

# **Design, Development and Testing of an Adjustable Above-Knee Prosthetic Leg for Toddlers**

by  
Janelle Theron

*Thesis presented in partial fulfilment of the requirements for the degree  
of Master of Engineering (Mechatronic) in the Faculty of Engineering at  
Stellenbosch University*



Supervisor: Dr Dawie Van den Heever

December 2017

## DECLARATION

By submitting this thesis electronically, I declare that the entirety of the work contained therein is my own, original work, that I am the sole author thereof (save to the extent explicitly otherwise stated), that reproduction and publication thereof by Stellenbosch University will not infringe any third party rights and that I have not previously in its entirety or in part submitted it for obtaining any qualification.

Date: December 2017

## Abstract

The aim of this research was to design and develop an above-knee lower limb prosthetic that can be adjusted to facilitate the growth of a child for a duration of three-years, between the ages of three and five years. The lower age limit is selected to accommodate for the occurrence of a mature gait pattern. Engineering requirements include a low-cost design and adjustability with respect to height, foot length and stiffness of the components. All requirements were met. Design parameters were then determined to ensure a natural gait. Concept designs were rated according to their respective design parameters so that a final design could be chosen.

The final design is lightweight, weighing 933 g (excluding a socket and foot cover). A low prototype cost of only R21 458 (Aug 2017) is incurred. The design consists of an ankle and foot prosthetic that is a single-axis, hinge-joint with a torsion spring of stiffness 808.59 Nmm/° which simulates the ankle stiffness and a removable footplate allowing for foot length adjustment. The pylon component of the prosthetic consists of two overlapping tubes, constrained by a clamp to allow for a height adjustment of 45 mm. The knee component consists of an Automatic Stance Phase Lock (ASPL) mechanism with an extension assist spring to allow for swing phase control. This design allows for the replacement of the spring of 3.34 N/mm to adjust the swing speed. The overall knee flexion is 67.3°, which is large enough to allow for adequate toe clearance. The overall design uses standard paediatric adapters, thus ensuring compatibility with other prosthetics.

To evaluate the functionality of the prosthetic device, prior to testing with children, a gait emulator was designed. This emulator controls a linear actuator emulating vertical excursion of the hip during swing-phase; a rotary actuator emulating the extension and flexion angles of the hip, and the use of a Bertec treadmill to emulate the horizontal motion of gait. Due to microcontroller timing limitations, the gait emulator did not allow for sufficient movement to occur during toe-off, thus preventing the knee from unlocking and the ankle flexing. When adjustments in height or foot length were made no changes in the gait kinematics occurred as is evident from the standard deviation for each age range being smaller than 2.1°. It was noted that an extension assist spring of a lower stiffness, 2.416 N/mm, resulted in the lowest standard deviation of the knee angle at only 0.76°. This was likely due to the low weight of the prosthetic limb during emulation. It is recommended that a spring with a lower stiffness be used for lighter individuals.

Though sufficient moment could not be applied during the emulation, it can be speculated that the knee can unlock and lock accurately via manual tests. In conclusion, this prosthetic is entirely adjustable to facilitate three-year growth of a child, between the ages of three to five years for a three year lifespan.

# Opsomming

Die doel van die studie is om 'n bo-die-knie onderste ledemaat protese te ontwerp en te vervaardig wat verstel kan word om sodoende die groei van 'n kind oor drie jaar, tussen die ouderdom van drie en vyf jaar, te kan akkommodeer. Die laer ouderdom is gekies om die voorkoms van 'n volwasse loop-patroon in ag te neem. Ingenieursvereistes sluit lae-koste ontwerp en verstelbaarheid, in terme van lengte, voetlengte en styfheid van die onderdele in. Daar is voldoen aan al die vereistes. Ontwerpsparameters (of -grense) is hierna vasgestel om 'n natuurlike loop-patroon te verseker. Konsepontwerpe is gemeet volgens hulle onderskeie ontwerpsparameters sodat die finale ontwerp gekies kan word.

Die finale ontwerp is lig en weeg 933 g (uitgesluit 'n potjie en voetbedekking). Die prototipe het 'n lae koste van slegs R21 458 (Aug 2017) beloop. Die ontwerp bestaan uit 'n enkel en voet protese op 'n enkele as, skarnier-gewrig met 'n wringveer met 'n styfheid van 808.59 Nmm/° wat die enkelstyfheid simuleer, en 'n verwyderbare voetplaat wat verstelbaarheid vir voetlengte moontlik maak. Die paal-komponent van die protese bestaan uit twee oorvleuelende buise, wat met 'n klamp begrens word vir 'n hoogteverstelling van 45 mm. Die knie-komponent bestaan uit 'n geoutomatiseerde houdingsfase klem (*Automatic Stance Phase Lock (ASPL)*) meganisme met 'n verleng-hulp veer om toe te laat vir beheer tydens die swaifase. Hierdie ontwerp laat die vervanging van die veer van 3.34 N/mm toe om die swaaispoed aan te pas. Die algehele kniebuiging is 67.3°, wat groot genoeg is vir voldoende toonspeling. Die algehele ontwerp gebruik standaard pediatriese koppelings en verseker dus aanpasbaarheid met ander protese.

Om die funksionaliteit van die protetiese toestel te evalueer, voor dit op kinders getoets word, is 'n loop-nabootser ontwerp. Die nabootser beheer 'n lineêre aandrywer wat vertikale uitwyking van die heup gedurende die swaai-fase naboots; 'n roterende aandrywer boots die verlengings- en buigingshoeke van die heup na, en die gebruik van 'n Bertec trapmeul boots die horisontale loop-aksie na. Weens die tydsbeperkings van die mikrobeheerder het die loop-nabootser nie toegelaat vir voldoende beweging tydens die fase waar die toon van die grond af gelig word nie, wat dus die knie verhoed om te ontsluit en die enkel om te verleng. Nadat verstellings aangebring is in lengte of voetlengte was daar geen veranderinge in die loop-kinematika nie soos dit blyk uit die standaard afwyking van minder as 2.1° vir elke ouderdomsgroep. Daar is egter gesien dat 'n verleng-hulp veer met 'n laer styfheid, 2.416 N/mm, lei tot die laagste standaard afwyking van die knie se hoek teen slegs 0.76°. Hierdie is heel moontlik as gevolg

van die lae gewig van die prostese tydens nabootsing. Daar word voorgestel dat 'n veer met 'n laer styfheid gebruik word vir individue met 'n laer liggaamsmassa.

Alhoewel genoeg moment nie aangeheg kan word in die nabootser toets nie, kan dit gespekuleer word dat die knie kan sluit en ontsluit wanneer voldoende beweging aangewend word. Ter afsluiting, hierdie prostese is ten volle verstelbaar om 'n kind tussen drie en vyf jaar te ondersteun vir drie groeijare.

## Acknowledgements

I would like to thank my Supervisor, Dawie van den Heever for his guidance in my thesis writing, John Cockroft and Cara Mills who helped me with the testing of my prosthetic device and Joka Plotz for her help and guidance with the Finite Element Analysis of the prosthetic components.

I would like to thank my family and friends, especially Gavin, for their guidance and helping me emotionally through this journey. Most importantly I thank God, this is only possible through Him.

# Table of contents

	Page
<b>Abstract</b> .....	<b>ii</b>
<b>Opsomming</b> .....	<b>iv</b>
<b>Table of contents</b> .....	<b>vii</b>
<b>List of figures</b> .....	<b>x</b>
<b>List of tables</b> .....	<b>xiii</b>
<b>Nomenclature</b> .....	<b>xv</b>
<b>1 Introduction</b> .....	<b>1</b>
1.1 Background.....	1
1.2 Objectives.....	2
1.3 Motivation.....	2
<b>2 Literature review</b> .....	<b>3</b>
2.1 Considerations for paediatric prosthetics.....	3
2.2 Gait analysis.....	3
2.2.1 Kinematic data of the gait cycle .....	5
2.2.2 Ground Reaction Force (GRF).....	8
2.3 Overall engineering requirements .....	10
2.4 Foot and ankle prosthetics.....	12
2.4.1 Determination of Functional Requirements (FRs) and Ankle Design Parameters (ADPs).....	13
2.4.2 Types of prosthetic feet .....	16
2.5 Pylon prosthetics.....	18
2.6 Knee prosthetics.....	20
2.6.1 Functional Requirements (FRs) and Knee Design Parameters (KDPs) .....	21
2.6.2 Knee stability (KDP1) .....	24
2.6.3 Swing-phase control (KDP2).....	25
2.6.4 Types of prosthetic knee joints .....	26
2.7 Materials.....	30
2.7.1 Metals.....	30
2.8 Safety considerations .....	31



<b>3</b>	<b>Concept Design.....</b>	<b>33</b>
3.1	Foot and ankle.....	33
3.1.1	Design Option 1: SACH foot (Figure 42) .....	34
3.1.2	Design Option 2: Single-axis foot (Figure 43) .....	34
3.1.3	Adjusting the length of the foot (Figure 44, Figure 45 and Figure 46) (ADP6).....	35
3.1.4	Additional considerations: Adding another dimension .....	36
3.1.5	Final design.....	36
3.2	Pylon.....	37
3.2.1	Design Option 1: Based on crutches (Figure 49) or a pin (Figure 50) .....	37
3.2.2	Design Option 2: Clamp design (Figure 51) .....	38
3.2.3	Design Option 3: Screw designs (Figure 52 and Figure 53) .....	38
3.2.4	Design Option 4: Key/slot design (Figure 54) .....	39
3.2.5	Final design .....	39
3.3	Knee.....	39
3.3.1	Design Option 1: Single-axis with spring (Figure 56).....	40
3.3.2	Design Option 2: Single-axis free swinging knee (Figure 57) ....	40
3.3.3	Design Option 3: Polycentric knee (Figure 58).....	41
3.3.4	Design Option 4: PASPL knee .....	41
3.3.5	Final design.....	41
<b>4</b>	<b>Detailed Design .....</b>	<b>42</b>
4.1	Foot and ankle.....	42
4.1.1	Design decisions based on calculations .....	43
4.1.2	FEA analysis .....	44
4.2	Pylon.....	48
4.2.1	Design decisions .....	48
4.2.2	Analysis results .....	49
4.3	Knee.....	49
4.3.1	Design decisions based on calculations .....	50
4.3.2	FEA analysis .....	52
4.4	Overall design.....	57
<b>5</b>	<b>Design of the gait emulator .....</b>	<b>59</b>
5.1	Introduction.....	59
5.2	Desired output data .....	60
5.2.1	Vertical excursion of the centre of mass.....	60
5.2.2	Speed and stride length.....	62
5.2.3	Flexion and extension angles .....	63
5.2.4	Kinetics .....	63
5.2.5	Measurement devices .....	64

5.3	Mechanical design.....	64
5.3.1	Existing gait emulator designs.....	64
5.3.2	Linear actuator .....	66
5.3.3	Rotary actuator.....	67
5.3.4	Structure design .....	67
5.4	Control requirements and strategy.....	68
5.5	Results .....	71
5.6	Discussion.....	76
<b>6</b>	<b>Conclusion.....</b>	<b>79</b>
<b>7</b>	<b>References .....</b>	<b>83</b>
<b>Appendix A</b>	<b>Information for the design of the prosthetic.....</b>	<b>90</b>
<b>Appendix B</b>	<b>Structural strength test requirements .....</b>	<b>102</b>
<b>Appendix C</b>	<b>Design calculations.....</b>	<b>110</b>
<b>Appendix D</b>	<b>Safety procedure.....</b>	<b>128</b>
<b>Appendix E</b>	<b>Gait emulation testing.....</b>	<b>130</b>

# List of figures

	Page
Figure 1: Components of the gait cycle (Andrysek 2009).....	4
Figure 2: Vertical excursion of the hip, represented as a sine wave (Choi & Kim 2008) .....	5
Figure 3: Mean normative data for percentage gait of paediatric patients of a) Hip flexion/extension angles, b) Knee flexion/extension angles and c) Ankle dorsi-/plantar-flexion angles (Chester et al. 2006).....	6
Figure 4: The effect of speed on the a) Hip flexion/extension angles, b) Knee flexion/extension angles and c) Ankle plantar-/dorsi-flexion angles(Schwartz et al. 2008) .....	6
Figure 5: Abstraction of the natural torque-angle characteristic of the human ankle (Brackx et al. 2012).....	8
Figure 6: Effect of speed on ground reaction force (Schwartz et al. 2008).....	9
Figure 7: Contributions of gravity and centrifugal force to the vertical GRF (Total) generated by the single pendulum model (Buczek et al. 2006) .....	10
Figure 8: Types of foot and ankle prosthetics a) SACH foot and flexible keel, b) Single axis foot, c) Multiaxis foot and d) Carbon fibre and flex foot (Military in-step 2014; Rush 2016; Ossur 2016a) .....	17
Figure 9: Zones of instability for prosthetic knees: a) Single-axis knee; b) Four-bar knee; c) Six-bar knee, d) Six-bar knee during stance-flexion; and e) ASPL knee (Andrysek 2009) .....	25
Figure 10: a) BMVSS manual locking knee, b) ICRC manual locking knee, c) BMVSS single-axis free-swinging knee, d) Stanford-Jaipur knee joint, a polycentric knee, e) ASPL mechanism (Narang 2013) .....	28
Figure 11: The shortening of a polycentric knee (Greene 1983).....	29
Figure 12: Automatic stance phase lock (ASPL) mechanism (Andrysek 2009).....	30
Figure 13: Final foot and ankle design .....	42
Figure 14: FEA model of ankle joint (Plotz 2016) .....	45
Figure 15: FEA how forces are applied, a) Front pressure (467 kPa), b) Centre pressure (117 kPa) and c) Back pressure (467 kPa) (Plotz 2016) .....	45
Figure 16: Fringe plot of Von Mises stress when centre pressure is applied (Plotz 2016) .....	46
Figure 17: Design adjustment of hinge joint to reduce stress points.....	47

Figure 18: Fringe plot of translational displacement when front pressure applied (Plotz 2016) .....	47
Figure 19: Final pylon design a) Components overlapping, b) Clamp, c) Components separated.....	48
Figure 20: Final knee design .....	50
Figure 21: Half model of the knee (Plotz 2016).....	53
Figure 22: FEA how forces are applied, a) Back pressure (439 kPa), b) Centre pressure (219 kPa), c) Front pressure (439 kPa) (Plotz 2016) .....	53
Figure 23: Von Mises stress fringe plot - Centre pressure (Plotz 2016).....	54
Figure 24: Back pressure FEA analysis (Plotz 2016).....	55
Figure 25: Front pressure applied, with close up (Plotz 2016).....	56
Figure 26: Displacement fringe plot – Centre pressure is applied (Plotz 2016)....	56
Figure 27: Final prototype of the adjustable prosthetic leg.....	57
Figure 28: The kinetic and potential energy curves during optimal speed (Schepens et al. 2004).....	61
Figure 29: Test robot by Richter et al. (2015).....	65
Figure 30: Depiction of uncoupled actuator.....	66
Figure 31: Final test structure with prosthetic attached.....	68
Figure 32: Linear actuator requirements for only the swing-phase.....	69
Figure 33: Control strategy diagram of gait emulator .....	69
Figure 34: Testing procedure.....	70
Figure 35: Marker location points on prosthetic device .....	71
Figure 36: GRF - gait emulator results .....	72
Figure 37: Vertical hip excursion - gait emulation results.....	73
Figure 38: Hip flexion and extension angles - gait emulation results.....	73
Figure 39: Knee flexion and extension angles - gait emulation results.....	74
Figure 40: Ankle dorsi/plantar flexion - gait emulator results .....	74
Figure 41: Screenshot of gait emulation when insufficient toe-clearance .....	78
Figure 42: Design Option 1: SACH foot.....	92
Figure 43: Design Option 2: Single-axis foot.....	92
Figure 44: Length adjustment option 1: Padded Socks/Straps .....	92
Figure 45: Length adjustment option 2: Slide mechanism.....	93

Figure 46: Length adjustment Option 3: Replace flat foot component .....	93
Figure 47: Auxetic tri-star sole (Nike 2016) .....	93
Figure 48: Adjustable pylons (Kinetic revolutions 2016) .....	94
Figure 49: Leg design 1 version 1: Based on crutches .....	94
Figure 50: Leg design 1 version 2: Based on pin adjustments .....	94
Figure 51: Leg design 2: Clamp design .....	95
Figure 52: Leg design 3 version 1: Use of the Kinetic Revolution (2016) adjustable pylon .....	95
Figure 53: Leg design 3 version 2: Use of screw design .....	95
Figure 54: Leg design 4: Key/slot design .....	95
Figure 55: Pyramid adapter (Haun, 2012) .....	96
Figure 56: Design Option 1: Single-axis with spring .....	96
Figure 57: Design Option 2: Single-axis, no spring .....	96
Figure 58: Design option 3: polycentric knee .....	97
Figure 59: Final assembly drawing of test structure .....	100
Figure 60: Fcr with respect to weight for condition I .....	103
Figure 61: Fcr with respect to weight for condition II .....	103
Figure 62: Specific configuration with $u_b=0$ , showing coordinate systems with reference planes, reference lines, reference points and test force, F, for right and left-sided application (ISO 2006) .....	104
Figure 63: Moment vs Fcr for condition I .....	106
Figure 64: Moment vs Fcr for condition II .....	107
Figure 65: Testing the prosthetic leg using Bertec treadmill and Vicon motion capture .....	130
Figure 66: Second figure of testing of the prosthetic leg using Bertec treadmill and Vicon motion capture .....	130

# List of tables

	<b>Page</b>
Table 1: General engineering requirements (ERs).....	11
Table 2: FRs and ADPs for the foot and ankle prosthetic.....	13
Table 3: Activity level of patient and what type of prosthetic foot to design for (Ottobock 2016).....	15
Table 4: FRs and PDPs of the pylon component.....	18
Table 5: FRs and DPs for evaluating knee joints.....	22
Table 6: Relationships between the DPs and the placement of the knee axis (single-axis) (Andrysek 2009).....	23
Table 7: Ankle rated concept designs according to ADPs.....	34
Table 8: Pylon rated concept designs according to PDPs.....	37
Table 9: Knee rated concept designs according to KDPs.....	40
Table 10: The determination of DeltaZ using the data determined by Eames et al. (1999).....	62
Table 11: Average optimal speed and Tc values for ages 3 to 5 years.....	63
Table 12: Data from gait emulation testing.....	75
Table 13: Standard deviation of gait emulator testing with respect to age and spring.....	75
Table 14: Measurement data.....	90
Table 15: Material properties.....	91
Table 16: Parts list for foot and ankle design.....	97
Table 17: Parts list for pylon design.....	98
Table 18: Parts list for the knee design.....	98
Table 19: Parts list for test structure, see Figure 59.....	101
Table 20: Structural test forces (Principal tests).....	108
Table 21: Structural test forces (Separate tests).....	109
Table 22: Calculation results for each design component.....	110
Table 23: Summary of ankle FEA results.....	111
Table 24: Summary of knee FEA results.....	111
Table 25: Summary of engineering requirements for final design.....	112

Table 26: Summary of Design parameters, see Table 25 for additional ERs.....	113
Table 27: Overall cost of final design.....	113
Table 28: Risk analysis.....	129

## Nomenclature

BW	Body weight
ASPL	Automatic Stance-phase Lock
CNC	Computer Numerical Control
DP	Design Parameters
ISO	International Organisation for Standardisation
ER	Engineering requirements
F-axis	Extends from the origin 0 perpendicularly to both the o-axis and the u-axis. Its positive direction is forward towards the toe.
FEA	Finite Element Analysis
Fcr	Cyclic load
FR	Functional Requirements
Fu	Axial force
GCSH	Gillette Children's Specialty Healthcare
GRF	Ground Reaction Force
K	Mechanical knee centre
KM	Kinematic Model
L-value	Amount of shortening of the polycentric knee
O-axis	Extends from the origin 0 perpendicularly to the u-axis and parallel to the effective knee-joint centre line. Positive direction outwards (left for left prostheses)
PASPL	Paediatric Automatic Stance-phase Lock
ROM	Range of Motion
S.D.	Standard deviation
TKA	Trochanter Knee Ankle
U-axis	Extends from origin, passes through the effective ankle-joint centre and the effective knee joint centre, positive direction upwards
VFC	Variable Friction Controller



# 1 Introduction

## 1.1 Background

A large number of people in the world need some form of a prosthetic device. This can be due to an amputation or a congenital limb deficiency. The overall rate of limb deficiencies in the United States is between 0.3 and one per 1000 births in 2006, approximately 41.5% of all limb deficiencies affect the lower limb and about 15% of children with deformities or amputations require an above-knee prosthetic (Smith 2006). The purpose of a prosthetic is to restore functions, such as mobility, of the missing limb thus allowing the individual to participate in physical, recreational and occupational activities. When a good prosthetic is fitted for a child, independence and normal physical and psychological development ensue. Studies have shown that up to 95% of children (ages 1-18 years) who were fitted with an appropriate lower limb prosthetic became functional walkers with 89% using it for the entire day. This study included patients with congenital limb deficiencies and those with amputations (excluding those within one year of the amputation). In this study, a child with a congenital deficiency is fitted with a prosthetic on average at 18 months, and an articulating knee at 37 months (Boonstra et al. 2000). The costs of prosthetics for children is high, in 2003 the prosthetic cost from injury, at an average of 4.7 years, to the age of 18 years ranged between \$73 140 and \$116 140 per single lower extremity amputation. The total cost of an above-knee prosthetic ranged between \$118 047 and \$130 247 from the average age of 5.8 to 18 years. The cost remains high because prosthetics are patient-specific and therefore are not manufactured on a large scale (Loder et al. 2004).

Children experience a lot of changes as they grow. Changes in height, girth, activity and weight are aspects that all toddlers go through. These changes result in a need to adjust the prosthetic leg approximately every three months (Levesque et al. 1992). Lower limb prosthetics must be replaced every year up to the age of five, every two years up to the age of 12 and then every three to four years up to the age of 21. Often a new prosthetic may be required more often than this if the child experiences skin ulcers or bone growth problems (Lambert 1972). This constant need for adjustments can be difficult for the child to adapt to and can be expensive for the parents who pay for the replacement each time. Due to the high costs, the best prosthetic may not even be considered. Therefore, it is important to find a prosthetic leg solution that can improve the lifespan and the cost of the leg, thus improving the lifestyle and mobility of the child (Smith 2006).

Therefore, the purpose of this study is to design, manufacture and test an adjustable prosthetic leg focusing on the growth of toddlers.

## 1.2 Objectives

The aim of this project is to design and develop an adjustable above-knee prosthetic leg for growing toddlers between the ages of 3 and 5 years with respect to height, foot length and stiffness while ensuring the design is functional for the entire age range. To satisfy this aim the following objectives will be realised:

- Identification of key engineering requirements, this includes the total length in adjustment for height and foot length, stiffness requirements, total fatigue life, cost range, and manufacturing requirements.
- Identification of design parameters to ensure the functionality of the prosthetic design, that is to allow the user to achieve a natural gait.
- Design of a test procedure - Testing of the prosthetic device to evaluate the overall functionality by designing a gait emulator.

## 1.3 Motivation

As discussed in Section 1.1 the cost of prosthetics is extremely high due to each case being patient-specific and the requirements of adjustments due to growth changes. Additionally, the testing of a prosthetic device's functionality on young children is difficult due to safety concerns and communication challenges (Andrysek 2009). Therefore ensuring a safe way to test the paediatric prosthetic design would be necessary. Though research does exist for adjustable prosthetics, these are for older age ranges (5-16 years) and do not consider aspects of fatigue which will affect the overall lifespan of the prosthetic (Ngan 2015; Castellanos et al. 2016).

It is obvious that the lifestyle of the child and family will be improved by designing a prosthetic that can reduce costs by reducing the need for constant replacements. Through this design, the overall cost of paediatric prosthetics in developing countries will be reduced which will ensure a positive socioeconomic impact in developing countries.

## 2 Literature review

A typical lower limb prosthetic consists of a foot and ankle system, lower and upper leg, a knee mechanism and a socket. Connection components and shock absorption components are then added as required. According to Andrysek (2009) “It is the setup, interaction and alignment of all these components that contribute to a successful prosthetic treatment”. In this chapter design considerations for paediatric prosthetics will be discussed, in particular, this will involve paediatric specific recommendations, the gait, individual components that a prosthetic comprises of, overall functionality and safety.

### 2.1 Considerations for paediatric prosthetics

Prosthetics for children, especially prosthetic legs, have many different requirements depending on the stage of growth of the child – changes in height, weight, girth and activity are all important considerations and usually result in a need for a new prosthetic every three months for a toddler (Levesque et al. 1992). A child will use a prosthetic leg for more than nine hours per day, therefore, it is important to consider comfort in terms of pressure-pain – as often a child cannot fully explain where or what kind of pain they are experiencing (Andrysek 2009). The additional need for a cosmetically appealing prosthetic usually branches from a desire that the parents have (Jones & Nelson 1965).

A prosthetic should be designed towards children who are physically active. This can be done by considering energy storing, light materials. To design a paediatric prosthetic it is necessary to remember that in general, children are less responsible and more mentally and emotionally immature than the ideal adult, therefore, removable components will likely get lost and instructions can be forgotten or ignored (Cummings & Kapp 1992). It is also important to note that durability of the prosthetic is more important than the cosmetics. Prosthetics must facilitate function – if products are used that result in the need for the child to be careful, that product should rather be avoided (Fisk 1992).

### 2.2 Gait analysis

Gait refers to the manner of walking and a gait cycle to the time interval between two successive occurrences of one of the walking events. By comparing the kinematics and kinetics of the gait cycle of a prosthetic device to normative data it can be determined whether or not a patient will walk efficiently and how improvements can be made (Ngan 2015).

The full gait cycle is represented in Figure 1. During the gait cycle, two main phases occur, the stance-phase and the swing-phase. The gait cycle begins at the stance-phase, between the heel strike until toe-off, this is approximately the first 60% of the cycle. The swing phase occurs from toe-off until foot contact. A mature gait pattern is established by the age of 3. This is due to the presence of heel-strike at the age of 18 months old and the increase in limb lengths as the child grows. With an increased limb length a greater limb stability results thus increasing the duration of the single-limb stance (Sutherland et al. 1980; Ivanenko et al. 2005). It is noted that the normal heel-to-toe gait pattern is usually only reached by the age of five years and therefore complete rollover is not expected (Cummings & Kapp 1992).

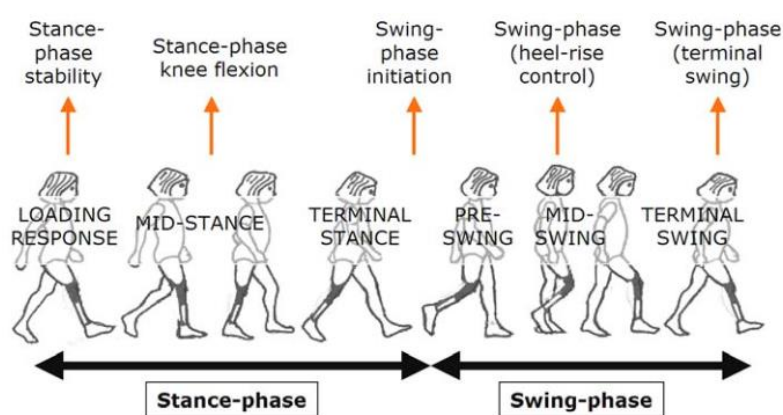


**Figure 1: Components of the gait cycle (Andrysek 2009)**

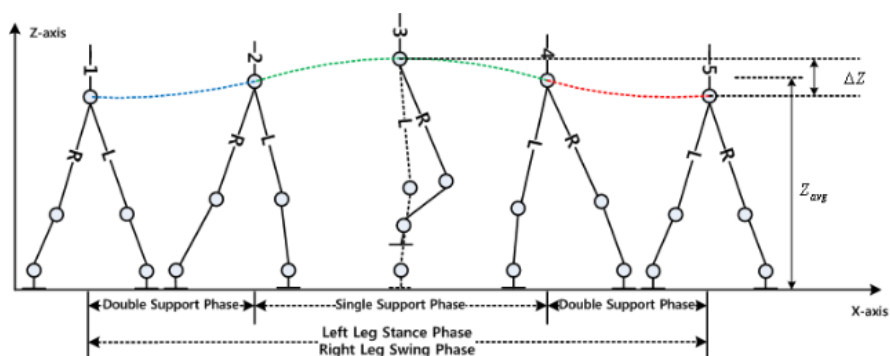
During a gait analysis, kinetic data are measured and calculated such as the ground reaction force (GRF); the power of the hip, knee and ankle; and moments due to abduction and adduction of the hip. Additionally, kinematic data are collected which include flexion and extension of the ankle, knee and thigh; hip displacement; cadence; stride length; and step frequency. This data is determined by comparing the GRF measured from a force plate with the coordinates measured in 3D space. This data can be used to analyse anomalies of a prosthetic with respect to a normal gait pattern (Andrysek 2009; Schmalz et al. 2002; Eng & Winter 1995; Kaufman et al. 2016; Eastlack et al. 1991; Cupp et al. 1999). Kinematic and kinetic data are discussed further in the following sections.

## 2.2.1 Kinematic data of the gait cycle

During the gait cycle, the hip moves laterally for balance, horizontally for forwarding progression and vertically. The vertical motion is known as a vertical excursion and fluctuates around the centre of body mass, moving similar to a sinusoidal pattern having twice the frequency of gait, as determined in the theory of ballistic walking (Mochon & McMahon 1980). This motion can be seen in Figure 2. Choi and Kim (2008) determined a sinusoid waveform to simulate the movement of the hip with respect to walking time, see Equation 1, in which  $y(t)$  is equal to the vertical excursion.  $Z_{max}$  and  $Z_{min}$  are the maximum and minimum excursions of the centre of mass during the gait cycle;  $Z_{avg}$  is the centre of mass height when standing (standing CG Table 14); and  $T_c$  is the time for a full gait cycle to occur.

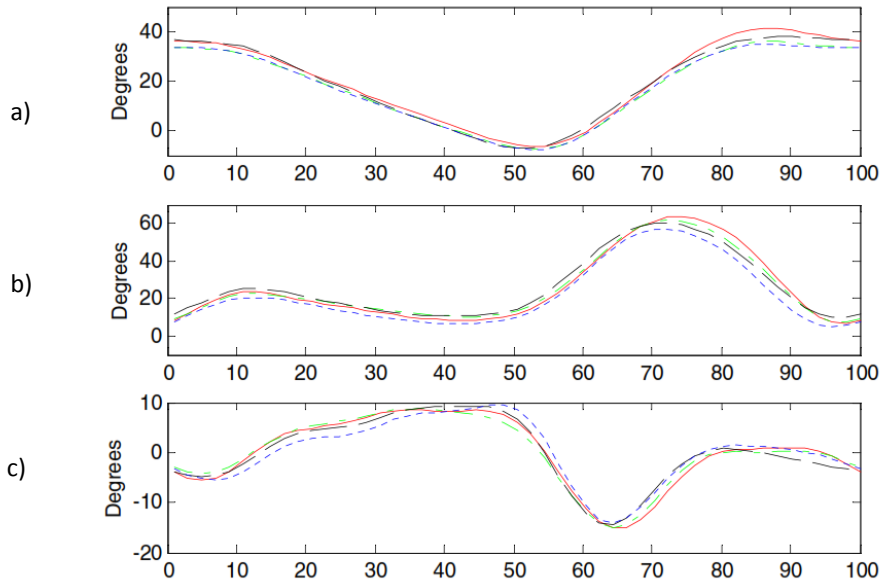
$$y(t) = \frac{\Delta Z}{2} \sin\left(\frac{4\pi}{T_c} t + \frac{\pi}{4}\right) + Z_{avg} \quad (1)$$

With  $\Delta Z = Z_{max} - Z_{min}$



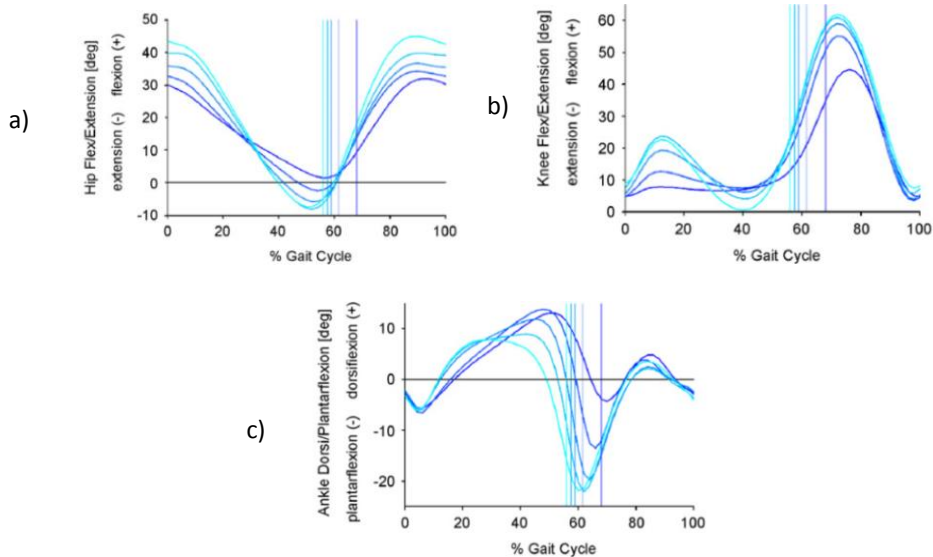
**Figure 2: Vertical excursion of the hip, represented as a sine wave (Choi & Kim 2008)**

Figure 3 shows the flexion and extension angles for the hip, knee and ankle for ages 3 to 13 years of age at free speed. From the curves depicted in this figure, it can be seen that the age increase from 3 years to 13 years of age does not have a large effect on the magnitude or curve of the angles (Chester et al. 2006). Figure 4 shows the effect that speed has on the flexion and extension angles. As can be seen in the figures the shape of the curves remain similar, however, the peaks occur earlier as the speed increases (Schwartz et al. 2008).



**Figure 3: Mean normative data for percentage gait of paediatric patients of a) Hip flexion/extension angles, b) Knee flexion/extension angles and c) Ankle dorsi-/plantar-flexion angles (Chester et al. 2006)**

Key for Figure 3: 3-4 year olds (—); 5-6 year olds (---); 7-8 year olds (-.-.); 9-13 year olds (—)



**Figure 4: The effect of speed on the a) Hip flexion/extension angles, b) Knee flexion/extension angles and c) Ankle plantar-/dorsi-flexion angles(Schwartz et al. 2008)**

Key for Figure 4: Very Slow; Slow; Free; Fast; Very Fast

Figure 3a) shows the flexion and extension angles of the hip during the gait cycle. The hip flexes on average between  $39.16^\circ$  flexion and  $7.95^\circ$  extension, the total range of motion (ROM) is therefore  $47.11^\circ$  (Chester et al. 2006). The shape of this curve is due to the pendulum-like motion of the hip joint as it swings back and forth during gait. The hip angle decreases as the body moves forward during the stance phase. To ensure foot clearance, the hip begins to flex slightly earlier than the end of the stance phase. This range of motion ensures an adequate step length. The angles represented in the graph are with respect to the initial  $14^\circ$  hip flexion of the hip when standing. This flexion is due to the assumption that the transverse plane of the pelvis is that containing the anterior and posterior superior iliac spine. (Schache & Baker 2007)

The knee flexion and extension angles are shown Figure 3b). The knee flexes between an average of  $64.33^\circ$  flexion and  $6.48^\circ$  extension, a total ROM of  $70.81^\circ$  (Chester et al. 2006). As seen in the figure the knee flexes slightly during the stance phase to accommodate for the transfer of weight followed by a large amount of flexion during the swing phase. It is necessary for a minimum of  $50^\circ$  during the mid-swing to ensure toe clearance. (Schache & Baker 2007)

Figure 3c) shows the ankle plantar- and dorsiflexion. The flexion angles of the foot range from  $8.77^\circ$  for dorsiflexion and up to  $19.56^\circ$  for plantar flexion, a total ROM of  $28.33^\circ$  (Chester et al. 2006). Inversion and eversion are necessary when walking on uneven surfaces; this reduces the chances of the prosthetic leg being displaced (Rihs & Polizzi 2001). The ankle joint exhibits a small plantar flexion during the first 10% of the gait cycle, it then progresses from plantar flexion to dorsiflexion between 10 to 62% of the stance (See Figure 5). The ankle joint then generates a large amount of torque during this progression stage to contribute to the forward movement of the body. The maximum amount of torque is generated at the end of terminal stance (Shamaei et al. 2011).

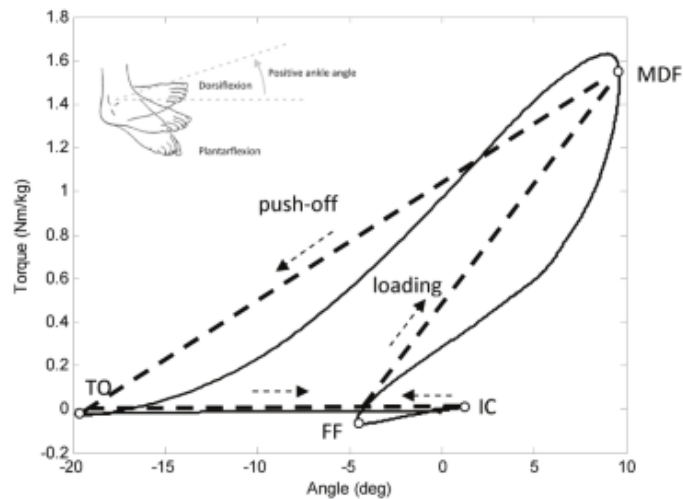


**Figure 5: Abstraction of the natural torque-angle characteristic of the human ankle (Brackx et al. 2012)**

*Key for Figure 5: TO – Toe-off, FF – Foot-flat, IC – Initial contact, MDF – Maximum Dorsiflexion Angle*

### 2.2.2 Ground Reaction Force (GRF)

The graph for the Ground Reaction Force (GRF) during walking is shown in Figure 6 (refer to free walk). As seen in the figure, the curve increases above the body weight line then fluctuates below and above this line and finally decreases back to zero. The initial increase in the GRF occurs as weight is transferred from one foot to the other. The slope is also affected by the friction force which becomes more prominent as the foot is placed on the ground. Similarly, the friction force and weight transfer will cause a decrease in the slope during toe-off. (Kirtley 2016)

The GRF then fluctuates above and below the body weight line. This is due to the acceleration of the leg having a strong effect on the force. According to Newton's second law, the reaction force is affected by the acceleration of the body. Following this increase, a dip occurs due to the angle at the thigh decreasing as the leg starts to straighten. The angular acceleration of the leg is strongly related to this angle as seen in Equation 2 and 3. The second peak is as the body moves in front of the leg, increasing the angle and thus the acceleration. (Kirtley 2016)

The curve of the GRF is affected by the speed of walking, as can be seen in Figure 6, the peaks increase as the speed increases. This is clear from the previous discussion as an increase in acceleration will increase the angular acceleration. In this figure, it can also be noted that speed has a higher effect on the first peak in



the gait cycle than the second peak (Stansfield et al. 2001). A number of additional factors can affect the ground reaction force, the first peak can be affected by a stomping motion or weak thigh muscles which have less control of the leg (Baker 2011).

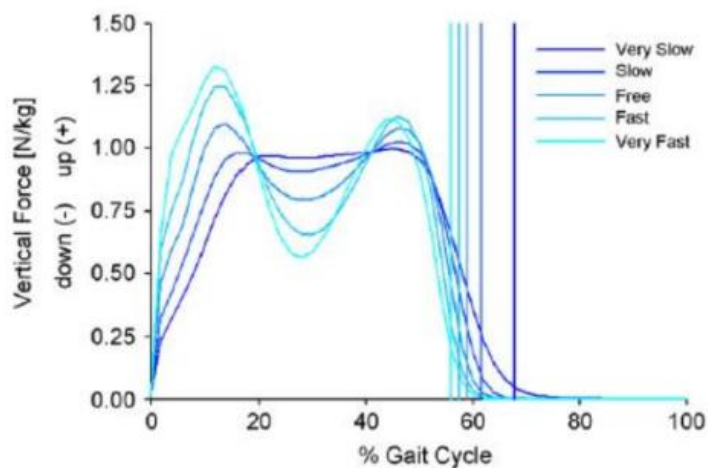


**Figure 6: Effect of speed on ground reaction force (Schwartz et al. 2008)<sup>1</sup>**

$$\theta = g \sin \ddot{\theta} + \ddot{x} \cos \theta \quad (2)$$

With positive anti-clockwise,  $g$  = acceleration due to gravity ( $m/s^2$ ),  $\ddot{\theta}$  = angular acceleration ( $rad/s^2$ ),  $\ddot{x}$  = vertical acceleration ( $m/s^2$ ). (Kinematic angular acceleration, inverted pendulum design)

$$\ddot{\theta} = \frac{g \sin \theta}{\theta R} \quad (3)$$

With the assumption of constant velocity ( $\dot{x} = 0$ ),  $R$  = radius of curvature

In comparison, the GRF of an inverted pendulum design is shown in Figure 7, as can be seen in this figure the GRF does not peak above the body weight line, nor does it have two separate peaks. This is due to the inverted pendulum assumption not having the consideration of the leg bending and straightening. (Buczek et al. 2006)

<sup>1</sup> From literature it can be concluded that the units given for the vertical force N/kg is incorrect, based on the given range it is meant to be BW(kg/kg) and will be referred to as such in future sections. (Kirtley 2016)

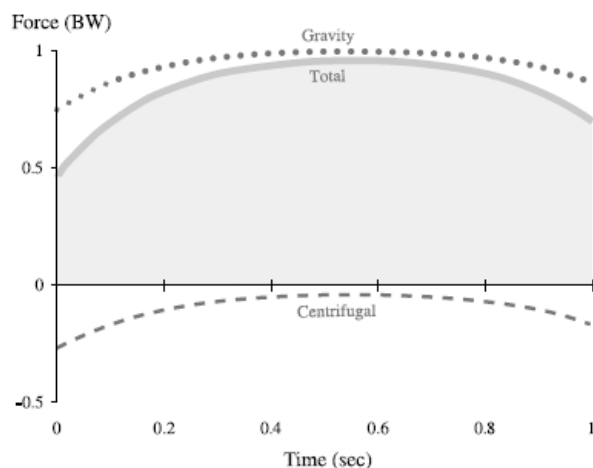


**Figure 7: Contributions of gravity and centrifugal force to the vertical GRF (Total) generated by the single pendulum model (Buczek et al. 2006)**

### 2.3 Overall engineering requirements

In the following chapters, each prosthetic component will be analysed separately to find the functional requirements so that design parameters can be determined. Before the component-specific requirements are determined it is important to first analyse the overall engineering requirements. The engineering requirements (ERs) are summarised in Table 1, these are labelled and numbered to allow for referencing throughout the document.

As stated in Section 2.2 a mature gait pattern is reached at the age of 3, improving until a normal complete rollover of heel-to-toe is reached at the age of five years (Sutherland et al. 1980; Ivanenko et al. 2005; Cummings & Kapp 1992; Chester et al. 2006). During this time, however, a toddler experiences so much change with respect to weight, height and circumferential growth that the prosthetic must be replaced every three months (Sutherland et al. 1980; Levesque et al. 1992). Therefore it is the design goal to develop a prosthetic that can be adjusted with respect to the growth of the child as well as be strong enough to handle the changes in weight of a growing child over a three year period between the ages three and five. This will improve the cost of the prosthetic component immensely. The ERs are thus for adjustments for changes in length, changes in foot length and changes in stiffness requirements of the components while being strong enough to handle the changes in weight over a three-year lifespan (ER1, ER2, ER3, ER4, ER5). The ranges of the ERs are

determined based on the anthropometric data in Table 14 and are discussed in further detail in the sections referenced in Table 1.

**Table 1: General engineering requirements (ERs)**

Goal	ER ref no.	Engineering requirements	Further details
Adjustable for growth over 3 year period (age 3 to 5 years)	ER1 /PDP3	Height adjustments	Section 2.5, 50 mm
	ER2 /ADP6	Foot length adjustments	Section 2.4, 22 mm
	ER3 /ADP4 /KDP7	Stiffness adjustment	Component specific, Section 2.4, 2.5 and 2.6
	ER4	Overall strength	Maximum weight of child, 20 kg, rounded up for safety
3-year lifespan	ER5	Fatigue strength	Lifespan: $2.37 \times 10^7$ cycles
Locally sourced materials	ER6	South Africa	
Manufacturable	ER7	Easy to manufacture	Basic engineering workshop facilities
Low cost	ER8	Material and manufacture cost	Less than R378 480.93 – R417 596.43
Safe	ER9	Safe	Especially stability
Cosmetically appealing	ER10 /PDP4	Cosmetically appealing	To the eye, putting on clothing
Allow for use of standard products	ER11	Standardized	Use of standard mechanisms for attachment

Prosthetic components are normally rated for one year, therefore the total lifecycle of the component will need to be adjusted for this longer cycle of three years (Rush 2016; Ossur 2016a; Faulhaber 2011). With the prosthetic leg having a minimum of a three-year lifespan the leg must be durable and strong enough to handle the cyclic stresses over this time. If this is not achievable, designs must be considered as to how to replace parts to ensure the overall lifespan. The lifespan can be lengthened as is feasible. The design should handle the cyclic loads resulting from the constant use of the leg. Stress cycles are determined based on the following assumptions: nine hours of use a day (Andrysek 2009), with an average of 80 steps per minute (determined from a

slow walk) – therefore 40 steps per leg. The total cycles for three years are  $2.37 \times 10^7$  cycles (ER5).

To design components that are cost effective for people in South Africa it would be important to have a low-cost design, using locally sourced materials (ER6) to ensure a positive socioeconomic impact in South Africa. It will also be necessary to ensure that the components are easy to manufacture to ensure that they can be made anywhere where there are basic engineering workshop facilities (ER7). As stated in Section 1.1, the total above knee prosthetic cost from injury, at an average of 5.8 years, to the age of 18 years is between \$118 047 - \$130 247 (\$, 2003) (Loder et al. 2004). In 2017, excluding inflation considerations, the total cost of an above knee prosthetic from injury in South African Rands is approximately between R1 539 155.81 and R1 698 225.51. The cost per year resulting between R126 160.31 and R139 198.81 (for the average total of 12.2 years). Therefore, the prosthetic design should cost less than the normal cost of an above knee prosthetic component over three years, R378 480.93 – R 417 596.43. (ER8)

Additionally, the following requirements are based on the parent, the physiotherapist and socioeconomic factors:

- Safe – This not only means stability and prevention of falling but considerations should also be considered in terms of what is safe for a toddler to use – avoid too many parts that can be detached, design for high activity in terms of cyclic stresses to avoid breakage, durability and prevent abrasive edges that can hurt the toddler (Section 2.1). (ER9)
- Cosmetics – appealing to the eye as well as being able to easily put on clothing. (ER10)
- The design should be such that components can easily be replaced by standard products – the attachments should use standard mechanisms. (ER11)

Due to the different lengths of amputations for all individuals, for adults and children alike, the design of the prosthetic will be considered with respect to individual components of the ankle, the pylon and the knee. This will allow users of different amputation lengths to be able to use this technology and overall increase the number of patients that can be reached.

## **2.4 Foot and ankle prosthetics**

The functional requirements for the ankle and foot prosthetic system are analysed and from this, the design parameters are determined. The design parameters are then further analysed to ensure that each has a measurable

amount. Finally, different types of ankle and foot prosthetics are discussed so that concepts can be developed.

### 2.4.1 Determination of Functional Requirements (FRs) and Ankle Design Parameters (ADPs)

The functional requirements (FRs) for the prosthetic ankle and foot system are determined so that the ankle design parameters (ADPs) and means of measurement can be found. ADPs are labelled and numbered to allow for referencing throughout the document. With these ADPs, the final design can be constructed to ensure that all FRs and ERs are met. Table 2 summarises these results, FRs are grouped by shading rows – the ADPs apply to these respective groupings.

**Table 2: FRs and ADPs for the foot and ankle prosthetic**

Functional requirements	Design Parameters	DP/ER ref no.	Method of measurement	Unit	Range	Rate (5)
Achieve natural gait (Ottobock 2013)	Lightweight	ADP1	Weight excl. connections	g	276-400	4
	Shock absorption	ADP2	Energy absorption	J	N/A	3
	Activity level	ADP3	Table 3	N/A	K2-K3	3
	Ankle stiffness	ADP4 (ER3)	Deflection under maximum force	<sup>0</sup> Nmm/ <sup>0</sup>	Dorsi: 8.77 Plantar: 19.56 855.7	4
Small - fit into foot shell (Klute et al. 2004)	Length and breadth	ADP5	Fit normal shoe dimensions, Table 14	mm	159-181	5
Growth adjustment	Adjustability	ADP6 (ER2)	mm adjustment (Table 14)	mm	22	5

From literature, it is determined that the FRs for the user of a prosthetic ankle and foot system are to achieve a natural gait and be small enough to fit into a shoe (Ottobock 2013). Additionally, the ERs determined in Section 2.3 must be designed for. Foot length adjustment (ER2) and stiffness (ER3) are analysed in

more detail, therefore these are noted as ankle-specific design parameters ADP6 and ADP4 respectively.

A natural gait is achieved by designing for a lightweight system. When the system is too heavy the suspension and connection system can be affected poorly (Ottobock 2013). The ranges of weight in prosthetic foot products are between 276 and 400 g. The weight of the prosthetic foot system is dependent on the materials used as well as the shock absorption systems (Imasen 2009; Ossur 2016a; Trulife 2011; Rush 2016). (ADP1)

Shock absorption reduces the impact of heel strike; allows for a smooth rollover; provides a rigid lever during toe-off and allows the patient to walk over different terrains (Ottobock 2013). It is also important to absorb shock as the impact of walking can often lead to residual limb tissue breakdown and pain (Klute et al. 2004). The more flexible a component the more energy that will be absorbed, if too little energy is absorbed a shock absorption device may be required – this does, however, add more weight to the component (Beardmore 2013). The impact force experienced on the ankle and thus the rest of the leg is with respect to the body weight (BM) of an individual, the peak amplitude of the vertical reaction force increases from 1 to 1.5 BW as the walking speed increases (Nilsson & Thorstensson 1989). (ADP2)

Wearing shoes has a large effect on the impact of shock absorption. By wearing running or orthopaedic shoes a large increase of up to 63% in energy dissipation occurs when compared to no shoes. If residual limb injury is a concern, prosthetics that dissipate more energy is recommended (Klute et al. 2004). From this, it is concluded that the prosthetic device should be made such that a shoe can be worn. Shoe sizes for a child depend on the child's growth, Table 14 in Appendix A.1 shows that on average a three-year-old will have approximately 159 mm shoe length and at five years approximately 181 mm (Healthyfeetstore 2016). It is important to ensure that the prosthetic foot can be adjusted to fit the required shoe length to ensure the required minimum lifespan of three years. (ADP2, ADP5, ER5)

Choosing the correct activity level is necessary to avoid difficulty in walking, especially with regards to stability. Table 3 summarises the activity levels in the prosthetics industry as well as what is recommended for these designs (Ottobock 2013). Ideally, an activity level of K3 or K4 would be desired for a toddler as toddlers usually have high amounts of energy and want to explore (APC Prosthetic 2016). (ADP3)

Ankle stiffness is an important factor with regards to a natural gait. An ankle which is too stiff will cause the foot not to rotate forward to a flat position which can cause the knee to buckle forward. Alternatively, an ankle that is too flexible

will reduce sound limb loading as well as preventing adequate forward progression, resulting in a reduction in the effective ankle moment. Therefore, it is important to find a balance for ankle stiffness (Klodd et al. 2010; Ottobock 2013). Ankle torque supplies the force that propels the individual forward when walking. Figure 5 shows the comparison of the ankle torque in Nm/kg compared to the ankle angle ( $^{\circ}$ ). The energy return during ambulation ensures that natural gait occurs by providing momentum. In a normal foot, the energy is stored during the stance phase and released on the transferral of weight (Rihs & Polizzi 2001). The ankle rotational stiffness can be compared to a torsion spring's stiffness. A stiffness of  $858.7 \text{ Nmm}/^{\circ}$  was determined for young patients with an average age of 12.9 years (standard deviation (S.D.) 3.3 years). This stiffness can be lowered when considering younger patients (Shamaei et al. 2011; Liu et al. 2008). (ADP2, ADP4)

**Table 3: Activity level of patient and what type of prosthetic foot to design for (Ottobock 2016)**

	<b>Activity level K0</b>	<b>Activity level K1</b>	<b>Activity level K2</b>	<b>Activity level K3</b>	<b>Activity level K4</b>
<b>Description:</b>	Non-ambulatory	Household	Limited community walker	Unlimited community walker	Very active
<b>Design for:</b>	Doesn't support the weight	Maximum stability maintain balance	Stability, comfort	Combination: K2 and K4	Withstand shock, tension, torsion Respond to changing speed

The ADPs and ERs are scaled for analysis purposes for concept development. A scale of five is used, with five being highly important. The ADPs and ERs for size, adjustability, strength and manufacturability are rated five due to the effect on the main objectives. The ADPs and ERs for lightweight, ankle stiffness and durability are rated four due to their strong effect on ADPs such as shock absorption and activity level which in turn is rated at three. The ERs for low-cost and locally sourced materials are then rated two- due to the effect that all ADPs have on this. Other ERs are not rated as they will be designed for in the design stage.

## 2.4.2 Types of prosthetic feet

A prosthetic foot can be categorised in terms of its structure: non-articulated – having a rigid connection to the prosthetic shank, and articulated – having a hinged ankle mechanism. An articulated prosthetic foot can be further improved by a dynamic response foot (Military in-step 2014).

The SACH foot (Figure 8a) is the most basic prosthetic foot. The design consists of neoprene or urethane foam moulded over an inner keel, shaped to resemble a human foot. The keel is the device in which energy is stored; it bends the foot upwards when weight is applied to the toe. This foot has no hinged parts and is, therefore, inexpensive, durable and virtually maintenance free. The foot offers cushioning and energy absorption but does not store and return the same amount of energy as a foot would. A similar design is an elastic keel (or flexible keel) foot, this design involves a keel that is flexible with no moving parts. The elastic keel foot allows the forefoot to conform to uneven terrain but still remains stiff and stable when standing or walking. Both SACH feet and flexible keel feet (Figure 8a) are designed for patients with a low activity level K0 and K1 (see Table 3), with little variation in speed. These feet work well as a first prosthetic and are often later replaced for a more dynamic foot (Military in-step 2014). The MightyMite foot is an elastic keel foot that costs \$92.40, these feet come in size 140 mm to 210 mm (Fillauer Companies 2011).

Articulated prosthetic feet are those that move in one or more of three different planes. This allows for rotation of the leg while the foot is in contact with the ground. Single-Axis Feet (Figure 8b) allows the ankle to move only up and down, this design enhances the knee's stability (compared to the SACH foot). This design is better for above-knee designs and reduces the effort of walking. The wearer is required to actively control the prosthetic to prevent the knee from buckling. This design does, however, add more weight to the overall prosthetic, requires periodic servicing and is more expensive than the SACH foot. This foot would be appropriate for individuals whose major concern is stability, i.e. a K2 activity level (Table 3). (Military in-step 2014)



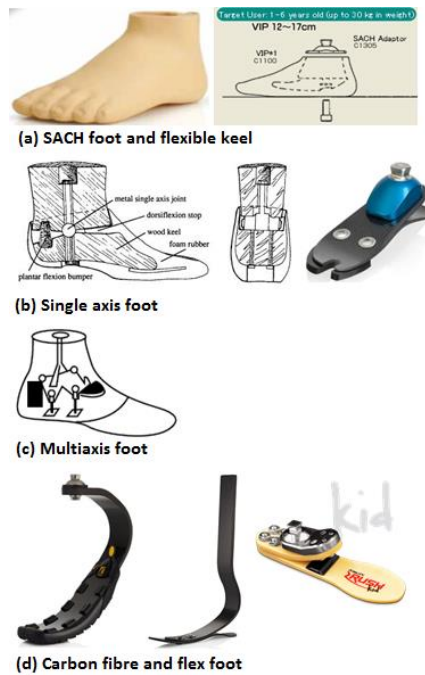


**Figure 8: Types of foot and ankle prosthetics a) SACH foot and flexible keel, b) Single axis foot, c) Multiaxis foot and d) Carbon fibre and flex foot (Military in-step 2014; Rush 2016; Ossur 2016a)**

Multi-axis feet (Figure 8c) are similar to single-axis feet with the addition to conform better to uneven surfaces; this is due to the added movement from side to side. This additional ankle motion absorbs some of the stresses that occur when walking and protects the skin and prosthetic from wear and tear – thus increasing the overall lifespan of the prosthetic. These feet are recommended for individuals who need significant mobility for their work or recreational needs such as hiking and dancing (K3 and K4 Table 3). (Military in-step 2014)

An articulated foot usually requires a foot shell. A foot shell allows the user to wear shoes and improves the lifespan of the foot. For an adult foot shell, the cost is around \$112.00, the cost of a foot shell is separate from the cost of buying the ankle and foot prosthetic. (Fillauer Companies 2011) The element foot system (\$988), element DS foot system (with shock absorber) (\$1889.00) and the Ibx foot system (\$1089.00) are all articulated feet that are designed for adult users (Fillauer Companies 2011). These prices give the designer an idea of the cost of articulated feet, though inflations should be considered and prices do vary.

Dynamic response feet are ideal for those who vary their walking speed or who walk long distances (K3 and K4). These feet are designed to store and release energy when walking. Some even have less impact on the heel than a normal

foot during motion. The carbon fibre heels and the Rush foot (Figure 8d) allow for additional energy storage compared to the SACH foot (Military in-step 2014). The Rush foot is made from a glass composite and has a smooth transition from heel to toe-off, being extremely flexible with no dead spots. Both of these materials are highly strong and durable. Rush (2016) also states that this foot allows walking on different terrains and at different speeds.

## 2.5 Pylon prosthetics

The pylon is the external frame of the prosthetic system. It is connected to the foot prosthetic, knee and socket by means of various adapters (Clements 2016). The pylon functional requirements (FRs) are determined and from this, the pylon design parameters (PDPs) are made – these are summarised in Table 4. PDPs are labelled and numbered to allow for referencing throughout the document. FRs are grouped by shading rows – the PDPs apply to their respective groups. The PDPs are then further analysed to ensure each has a measurable amount. Finally, different types of pylon prosthetics are analysed and discussed so that concept designs can be developed.

**Table 4: FRs and PDPs of the pylon component**

Functional requirements	Design Parameters	DP/ER ref no.	Method of measurement	Units	Range	Rate
Achieve natural gait	Lightweight	PDP1	Weighing of all components excl. adapters	g	114-160	4
	Shock absorption	PDP2	Measure units of acceleration	m/s <sup>2</sup>	N/A	1
Growth adjustment	Adjustability	PDP3 (ER1)	See Table 14	mm	50	5
Ease of use	Smooth	PDP4 (ER10)	Ensure no protruding components to prevent difficulty when dressing		N/A	4

The functional requirements for the pylon component are to achieve a natural gait. Additionally, the ERs determined in Section 2.3 must be designed for. Length adjustment (ER1) and a cosmetically appealing product (ER10) are analysed in more detail, these are noted as pylon-specific design parameters PDP3 and PDP4 respectively.

To allow for a natural gait, the pylon prosthetics should not add too much additional weight. The weight of the pylon is dependent on the strength requirements as well as the shock absorption design. Commercial pylons are made of carbon, aluminium or steel with adapter materials consisting of titanium, Titanium-HD, stainless steel or aluminium (ER6). Paediatric pylons are designed for a weight limit between 45 kg and 60 kg, these usually have a 12-month warranty (ER5). The aluminium and composite flex tubes by Trulife and WillowWood weigh between 114 and 160 g (WillowWood 2016; Fillauer Companies 2011; Trulife 2011). (PDP1)

Natural gait is affected by the ability of the pylon to absorb shock. A pylon can either be static or dynamic. A static pylon will serve to bear the weight of the person, connect the components together and allow for the appropriate height. A dynamic pylon has the same functionalities as the static pylon with the addition of shock absorption – this reduces the forces felt by the residual limb when a person walks, particularly during heel strike. A dynamic pylon's spring-like action also helps to propel the person forward allowing for improved movement (Hanger Clinic 2016). A shock-absorbing pylon does not have a large effect on the speed of walking for transtibial patients, however, it is preferred with regards to comfort. Shock-absorbing pylons are recommended when the patient is able to walk routinely at speeds above 1.3 m/s (Gard & Childress 2001) (PDP2). A toddler's average walking speed is 1m/s based on literature, therefore a shock absorbing pylon is not necessary (Schepens et al. 2004; Rose-Jacobs 1983; Shriners Hospital 1987; Hof 1996; Schwartz et al. 2008).

Some pylons have torque-absorption qualities, this allows for rotation of the foot for up to 45° in either direction, with adjustable resistance for different activities. This is a useful addition for those who wish to play golf, tennis or dance (Hanger Clinic 2016). Ankle shock components such as the MiniShock absorbs 5 mm of vertical shock as well as allowing for up to 60° of axial rotation (30° in each direction), it is a lightweight component (130 g) and is 60 mm in height (Fillauer LLC 2016) (PDP2).

According to Lenka et al. (2008), shank deformability can be altered to mimic the natural ankle joint motion, however, structural integrity should be considered to avoid permanent deformation and buckling. Shank flexibility changes may alter the stress distribution of the socket-residual limb interface – this can result in discomfort and affect the patient's gait. (PDP2)

The PDP for length adjustability is especially important as a shortening of 10 mm for above-knee prosthetics as tolerance limits were inadequate. Only 15% of the group analysed found this acceptable – if too short, chronic hip pain occurred mainly on the long leg side (Friberg 1984). From the data in Table 14, a total adjustment of 50 mm will be required (PDP3/ER1). Adjustable pylons such as

those made by Kinetic Revolutions (2016) are made for high activity levels. It is adjusted by revolutions, one full revolution accounts for 1.59 mm. It is constructed from 7075-T6 aluminium. The models can be seen in Figure 48 in Appendix A.4. The paediatric model can extend by 25.4 mm. It has a retail pricing of \$550.00.

It is important for prosthetic components to be cosmetically appealing, the way that a prosthetic looks affects the perceived functionality of the prosthetic as well as the chance of use. Not only should the prosthetic look appealing, it should also be easy to cover with clothing – parts that can catch or tear clothing would not be ideal. (Ngan 2015) (PDP4/ER10)

The cost of a MightyMite pylon tube is between \$24.98 and \$27.49 (in 2011) and with adapter costs between \$90.41 and \$92.04 (in 2011) (WillowWood 2016; Fillauer Companies 2011; Trulife 2011). This can be used to compare concept design costs (ER8). A pylon design exists which involves the use of bicycle components. Though the design was heavier than most other options it was concluded that this improved the sense of stability for the patient (Strait & Resident 2006). A plain bicycle seat post with a clamp can be used to easily adjust to any height within a particular range. A more advanced seat post, a suspension seat post, can be used to adjust the height as well as absorb impact from bumps when riding (Bicycle riding 2016).

The PDPs and ERs are scaled for analysis purposes in the concept development stage. A scale of five is used, with five being highly important. The PDPs and ERs for adjustability, strength and manufacturability are rated five due to the effect on the main objectives. Durability and lightweight are rated at four due to their effect on the other PDPs especially shock absorption. The cosmetic appeal is also rated at four due to the need for the design to be useful for the customer. Low cost and locally sourced materials are then rated two due to the effect that all PDPs have on this. Shock absorption is rated one as it is determined not as important in literature. Other ERs are not rated as they will be designed for in the design stage.

## **2.6 Knee prosthetics**

The following chapter reviews the literature with regards to the design of a prosthetic knee for a paediatric patient. The FRs for the user are determined followed by the corresponding Knee Design Parameters (KDPs), these are summarised in Table 5. KDPs are labelled and numbered to allow for referencing throughout the document. Literature is then summarised to determine ranges for the KDPs and finally available solutions are discussed.

### 2.6.1 Functional Requirements (FRs) and Knee Design Parameters (KDPs)

The first user functional requirement is to allow for a normal gait. This can be classified further as a need for comfort, stability, and a prosthetic that does not result in fatigue. The KDPs that result from this are respectively lightweight, stance-phase stability, swing-phase initiation and toe clearance to reduce tripping (Mohd 2014; Andrysek 2009). Additionally, the ERs are considered, stiffness adjustment (ER3) is analysed in more detail, it is noted as a knee-specific design parameter KDP7.

It is recommended to design a prosthetic leg that has more mass at the knee rather than at the ankle to allow the knee to swing forward easily. The centre of gravity of the leg will be closer to the body and therefore easier to control. Therefore a lightweight knee is not a high priority KDP. (Thompson 2002) (KDP3)

Toe clearance is important to prevent tripping, the larger the toe clearance the less likely the chances of tripping are. The addition of toe clearance also improves gait by reducing asymmetrical behaviour in which a patient would adjust their gait to prevent the toe from hitting the floor, such as hip hiking, vaulting or circumducting (KDP4). An asymmetrical gait can result in muscular pain, particularly in the hip joint (Ngan 2015; Radcliffe 2003; Andrysek 2009). Toe clearance is affected by the trajectory of the lower-limb during the swing-phase which is defined by the knee and hip kinematics in relation to the ground. Toe clearance is also affected by the alignment of the knee as shown in Table 6 as well as the design of the prosthetic knee. No specific data on the amount of toe clearance has been found, however, providing as much as possible will improve the gait (Andrysek 2009). A four-bar prosthetic knee design has the benefit of the knee shortening during the swing phase as seen in Figure 11, Section 2.6.4 (Greene 1983).

**Table 5: FRs and DPs for evaluating knee joints**

Functional requirements	Design Parameters	DP ref no.	Method of measurement	Units	Range	Rate
Allow for a normal gait. (Mohd 2014; Andrysek 2009)	Stance-phase stability	KDP1	Alignment- Zones of Instability	%	Ideal 55.8%	4
	Swing-phase control	KDP2	Allow smooth control during swing phase	N/A		4
	Lightweight	KDP3	Weight of all components, including adapters	g	130-369	2
	Toe-clearance	KDP4	Length of prosthetic in varying degrees of knee flexion	N/A	N/A	3
Adequate knee flexion (Andrysek 2009)	Maximum knee flexion angle	KDP5	Angle between thigh and shank when knee joint is maximally flexed	<sup>0</sup>	150-165	3
Sitting appearance (Andrysek 2009)	Thigh portion length	KDP6	Distance from centre of hip joint to knee cap while sitting	mm	Inline with the other thigh	1
Adjustability	Adjustability	KDP7 (ER3)	Allow for the changes in weight of the child			5

The maximum knee flexion of a prosthetic knee can affect the activities of the patient. A minimum of  $50^{\circ}$  is required for toe clearance during the swing phase (Schache & Baker 2007). However,  $120^{\circ}$  is usually considered to be a necessary minimum. According to Andrysek (2009), additional maximum knee flexion for children can enhance the functionality of the knee by allowing activities such as playing on the floor, therefore a maximum  $150^{\circ}$  or more is desirable (KDP5). The axis location of the knee design can affect the amount of knee flexion (Table 6). In general placing, the knee axis posteriorly helps to increase the maximum knee flexion. When the posterior alignment of the knee axis is done via a rotation, the maximum knee flexion is reduced.

**Table 6: Relationships between the DPs and the placement of the knee axis (single-axis) (Andrysek 2009)**

Design Parameter	Move axis posteriorly	Move axis anteriorly
Stance-phase stability (KDP1)	More, but more difficult initiation of swing-phase	Less, but easier initiation of swing-phase
Toe-clearance (KDP4)	Less	More
Maximum knee flexion angle (KDP5)	Increased	Decreased
Thigh portion length (KDP6)	Thigh may appear too long	Thigh less likely to appear long

Aesthetics (ER10) is an important factor in the design of a component. Though the knee can logically be covered by the user, aesthetics affect the perceived usability, satisfaction and pleasure in the component (Ngan 2015). Therefore it is important to not only design for stability and low-cost but also to ensure perceived effectiveness is achieved.

A market analysis was done to determine the available varieties of paediatric prosthetic knees on the market. The largest challenge determined in paediatric prosthetics are for the provision of compact and lightweight knees that can provide effective stance- and swing-phase control. A range of some of the KDPs can be determined from this market analysis, however, note that these designs are for much older children than the range designed for in this thesis. The larger values for the ranges of weight and total length are due to the more complex knees such as polycentric designs (Table 5).

The KDPs and ERs are scaled for analysis purposes for concept development. A scale of five is used, with five being highly important. The ERs for strength and manufacturability are rated five due to the effect on the main objectives. The KDPs and ERs for stance-phase stability, swing-phase control and durability are rated four due to their strong effect of achieving natural gait. Toe clearance and maximum knee flexion are rated three due to the effect other KDPs have on these. KDPs and ERs for lightweight, low-cost and locally sourced materials are rated two due to the strong effect other KDPs have on them.

The following chapters discuss the most important FRs which are stance-phase stability (KDP1) and swing-phase control (KDP2). Finally, existing designs of knee prosthetics are discussed.

## 2.6.2 Knee stability (KDP1)

One of the most important aspects of the knee is to provide stability when standing and during gait. The following section discusses methods to provide stability such as voluntary control, required hip flexion moment, initial flexion, alignment and stance-phase stability design.

The stability of the knee is affected by the effort required to flex the knee prior to toe-off, known as the hip flexion moment. Maximum voluntary knee control by the stump should be provided as this results in the smoothest and most effortless gait. The muscle action of the stump should be used, however, the stump should never approach the limits of its motion while the patient performs normal activities (Radcliffe 1955). The stump can also be aligned with initial flexion which will result in greater control of knee stability during the entire stance phase of the walking cycle. This design will allow for shock absorption and the reduction of the rise of the centre of gravity. This was done in the design of a 6-bar mechanism, the Otto Bock 3R60 prosthetic knee, in which the knee gradually flexes up to 15° during the stance phase thereby cushioning the impact of weight acceptance (Schmalz et al. 2002; Andrysek 2009).

To reduce buckling problems a technique is used known as alignment stability – this is when the axis of the knee is placed posterior to the centre line of the leg. This allows the ground reaction force from early to late stance to result in a large extension moment about the knee which then prevents buckling. This technique can delay the initiation of knee flexion during pre-swing to the beginning of swing phase which will make it more difficult to clear the foot from the ground. As can be seen in Table 6, the effect of the stance-phase stability, the toe clearance (KDP4), the maximum knee flexion angle (KDP5) and the thigh portion length (KDP6) are affected by this alignment. (Radcliffe 2003; Andrysek 2009; Ngan 2015; Narang 2013)

Knee instability diagrams are used to analyse the stability characteristics of different prosthetic knees. The stability of a knee is the function of the line of action of loads placed on the prosthetic knee, referred to as the load line vector. Load line vectors are combined from those which originate at the toe, creating a flexion moment at the knee axis; those that originate at the heel and cause a flexion moment at the knee axis; and those that pass through the knee axis and in between the toe and heel boundaries. Zones of instability can be seen in Figure 9, the smaller the zone of instability the better. From the figure it can be noted that the stability is lowest for a single-axis knee, improved in four- and six-bar knees and most stable in the Automatic Stance-phase Lock (ASPL) knee developed by Andrysek (2009). It has been determined that a small zone of instability of 55.8% is sufficient, a smaller zone will result in difficulty in the initiation of the swing phase (Radcliffe 1994; Ngan 2015).



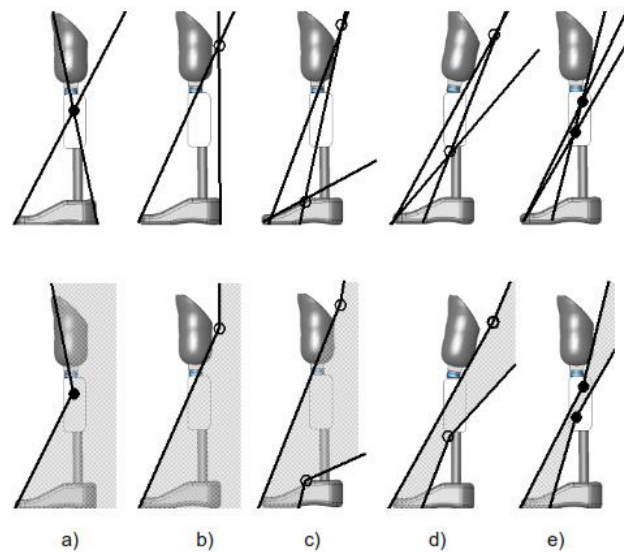


**Figure 9: Zones of instability for prosthetic knees: a) Single-axis knee; b) Four-bar knee; c) Six-bar knee, d) Six-bar knee during stance-flexion; and e) ASPL knee (Andrysek 2009)**

### 2.6.3 Swing-phase control (KDP2)

During the swing phase, it is important to limit the heel-rise (occurring during mid-swing) and ensure adequate deceleration of the shank during terminal swing. Poor control of the swing phase of the knee can affect foot clearance and thus increase the potential of tripping (Andrysek 2009). It is important to design a swing-phase control component that can be adjusted with respect to how much swing is required, this allows for patient-specific needs as well as the changes in need as a child grows older and more active (ADP7).

By designing a knee that has good swing-phase control a more natural gait will occur by helping the user control the duration of the swing phase. The swing-phase control has the following functions: (Ngan 2015)

- Limiting maximum knee flexion angle;
- Cause the shank-foot to swing forward smoothly in a manner similar to a normal knee;
- Allow the knee to extend smoothly into full extension without impact;
- Provide automatic changes in the level of the resistance patterns to allow walking over an extended range of walking speeds

Mechanisms to accomplish this include mechanical friction, fluidic damping and extension assist aids such as internal springs or external elastomeric straps (Ngan 2015). See Section 2.6.4 for a further discussion of types of prosthetic knee joints.

Mechanical friction is usually used in a single-axis type joint that swings in both flexion and extension. It is the simplest method to limit the maximum flexion angle during the swing phase, is low in cost, light, easily adjustable and requires little maintenance. The friction between the rotating parts interface limits the extension that is caused by the inertia of the swinging shank. The friction can be adjusted by tightening the bolt and bushing that applies friction to the knee. Due to the manual adjustment changes in walking speed not accounted for, a suboptimal swing phase performance can result. (Ngan 2015)

Fluidic damping control offers a better swing-phase control and can be designed to match the desired joint kinematic and kinetic curves closely, thus being a more effective mechanism for swing-phase control. This control is usually accomplished through hydraulic or pneumatic devices. These designs also allow for automatic adjustments to the changes in the walking speeds. These are, however, impractical for paediatric knees as they require a large amount of maintenance, and are larger and heavier than the mechanical friction alternatives. (Ngan 2015)

An extension assist mechanism is used to reduce the length of the swing-phase and energy expenditure by facilitating the extension of the leg. Mechanisms include mechanical springs or elastic band-type assistance. The inertia of the shank, which would naturally flex the knee during mid-swing is counteracted by the force applied by the extension assist. A dual spring system design can also be used, this utilises two different spring stiffness to better approximate the action of leg muscles during flexion and extension. It is important to use a compression spring which has a high spring rate and long life cycle so that the desired torque can be generated while ensuring reliability and durability of the mechanism. It is also important to design for a flexion stop feature so that the extension assist mechanism is protected when the knee is hyper-flexed. (Ngan 2015; Furse et al. 2011)

#### **2.6.4 Types of prosthetic knee joints**

Due to the cost of technical items such as power sources and actuators, prosthetic knee control is normally achieved passively through mechanisms such as dampers, brakes, locks and linkage mechanisms. Passive methods work well during level or downhill walking, however, it does make walking up inclines and stairs difficult due to the absence of torque (Andrysek 2009). The use of manual locking systems is advised if a child requires additional stability, however, by the

age of three-years-old, it is generally accepted for a child to have an unlocked knee (Myers 2016).

There are two types of prosthetic knee joints, monocentric and polycentric. A monocentric joint, also known as a single-axis joint, has the centre point at the anatomical location of the knee. When this type of knee has no additional stance-phase control the stability of the knee is accomplished through alignment stability and voluntary control of the hip muscles (Andrysek 2009). Monocentric joints include manual-locking knees, single-axis free-swinging knees and single-axis braking knees, shown in Figure 10. Examples of manual-locking knees are shown in Figure 10a) and b), Figure 10a) shows a model that is locked and extended during walking and can be unlocked and flexed when sitting. This type of knee is normally for older patients who are not able to control the knee when walking. The problem with this design is that it does not allow for any flexion at the beginning or end of stance. A normal knee will, on flat ground, flex up to 20° during the loading response to provide shock absorption and flex up to 40° during the pre-swing phase which allows for clearance of the foot from the ground. Finally, these knees do not allow for flexion during the swing phase. Figure 10b) can be used in the locked position (with the disadvantages as described above) or can be used unlocked in which case it becomes similar to a single-axis free-swinging knee. (Narang 2013)

The single-axis free-swinging knee is shown in Figure 10c), this knee resists flexion only through friction in the joint. Models can exist with a band in the front of the knee which can reduce the knee from flexing too far when walking. This knee has the disadvantage of no flexion at the beginning of stance, as with the manual-locking knees. This model also has the disadvantage that buckling can occur during mid-stance when the ground reaction force causes a flexion moment about the knee. The free-swinging knee does not allow for the leg to swing with appropriate timing, especially when walking quickly. (Narang 2013)

Single-axis braking knees (also known as a safety knee), lock when weight is placed upon it thus preventing flexion during most of the stance phase. However, similarly to an alignment stabilised knee, the braking knee can delay the initiation of knee flexion during pre-swing. Braking knees can also make sitting-to-standing and standing-to-sitting motions more difficult compared to the knees discussed previously. (Narang 2013)

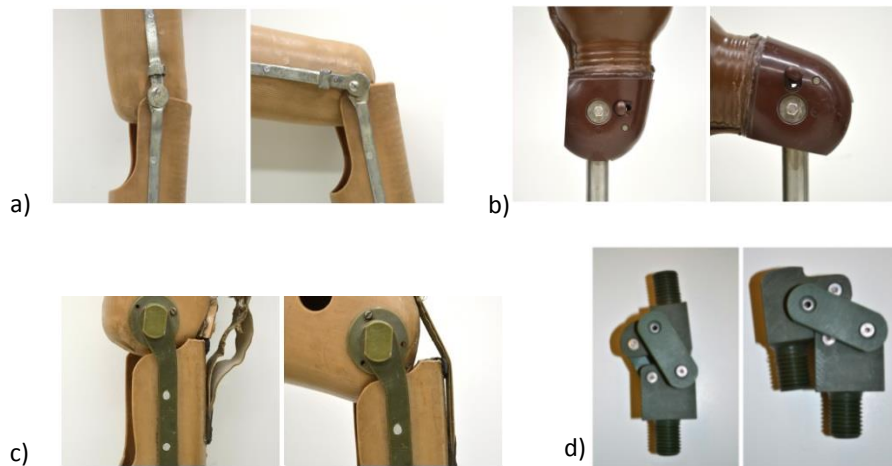


**Figure 10: a) BMVSS manual locking knee, b) ICRC manual locking knee, c) BMVSS single-axis free-swinging knee, d) Stanford-Jaipur knee joint, a polycentric knee, e) ASPL mechanism (Narang 2013)**

Finally, the four-bar knee is shown in Figure 10d). This knee is constructed as a four-bar linkage, with the centre of rotation changing as the link position changes. This allows for the centre of rotation to be behind the knee during stance – similar to an alignment-stabilized knee (Narang 2013). These knees are part of a broader category known as polycentric knees which also include six-bar knees. They address the stability concerns faced with a monocentric joint. The centre of rotation relocates as a function of the knee angle; thus enhancing the stability of the knee by ensuring a posterior centre of rotation when the knee is extended and a more anterior one when the knee is flexed (Andrysek 2009). The four-bar linkage system also increases the clearance of the foot during the swing phase. This is accomplished by the leg shortening during flexion as can be seen in Figure 11 (Greene 1983).

Radcliffe (2003) stated that

*“Four-Bar knees are not just a “safe” knee with improved security at heel contact. Their most unique feature, when properly applied, is the ability to provide conservation of energy by improved voluntary control of knee flexion during push-off”.*

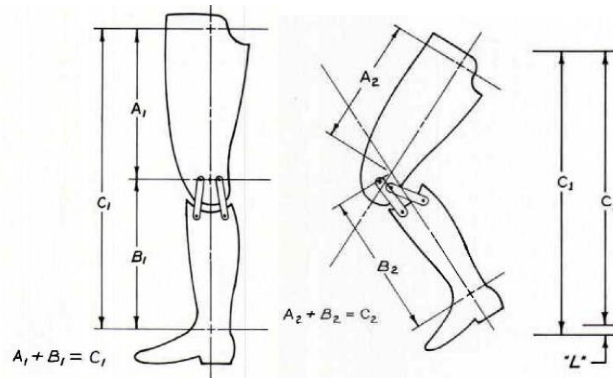


**Figure 11: The shortening of a polycentric knee (Greene 1983)**

A major disadvantage of a four-bar knee, however, is that they tend to be larger and heavier than a single-axis knee, this makes the design unsuitable for very small children. A single-axis knee design is a better alternative as they are simpler, more durable, lighter and lower in cost. (Ngan 2015)

A design that has similar stability characteristic to a four-bar knee is the ASPL knee, as noted in Section 2.6.2. The design involves a knee based on a lock that engages or disengages depending on the moment caused at the control axis, as seen in Figure 12 (Andrysek 2009). The design was later improved to become the AT-knee, sold by Legworks (2015) and has been further analysed by Ngan (2015) to develop a paediatric version, the PASPL knee. The PASPL knee was tested on five children, average age 10, and it was determined that less tripping occurred (compared to single-axis knees). Little maintenance was required for the less active children and a replacement of the extension bumpers was required every six months for the active children.

The ASPL design consists of two axes, shown in Figure 12, the knee axis and the control axis. The lock engages when a flexion moment is caused, this is due to the posterior alignment of the control axis with the GRF. The flexion moment is further increased by the use of a lock spring, this ensures stability in the stance phase. As the knee moves over the forefoot an extension moment is caused, this moment overcomes the lock spring force and allows the knee to become unlocked. The knee then enters the swing-phase. The ASPL knee has swing-phase control via mechanical friction with the use of shims. These shims can be adjusted, by tightening the screws, to result in a faster or slower swing (Andrysek 2009). The design was later improved by adding a variable friction controller (VFC) (AT-Knee for adults) (LegWorks 2016).

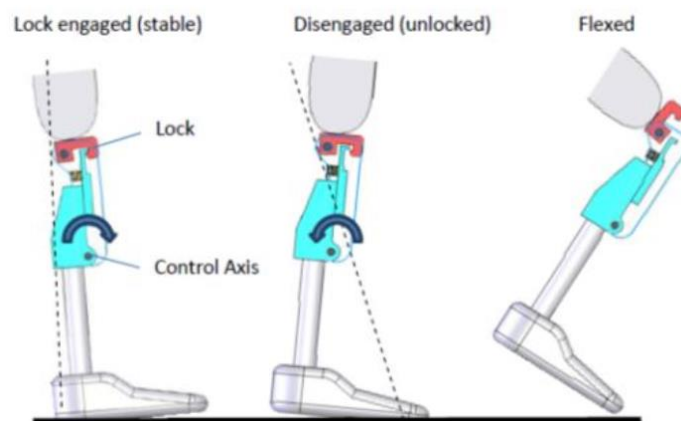


**Figure 12: Automatic stance phase lock (ASPL) mechanism (Andrysek 2009)**

## 2.7 Materials

Each component's material is chosen based on the design requirements for rigidity, strength, weight and the ability to handle fatigue (Radcliffe 1955). Though lightweight components are part of the design parameters for each prosthetic component discussed in Sections 2.4.1, 2.5 and 2.6.1 it is necessary to ensure that they are within the strength requirement range for each design component. The material characteristics of metals and plastics are summarised in Table 15.

Though a lightweight prosthetic has the advantage of reducing the energy requirements in gait, too light a component can cause problems with control of the prosthetic. When too light it can be difficult to control the swing phase as the inertial forces required to stop the swinging limb increases, this will, in turn, offset the energy saved in generating the motion. An unequal limb weight will also result in gait asymmetry due to the different centres of mass and the mass moments of inertia. (Selles 2002)

When the heavier masses are nearer to the knee the effect of additional mass is reduced. Increasing the mass nearer to the torso increases the stride time and single limb stance, which allow for more stability (Selles 2002). Therefore, in the design of individual prosthetic components, components that are further from the torso should be ideally lighter than those closer.

### 2.7.1 Metals

To ensure that a material is strong enough, it is necessary that the stresses experienced are smaller than the ultimate tensile and shear strength

respectively. When aluminium is analysed the Von Mises stress must be smaller than the fatigue strength which corresponds to  $50 \times 10^7$  completely reversed cycles. When steel is analysed the fatigue life is determined based on the ultimate tensile strength, yield strength and method of manufacture. (Budynas & Nisbett 2011)

Carbon fibre and fibreglass are lightweight materials that have energy storing capabilities. The material properties are anisotropic – having different properties in different directions, and involves layering of between 30 and 90 sheets to the required shape. These materials are expensive and require extensive computer analysis and mechanical testing. Due to the expensive nature of this material, it will not be considered in further detail. (Klasson 1995; Ossur 2016a; McHugh 2007)

If a material does not require high strength values, plastics can be considered. According to Ceri (2013), most designs in the developing countries use thermoplastics as the main material component. Thermoplastics have relatively low bulk cost, are easy to machine, have low friction low abrasion and low wear properties (with respect to density values). Thermoplastics are also recyclable to be reused in joints.

Thermoplastics include high-density polyethene (HDPE), nylon and oil-impregnated nylon (known as Oilon). HDPE has low wear properties but due to its high yield strength and low cost, it is often used in prosthetics. It also has excellent corrosion resistance and has favourable failure modes – it tends to rip rather than shatter. Nylon 6 has good strength and wear properties, it is highly abrasion resistant which is an ideal property for environments with large amounts of dust and dirt (Ceri 2013). Oilon is used in the Remotion Knee (D-Rev 2015). These nylons are used for unlubricated, highly loaded and slow moving parts. The nylon is blended with a non-drying lubricant that increases the nylon's sliding benefits. (Bay Plastics Ltd 2016)

3D printing commonly uses ABS or PLA to print out a design or prototype, it allows for more possibilities with respect to the design shape and does not involve a large amount of manufacturing time. ABS and PLA have much lower strength factors when compared to metals, as such, it is important to ensure that these materials can handle the required forces. (Otto 2014)

## **2.8 Safety considerations**

A prosthetic leg can injure the individual if a part fails which can lead to injury or prolonged muscle problems if the part is not fixed as soon as possible (Castellanos et al. 2016). A lower limb prosthetic device is classified according to

the FDA as class I - this means the device is deemed to have a low to moderate risk and only requires general controls. General controls are described as ensuring notification and recording procedures are followed as well as making provisions for custom devices (FDA 2016).

According to the ISO 10328 standard for adult prosthetics, the proof strength, ultimate strength, fatigue strength, static strength in torsion and security against slippage of clamped components should be tested to ensure the strength of the prosthetic is adequate. Appendix B discusses further methods to adjust these strength tests according to the ISO 10328 standard for children.

Testing is ideal when it can be done on individuals, however, it is important to ensure that the component is safe to use prior to testing on a patient. Therefore a test procedure is considered in Section 5 to test the prosthetic leg's gait characteristics mechanically prior to patient testing.



## 3 Concept Design

The concepts for each component of an above-knee prosthetic leg are considered. This is done with consideration for the engineering requirements determined in Section 2.3 which are adjustability (ER1-ER4), use of locally sourced materials (ER6), manufacturability (ER7), low cost (ER8), safe (ER9), cosmetically appealing (ER10) and allow for the use of standard products (ER11). The design parameters (DPs) determined in Sections 2.4.1, 2.5 and 2.6 are considered for the respective component. The detailed design considers whether the final design can be adjusted to ensure the lifespan of three years (ER5). Designs are discussed, are rated according to a scoring system determined in the literature review and then a final design is chosen.

### 3.1 Foot and ankle

The functional requirements (FRs) and design parameters (DPs) for the foot and ankle prosthetic are to achieve a natural gait, be small enough to fit into a shoe and allow for growth adjustment. Table 7 summarises the ADPs and ERs determined in Section 2.4.1 to achieve these FRs along with the scoring for each concept. (All ADPs are with reference to Table 2, in Section 2.4.1)

Concept designs were made by considering simplicity (ER7, ER8), allowable movement and available solutions. Two main designs are considered based on the SACH foot and the single-axis foot. Designs that consist of too much complexity, such as a carbon fibre foot, are not considered here. Additionally, designs are considered for length adjustment and adding additional dimensions for movement. The design options can be found in Appendix A.3.

An adjustable prosthetic foot design has been considered by Castellanos et al. (2016). It was determined to be complex and difficult to manufacture the product due to breakages. The team considered methods that could adjust the foot's length as the child grew older, however, did not consider alternative ankle designs.

**Table 7: Ankle rated concept designs according to ADPs**

Selection criteria (ADPs)		Rating	Concept design options	
			1	2
ADP1	Lightweight	4	2	2
ADP2	Shock absorption	3	1	2
ADP3	Activity level	3	0	2
ADP4	Ankle stiffness	4	1	2
ADP5	Small	5	2	2
ADP6/ ER2	Adjustability	5	2	2
ER4	Strong	5	2	2
ER5	3-year lifespan	4	2	2
ER6	Locally sourced materials	2	2	2
ER7	Manufacturable	5	2	2
ER8	Low cost	2	2	2
Total score		84	71	84

*Key for Table 7: 0 = not achieved, 1 = achieved but requires design considerations, 2 = achieved*

### 3.1.1 Design Option 1: SACH foot (Figure 42)

The SACH foot, shown in Figure 8a), is a simple design consisting of an inner keel with no moving parts. As a result, it is easy to manufacture and maintain, thus it is a low-cost design (ER7, ER8). The base material can be chosen such that it is sturdy yet has some flexibility to allow for smooth rollover when walking while ensuring a lightweight, low-cost component (ADP1, ADP4).

This design has few shock absorption abilities, this is due to only the foot deflection absorbing some of the shocks (ADP2 moderately affected). A shock absorption device can be added to the component, however, this will affect the overall cost and weight (ER8, ADP1 highly affected). The SACH foot is recommended for a very low activity level, K0, as noted in Table 3 – this does not allow for the required activity level, K3 to be achieved but design considerations can be made to increase the flexibility of the footplate to increase the activity level (ADP3 not achieved). As can be seen in Table 7, design option one has a total score of 71 out of 84.

### 3.1.2 Design Option 2: Single-axis foot (Figure 43)

A single-axis foot design can be seen in Figure 8b), this design involves a hinge joint which allows for up and down movement which enhances the stability of

walking in comparison to design option one (ER9). This design is similar to design option 1, in that it is relatively simple resulting in an easy to manufacture, thus low-cost design (ER7, ER8). The single axis foot would be similar in weight to the SACH design as the SACH design requires a metal component to handle the cyclic forces (ADP1).

The addition of a hinge joint increases the activity level of the prosthetic to between K1 and K2. The stiffness of the joint can be adjusted as required by adding a torsion spring of the required ankle stiffness as discussed in Section 2.4.1. The addition of the torsion spring will improve the shock absorption and increase the activity level to the range of K2-K3 (ADP2, ADP3, ADP4). The addition of a moving joint, which improves the activity level, increases the complexity of the design and may require maintenance to ensure that the hinge moves as required (ER8 moderately affected).

As toddlers grow older, becoming heavier, they require less stability and are likely to want to increase their activity level – this increase in weight will result in flexing the joint more easily. This means that it is possible to have a joint that adjusts to the changing weight and activity level with no actual adjustments required. However, with this design, it is possible to adjust the stiffness of the ankle by changing the torsion spring to a stiffer one (ADP4). As can be seen in Table 7, design option two has a total score of 84 out of 84.

### **3.1.3 Adjusting the length of the foot (Figure 44, Figure 45 and Figure 46) (ADP6)**

The requirement for adjustability states that a total adjustment of 22 mm is necessary (Table 2). These are approximate values as every child is different and additional shorter or longer length requirements should need to be considered. It is also important to remember that designing an adjustable foot involves the design to improve the lifespan of the product and therefore the foot must be made of a material that can last this extended amount of time.

The foot can be adjustable either through the metal component and foam surroundings or only the foam surrounding (resulting in a shorter metal part for the toe area as the child grows). It is noted that the normal heel-to-toe gait pattern is usually only reached by the age of five years and therefore complete rollover should not be the main priority, only balance (Cummings & Kapp 1992).

The first option is the use of padded socks or padded straps to lengthen the foot (Figure 44). The padded sock adds thickness to all sides of the foot whereas the 'toe-strap' adds toe length and some of the width required. The additional side view shows the padding going underneath the metal of the keel to improve rollover. Perfect rollover will not be achievable – due to the foot adjustment

being only 22 mm this should not cause extreme problems. These designs are simple and cost effective (ER7, ER8). The consideration with regards to what the padding is made of is important to ensure that sturdiness and lifespan are achieved (ER9).

The second option for length adjustment is through the use of a sliding mechanism (Figure 45). This design will result in an initially very stiff design which will become increasingly easier to damage as it is extended. The railings would also result in a higher stiffness than if no railings were considered. This is a complex design with movable parts and therefore is not an ideal design. Castallanous et al. (2016) considered designs of a foot length adjustment that included a pin based plantar extension, a threaded plantar extension or a slider-notch based plantar extension.

The final option shows replacing of the flat component (Figure 46). This concept is simple, has no moving parts and ensures smooth rollover (ER7, ER8, ER9). This design also allows for different materials to be used for the foot plate to adjust for the child's activity level. The design will require a visit to the prosthetist or training with the parents to ensure the foot component is adjusted correctly. With this design, the lifespan requirement is shortened to only a year (ER5).

#### **3.1.4 Additional considerations: Adding another dimension**

Adding additional dimensions mechanically can add to the complexity of the design, however, shoe soles such as the Nike auxetic tri-star outsole pattern as seen in Figure 47, Appendix A.3, allows for flexibility which allows the foot to stand on slightly uneven terrain as well as improving the grip. (Nike 2016)

#### **3.1.5 Final design**

Each design was given a score based on the ADPs and ERs each having a weighted value (discussed in Section 2.4.1), from this, it can be seen that design option 2, the single-axis foot has the highest score and thus the best design. It is the most feasible design, allowing all ADPs and ERs to be reached (ER6, ER8, ER9, ER10, ER11 and ADP5 will be ensured in the design stage).

Ensuring the correct length of the foot is important for balance. The padded socks are simple to manufacture but can result in poor rollover and can cause difficulty in walking if not attached well. The use of straps can also cause difficulty in putting on a shoe. The sliding mechanism is complex and increases the likelihood of the system breaking. Finally, the replacement concept is relatively simple to manufacture and allows the prosthetist to change the material of the foot if more or less stiffness is required. Therefore the best foot adjustment method is the foot replacement concept.

## 3.2 Pylon

As determined in Section 2.5, the FRs and DPs for the pylon are to achieve a natural gait, allow for height adjustment and be cosmetically appealing. The design options are discussed according to the pylon design parameters (PDPs) summarised in Table 8 to determine the most feasible design. Each concept design is focussed on adjustability (PDP3) and figures of the concepts are in Appendix A.4.

**Table 8: Pylon rated concept designs according to PDPs**

Selection criteria (PDPs)		Rating	Concept design options			
			1	2	3	4
PDP1	Lightweight	4	2	1	2	2
PDP2	Shock absorption	1	0	1	0	0
PDP3/ER1	Adjustability	5	2	2	2	2
PDP4/ER10	Smooth	4	0	2	2	2
ER4	Strong	5	1	2	1	0
ER5	3-year lifespan	4	1	2	1	0
ER6	Locally sourced materials	2	2	2	2	2
ER7	Manufacturable	5	2	2	1	1
ER9	Low cost	2	2	2	0	2
Total score			45	59	44	39

*Key for Table 8: 0 = not achieved, 1 = achieved but requires design considerations, 2 = achieved*

The use of paediatric growth plates exists such as those made by WillowWood (2016) to prevent the need to have to buy new components. The P-POD growth plates can be stacked on top of one another, however, should not exceed 22 mm which is less than the PDP for adjustability of 50 mm. A design can be developed to use the growth plate concept however it is not recommended to use components that can be easily lost when toddlers are involved.

### 3.2.1 Design Option 1: Based on crutches (Figure 49) or a pin (Figure 50)

This design involves overlapping rods that can be adjusted to a new height based on predefined holes which are pinned into place. With this design, the force will be concentrated onto the pins. This force can be reduced by having more than

one pin by using a crisscross pattern as seen in the figure – this will distribute the forces more evenly but more holes will be required. The holes can result in buckling of the pylon as they will be required to be closely spaced for the adjustment requirements (ER4 affected). This design involves removable components which are not recommended for children (ER9 affected), the pins will also result in difficulty in applying clothes (PDP4 not achieved). This design scored 45 out of 65.

### **3.2.2 Design Option 2: Clamp design (Figure 51)**

This design is based on the seat post of a bicycle. The design involves overlapping rods which are clamped together to the required position. This design allows for easy adjustment to any length. It would be important to ensure that the clamp can be tightened enough to ensure that the device is safe (ER9). The analysis will be required that the shafts are strong enough to be clamped and to ensure no buckling occurs when clamped (ER4). This design will result in a more distributed force than the pin design.

This design is relatively simple and cheap to manufacture (ER7, ER8). Bicycle posts can be used if shock absorption is required and offer a variety of light shafts (PDP1, PDP2). Alternatively only the bicycle clamp collar can be purchased and rods can be used for the leg. A clamp will not have any parts that would result in difficulty when dressing (PDP4). This design scored 59 out of 65.

### **3.2.3 Design Option 3: Screw designs (Figure 52 and Figure 53)**

Kinetic Revolution (2016) use an adjustable pylon design (Figure 52), these pylons can only adjust by a total 28 mm which is not enough for three years of a toddler's life. These components are also expensive at \$550 which does not allow for a low-cost design. (Kinetic revolutions 2016) (ER1, ER8 not achieved)

Instead, a screw design concept can be used as shown in Figure 53. Precision will be required to allow the leg to be adjusted by 50 mm in total (see Table 14) via a screw system. The screw system is similar to the pin design in that the leg height would be adjusted in increments. The screw design can be adjusted as shown in Figure 53 to have a fine adjustment screw section and a larger adjustment screw section – this can allow for more fine adjustments but does result in a more complex design (ER8 highly affected). It must also be ensured that the screw system does not loosen when walking (ER4, ER5, possibly unachievable). This design scored 44 out of 65.

### **3.2.4 Design Option 4: Key/slot design (Figure 54)**

This design involves the use of a slot that tightens two beams together at the required length. This design allows the component to be adjusted to any length. More bolts can be added to the component to reduce the load on each bolt (ER4). This design involves a simple manufacturing procedure and few components (ER7, ER8). It can make use of a flat or round pylon as shown in the figure depending on the required strength. Though toddlers do not have a large amount of weight, a key joint can become loose due to out of plane stresses (ER4, ER5 possibly unachieved). This design scored 39 out of 65.

### **3.2.5 Final design**

Each design was given a score based on the PDPs having a weighted value (discussed in Section 2.5), from this, it can be seen that design option 2, the clamp design has the highest score and thus is the best design. This design allows most PDPs to be reached as can be seen in Table 8, the design will be analysed in Section 4.2 to ensure that the strength (ER4) and lifespan (ER4) requirements are met.

As can be seen in Table 8 this design does have a score of 1 for lightweight and shock absorption, this is dependent on the detailed design stage in which strength requirements will be determined. Shock absorption can be resolved by a shock absorption component such as the MiniShock component by Fillauer LLC – this depends on weight and cost of the overall design. As stated in Section 2.5, this is not a high priority PDP as it does not have a large effect on walking (Fillauer LLC 2016; Gard & Childress 2001).

## **3.3 Knee**

As determined in Section 2.6.1, the FRs for the prosthetic knee are to achieve a natural gait, ensure adequate knee flexion, be cosmetically appealing, and be adjustable with respect to stiffness. The design options are discussed according to the knee design parameters (KDPs) and scored according to the ratings of the KDPs (Table 9). The final knee design is then chosen based on these scores.

**Table 9: Knee rated concept designs according to KDPs**

		Concept design options				
	Selection criteria (PDPs)	Rating	1	2	3	4
KDP1	Stance-phase stability	4	1	1	2	2
KDP2	Swing-phase initiation	4	2	1	2	2
KDP3	Lightweight	3	2	2	1	1
KDP4	Toe-clearance	3	0	0	2	2
KDP5	Maximum knee flexion angle	3	2	2	2	2
ER4	Strength	5	2	2	2	2
ER5	3-year lifespan	4	1	1	2	2
ER6	Locally sourced materials	2	2	2	2	2
ER7	Manufacturable	5	2	2	1	2
ER8	Low cost	2	2	2	1	1
ER10	Aesthetics	1	0	2	2	2
Total score			54	52	61	66

Key for Table 9: 0 = not achieved, 1 = achieved but requires design considerations, 2 = achieved

### 3.3.1 Design Option 1: Single-axis with spring (Figure 56)

The first design is based on a single-axis knee with mechanical friction and spring-assisted extension (KDP2). The hinge joint, as well as the spring, can be designed according to the amount of friction and movement required (KDP7). The knee can be locked if required, which will allow a toddler to walk without knee movement (KDP1, ER9). This is a simple design (ER7) however, it requires energy to bend the knee open. The knee is also unstable which can be improved through alignment (KDP2 low). This design can result in difficulty with sitting as forces are required to bend the knee (KDP6 low). The knee does not allow for foot clearance (KDP4 low) and thus it must be ensured that the design does not have too tight a spring so that the knee is prevented from closing too early. This knee design has a score of 54 out of 70.

### 3.3.2 Design Option 2: Single-axis free swinging knee (Figure 57)

This design involves a hinge joint with a band to prevent the knee from too much extension, only the tightness of the hinge joint can be adjusted to adjust the amount of swing (KDP2). This design also has a locking mechanism by using a band in the front if it is desired to have the knee locked when walking (KDP1, ER9). Similar to design option 1, this design does not allow for toe clearance (KDP4 low). Though this design is simple (KDP3, ER7, ER8), it does not allow for



stability control (KDP1 low). Alignment of the prosthetic can be considered to improve the stability. This design scored 52 out of 70.

### **3.3.3 Design Option 3: Polycentric knee (Figure 58)**

The third design is based on the Remotion knee (D-Rev 2015) and the design methods discussed by Greene (1963). This knee maintains stability (KDP1, as noted in Section 2.6.4) and allows for toe clearance (KDP4). The design has an increased number of moving parts, therefore, it is more complex than the previous designs (KDP3, ER7, ER8). The movement of the knee is nonlinear, which is difficult to accurately design. According to Radcliffe (1955), a four-bar knee is a heavy design which is not recommended for paediatric users. This design scored 61 out of 70.

### **3.3.4 Design Option 4: PASPL knee**

The Paediatric Automatic Stance Phase-Lock (PASPL) knee is discussed in Section 2.6.4. It consists of two axes, the knee axis and the control axis, which allows for a lock to engage when in the stance phase thus improving the stability of the knee (KDP1, ER9). The knee design makes use of mechanical friction through the use of shims and an extension assist spring to allow for swing-phase control (KDP2). The mechanical friction can be adjusted through the tightening of bolts and the extension assist spring can easily be changed if a stiffer spring is required, allowing for adjustability. It was determined by Ngan (2015) that the adjustment of the friction is a concern as the screws can come loose, it was recommended that the design should rather incorporate disc springs between the screw cap and the body component on both sides – this applies a tension force between the screw cap and the screw which could potentially prevent the screws from coming loose. This design scored 66 out of 70.

### **3.3.5 Final design**

Each design was given a score based on the KDPs having a weighted value (discussed in Section 2.6.1). From this, it can be seen that design option 4, the PASPL knee, has the highest score and thus is the best design. This design allows most KDPs to be reached as can be seen in Table 9. KDP for lightweight (KDP3) does require further evaluation in the design stage. Though it is clear that design options one and two are easier to manufacture, designing a knee that has improved stability is important when toddlers are considered as this improves their overall safety (ER9).

## 4 Detailed Design

The final design of each prosthetic component is chosen according to the FRs and DPs, iterative calculations are then done to ensure that each DP is met. In this chapter, the calculations are discussed followed by a discussion with respect to finite element analysis. Table 22 in Appendix C summarises the calculation results, only the final and maximum results are shown. All calculations are done with respect to a weight of a child of 20 kg to allow for safety factors. The final prototype design is shown in Appendix A.6, Figure 27.

A pyramid adapter, seen in Figure 55, is used to connect prosthetic components to one another. Set screws are used to tighten the female component to the male component. The purpose of this design is to couple the components and allow for minor adjustments but not significantly increase the length. A large variety of these components exists allowing for different types of attachments to each component to be possible. By using a pyramid adapter to connect each prosthetic component the design will be modular allowing for use of standard components (ER11). (Haun 2012)

### 4.1 Foot and ankle

As discussed in Section 3.1, the final concept design chosen was the single-axis foot. The final design can be seen in Figure 13, with the parts list in Appendix A.6 Table 16. In this section the design decisions based on calculations are discussed, the results are summarised in Table 26 in Appendix C with respect to the ADPs. The calculations can be found in Appendix C.1 with results summarised in Table 22. This discussion is followed by a Finite Element Analysis (FEA) of the hinge joint.

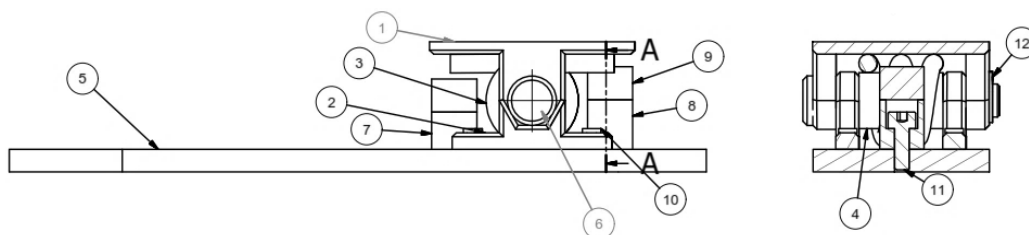


**Figure 13: Final foot and ankle design**

#### 4.1.1 Design decisions based on calculations

The design of the hinge joint dimensions required first the design of the torsion spring to replicate the ankle stiffness of the foot. This is due to the size requirements of bending the spring material. From literature, it was determined that a stiffness of slightly less than 858.7 Nmm/° would be adequate for paediatric prosthetics. The smallest feasible spring had an external diameter of 22.5 mm, and an internal diameter of 18 mm with a stiffness of 808.6 Nmm/°. This stiffness was smaller than the desired stiffness but allows for the much lower weight of the desired age range of three to five years. The maximum spring moment was determined to be at an angle of deflection of 16°. (Shamaei et al. 2011; Liu et al. 2008) (ADP4)

Following the spring design, it was necessary to ensure a lightweight design (ADP1), furthermore, the design was required to use locally sourced materials (ER6) and be low in cost (ER8). It was also necessary that the final design is strong (ER4) and durable to have a three-year lifespan (ER5). The final dimensions of the ankle joint were determined based on hinge joint calculations to ensure that the crushing failure, bending failure, tensile failure and shear failure would not occur in the components, see Appendix C.1 (Machine Design 2014). For the hinge joint, an 8 mm pin was determined strong enough. However, due to the inner diameter of the spring which is 18 mm, a PVC cylinder was used as a spacer around the pin to ensure a lighter hinge joint, while still ensuring the spring moves along the pin (ADP1). The strength analysis results of the hinge joint calculations are summarised in Table 22, the smallest safety factor was for bending failure of the pin at 8.59, therefore, this design has high safety and strength factors (ER4, ER9). The size of the top plate was designed so that it would be large enough for a junior Ossur paediatric prosthetic adapter (four-hole male) to be fixed on top (ER11) (Ossur 2016b). The final design has an activity level of between K2 and K3 (ADP3).

The footplate was analysed with respect to the strength of the foot during heel-strike, flat-foot and toe-off. The calculations can be found in Appendix C.1. The heel-strike analysis considers the total energy that would be absorbed by the spring during heel-strike and therefore how much would be required to be absorbed through the use of bumpers. Plantar flexion and dorsiflexion bumpers were considered according to the minimum deflection of 19.57 and 8.77° respectively, Section 2.2. The ideal stiffness for the bumpers was then determined to be 211.75 N/mm and 91.89 N/mm respectively. This was a low stiffness and could not easily be found for the design, therefore the bumpers were manufactured from silicon buttons and were glued to the top plate so that the foot plate can still be removed easily (ADP2, ER2).

The footplate was then analysed for foot-flat to toe-off, this was done by assuming that the aluminium toe was a fixed support and a moment was created by the body weight along the foot length (Rush 2016). The final thickness of the footplate was determined to be 6 mm, this ensured that the component would have the required strength and deflection. The Von Mises stress was determined to be 129.28 MPa which is larger than the fatigue strength of aluminium of 138 MPa for  $50 \times 10^7$  cycles of completely reversed stress, therefore the desired life cycle of  $2.37 \times 10^7$  cycles is feasible (Budynas & Nisbett 2011)(ER5). The deflection of the footplate was determined to be 6.07 mm (ADP2). The footplate was laser cut to allow for the smooth curves of the final shape which can then easily be placed inside a foot cover (ER7).

The final dimensions of the foot and ankle prosthetic can be found in the parts list in Table 16, Appendix A.6. The final prosthetic foot weight, including the weight of the adapter, is 227 g, this is smaller than the range determined for foot weight in Section 2.4.1. This lower weight will improve the overall weight of the component.

It will be important for the installation of the prosthetic leg to ensure that the ankle is aligned to ensure stability. According to Radcliffe (1955), the keel should be in line with the GRF vector as the leg does not move then and the prosthetic is stabilised.

#### **4.1.2 FEA analysis**

The FEA model is shown in Figure 14, this model was developed in Patran 2014 by Plotz (2016). FEA was done on the ankle component for solid meshes and for shell meshes. The results from these separate tests had similar outputs. Solid component designs were made with a quadratic tetrahedron (Tet10) mesh and shell component designs made use of IsoMesh Quad4, a quadrilateral plate with membrane-bending behaviour. The element size was chosen to ensure that the thinnest area on the solid had no less than a double layer. The quality of the mesh was ensured by using this element size along the remainder of the mesh to ensure that the element sizes remained relatively constant as well as ensuring symmetry when holes occurred in the solid. The total node count for the ankle FEA was approximately 40000.

The model in Figure 14 consists of a linear spring at each bumper location to simulate both the bumper as well as the torsion spring at both locations. Boundary conditions were placed on the ankle component to ensure no rigid body motion. This means that no movement in the x, y, z as well as rotation in these axes was prevented on the lower components to imitate the foot plate below. The load was then applied replicating the weight of a 20 kg child (added weight for safety, see Table 14) on the top of the ankle component as a pressure

force to ensure even distribution along the component. The pressures applied in this analysis can be seen in Figure 15, these are calculated based on the total weight which would be applied when the patient is standing on both legs onto the top of the ankle component. The model consists of the materials as seen in the parts list, Table 16, in Appendix A.6. All scales in FEA figures are in base units (Pa, m) and the results are summarised in Table 23, Appendix C.

The FEA results are compared to the results from analytical results. Where the FEA results have higher stresses than the analytical results discussions are made to ensure the manufacture of the component with a stronger material. It is necessary to apply ISO strength tests before testing on the patient as a final validation of the FEA results (See Appendix B).

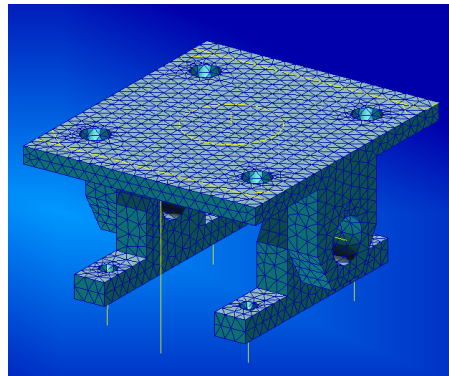


**Figure 14: FEA model of ankle joint (Plotz 2016)**

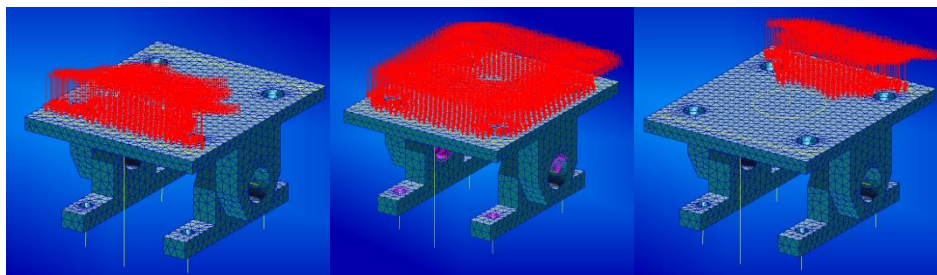


**Figure 15: FEA how forces are applied, a) Front pressure (467 kPa), b) Centre pressure (117 kPa) and c) Back pressure (467 kPa) (Plotz 2016)**

Figure 16 shows the fringe plot of the Von Mises stress when a centre pressure is applied. As seen in this figure the maximum stress is 24.7 MPa at the connection of the top and bottom hinge joints. The maximum is located at only one side due to some inaccuracy of pressure application points. As summarised in Table 23 (Appendix C) the Von Mises stress maximums for a front and back loading are 110 and 112 MPa respectively. These stresses are acceptable due to the components being made out of aluminium which has a fatigue strength of 138 MPa (Table 15, Appendix A.2). Design adjustments can be made to reduce the stress concentrations. These include the use of a washer placed between the components to reduce wear as well as designing the components to have smooth curves to reduce stress concentration points as shown in Figure 17. These design adjustments will reduce the stress concentrations at these connection points.

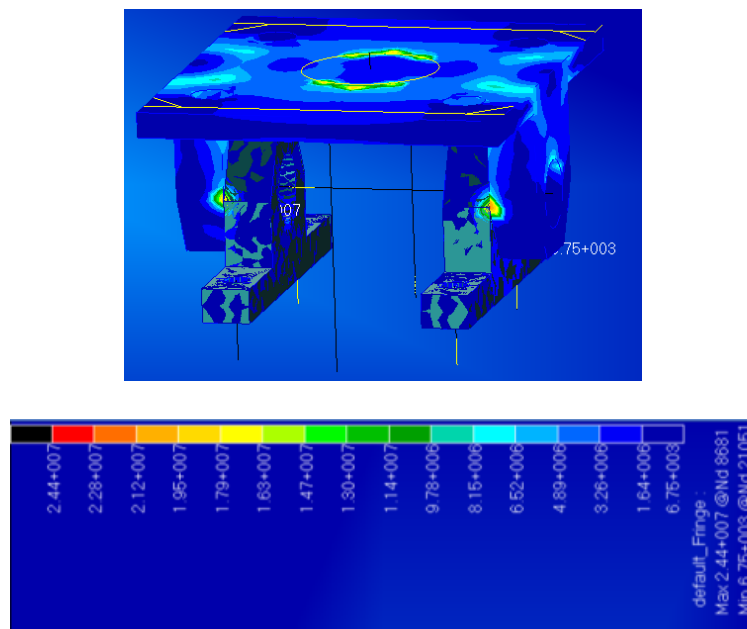


**Figure 16: Fringe plot of Von Mises stress when centre pressure is applied (Plotz 2016)**

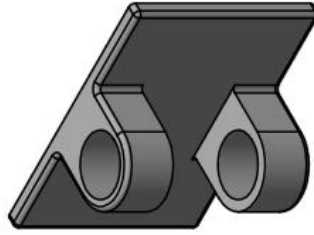


**Figure 17: Design adjustment of hinge joint to reduce stress points**

The maximum displacement occurs when front loading is applied as can be seen in Figure 18 at 0.0643 mm, this is a very small displacement and is likely due to springs that are simulated to have too high a stiffness. Due to modelling constraints, it will be necessary to see how these components realistically deflect. As can be seen in the figure, the displacement is not symmetrical, this is likely due to a slight asymmetrical placement of pressure points. This has not been adjusted for as it is more likely that a pressure will be applied with some asymmetry rather than with perfect symmetry.

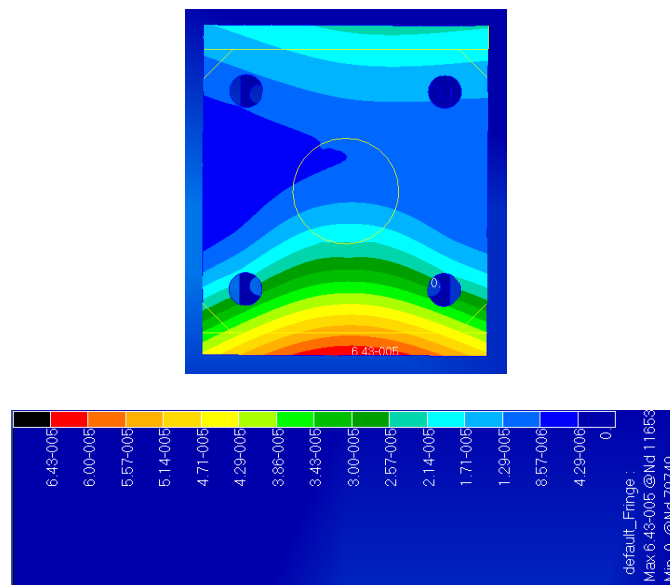


**Figure 18: Fringe plot of translational displacement when front pressure applied (Plotz 2016)**

## 4.2 Pylon

In Section 3.2.5, the final concept was chosen to use a clamp design. This section discusses the design procedure and strength analysis with regards to the shank pylon design parameters (PDPs) determined in Section 2.5 and summarised in Table 4. The final design can be seen in Figure 19 a), b) and c) with the parts list found in Appendix A.6 Table 17. The PDPs results are summarised in Table 13 in Appendix C. The femur was not analysed as the lengths are dependent on the individual's socket.

### 4.2.1 Design decisions

As discussed in Section 2.5, it would be ideal to use existing prosthetic adapters for the design of the prosthetic components to allow for standard components to be attached to the design (ER11). The pylon design was therefore constrained to the size of junior clamp prosthetic adapters which have an internal diameter of 22 mm (Ossur 2016b). This size requirement affected the choice of a clamp. A bicycle clamp could not be found for a 22 mm shaft, therefore another clamp was purchased with no shock absorption, with a weight of 105 g (PDP1) (PDP2: low to none). The clamp chosen ensures that there will be no difficulty when putting on clothes as there are no protruding parts (PDP4).

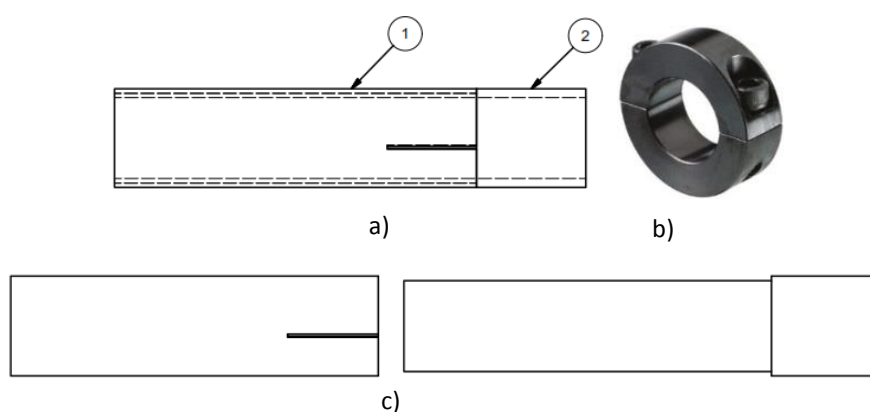


**Figure 19: Final pylon design a) Components overlapping, b) Clamp, c) Components separated**

It was initially desired to have the overall length to allow for 50 mm adjustability for the height difference of the leg up to the knee (PDP3) (Table 26 in Appendix C). However, due to size constraints of the height of the ankle; the size of the knee; and 25 mm of length for each junior adapter, this was determined



unfeasible. The final design has a 45 mm adjustment ensuring a minimum overlap of 36 mm according to Saint Venant's principle (Budynas & Nisbett 2011). This is within the range of 10 mm mentioned by Friberg (1984), the remaining 5 mm can be adjusted for through the use of growth plates for the older age group (WillowWood 2016).

#### **4.2.2 Analysis results**

The deflection, strength and fatigue of the pylon design were analysed by considering two overlapping rods, fixed at one end, with the moment caused by the weight of the child along the leg being applied to one side. See Appendix C.2 for these calculations. The inner tube is designed to have a thinner rim to allow for overlapping as can be seen in Figure 19c). The final material was chosen to be an aluminium pipe, see Table 17 (Appendix A.6) for the parts list, with thicknesses 2 mm for the inner component and 1 mm for the outer component (ER8, ER6). As can be seen in Table 22 (Appendix C), the maximum deflection of the shank was 0.28 mm, with a maximum weight of 20 kg. The largest Von Mises stress is at the outer part which is 116.24 MPa, this is smaller than the fatigue stress of 138 MPa which corresponds to a completely reversed lifecycle of  $50 \times 10^7$  (ER4, ER5).

The final weight of the pylon is 227 g (including the clamp adapters). This weight is higher than the ranges initially determined, however, these ranges do not include the weight of adapters. It will be necessary to consider the overall weight of the prosthetic to determine whether a lighter pylon would be required.

### **4.3 Knee**

In Section 3.3, the final design was chosen to be the PASPL knee. The knee design was based on the methodology determined by Ngan (2015). Below, the design decisions based on strength calculations are discussed followed by a further analysis into the FEA of the final component. Figure 20 shows the final design, the parts list can be found in Appendix A.6 Table 18. The following components will be discussed in further detail below, part 1 the body; part 4 the top; part 3 the base and parts 6, 8, 14, 15 and 27 composing the extension assist mechanism. Table 26 in Appendix C summarises how each design parameter for the knee is accomplished.

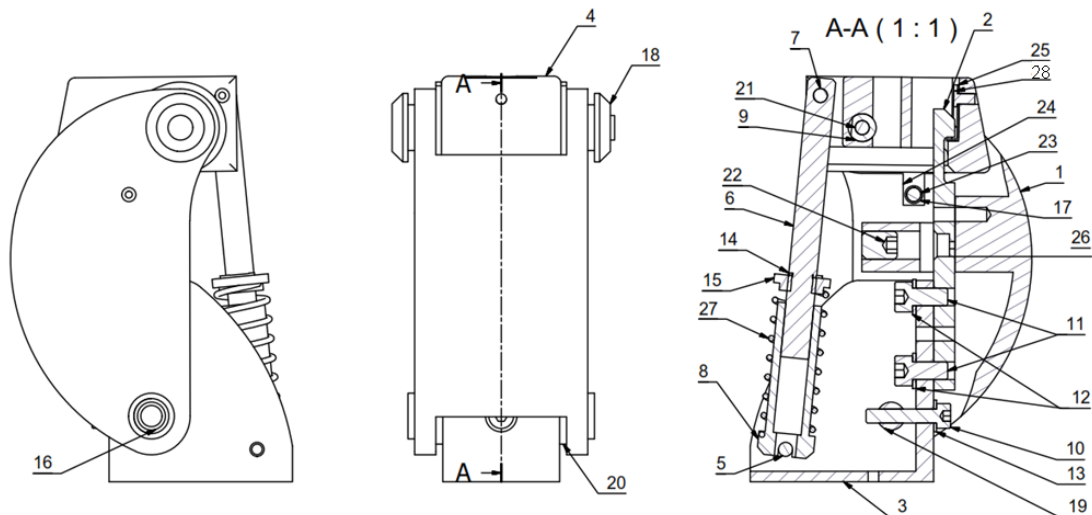


**Figure 20: Final knee design**

#### 4.3.1 Design decisions based on calculations

The axis alignment angle, the angle between the control axis and the knee axis, was determined by finding the zone of instability for each angle option. The zone of instability is determined from Equation 4. It was found that to aim for a zone of 55.8% an angle of  $5.5^\circ$  was required (average angle for ages three to five years). The alignment angle of  $5.8^\circ$ , used by Ngan (2015), resulted in an average zone of 54.8% for the data of three to five years olds. It was concluded that a smaller zone of instability would result in a more stable knee, which is preferable for toddlers using a prosthetic leg for the first time, even though this does result in some difficulty with starting the swing phase, therefore  $5.8^\circ$  was used in the final design.

$$\text{Zone of instability} = 1 - \frac{\text{Projected distance}}{\text{Foot length}} \quad (4)$$

To ensure that the knee remains locked during the stance phase, a small spring was added to keep the lock in place. The spring used is 0.35 N/mm, when tightened to the system a total force of 3.5 N results on the lock thus resulting in a moment of 0.1225 Nm, keeping the lock in place. With the foot length approximately 0.128 m (for the five-year-old data), a total GRF to unlock the knee is 0.957 N. This is a very small force to unlock the knee, if the knee does unlock too easily it will be necessary to tighten the spring more or use a stiffer spring.

The extension assist spring was determined by comparing the clinically proven AT-Knee torque of 2.54 Nm at  $60^\circ$  for a 100 kg user to the maximum of a 20 kg

user (Table 14, additional weight for safety), which is 20% of the original weight thus 20% of the torque is required resulting in 0.508 Nm or less. Using the PASPL lever arm length, the required stiffness was calculated to be 3.34 N/mm (Ngan 2015). Additional springs with higher and lower stiffnesses were then made based on the size constraints of the ideal spring size. The total height of the spring and inner diameter must stay the same due to the circlip and extension assist components. This spring can easily be removed so that a spring of a different stiffness can be used.

The maximum flexion of the design is 67.3° this is due to the constraining factor of the extension assist rod and the anchor which required constant overlapping when walking (KDP5). This also resulted in the spring having a smaller compression length than initially designed for. This flexion is much lower than the desired 150°. To rectify this, future designs should consider improvements on the design of the extension assist rod and anchor. This design, therefore, does not allow for an aesthetically appealing sitting posture (KDP6, ER10).

To ensure that the knee prosthetic could attach to standard components, the knee was designed to ensure that a prosthetic pyramid adapter could be placed on the top and bottom of the component, the final design has a junior SACH foot adapter on the top and bottom of the component (Ossur 2016b).

The deflection and fatigue of the knee component when an individual is standing on the knee with full-body weight was then analysed, see Appendix C.3. The top and bottom components each had a Von Mises stress of 1.94 MPa from the calculation of crushing failure in the eye and 15.77 MPa for the bending failure of the pin housed in these components (Machine Design 2014). Due to the low compressive yield strength of ABS plastic, it was determined that the body and top components would need to be 3D printed with PLA, which has a compressive strength of 17.9 MPa (Table 15). From this, it was determined that the body could be 3D printed, and thus the smooth curves were designed which allow for aesthetic appeal as well as ease in putting on clothing. The body and top component were 3D printed due to these results prior to the FEA analysis. The component was printed in the x-orientation, thus ensuring that the compression forces receive the least strain (Afrose et al. 2016).

The pins that are at the top and bottom axis points were calculated for strength, according to the hinge joint formulas (Machine Design 2014). Though aluminium was determined strong enough (safety factor = 7), the components were manufactured out of steel to ensure sufficient strength and safety.

The lock analysis involved deflection, strength and fatigue calculations, the results are summarised in Table 22. From the analysis, it was determined that the lock will be required to be manufactured of steel (1006 HR). This was due to

the lifecycle requirements and safety for any impacts that can result when locking and unlocking.

The total weight of the knee design is 479 g, this is larger than the ranges determined in Section 2.6.1, however, this range does not include the prosthetic adapters. The total weight is discussed in Section 4.4.

### **4.3.2 FEA analysis**

Strength, fatigue and deflection calculations were done to determine the material requirements for each component so that a prototype could be manufactured. Following this, a Finite Element Analysis (FEA) was done on the knee so that any stress concerns could be analysed and adjusted for.

The FEA model is shown in Figure 21, this model was developed in Patran 2014 by Plotz (2016) and is a symmetrical half model. FEA was done on the knee component for solid meshes and for shell meshes. The results from these separate tests had similar outputs. Solid component designs were made with a quadratic tetrahedron (Tet10) mesh and shell component designs made use of IsoMesh Quad4. The element size was chosen to ensure that the thinnest area on the solid had no less than a double layer. The quality of the mesh was ensured by using this element size along the remainder of the mesh to ensure that the element sizes remained relatively constant as well as ensuring symmetry when holes occurred in the solid. The total node count for the knee FEA was 112000.

Boundary conditions were placed on the knee half model components to ensure no rigid body motion, i.e. movement in the x, y, z as well as rotation in these axes was prevented on the lower components to imitate below the knee as well as along the length of the knee component to ensure the symmetry of the knee. The load was then applied replicating the weight of a 20 kg child (added weight for safety, see Table 14) on the top of the ankle component as a pressure force to ensure even distribution along the component. The pressures considered in this analysis can be seen in Figure 22, these are calculated based on the total weight which would be applied when the patient is standing on both legs on the top of the knee component. This amount is halved due to the model being a symmetric half model. The model consists of the materials as seen in the parts list, Table 18 Appendix A.6. All scales in FEA figures are in base units (Pa, m), the results are summarised in Table 24, Appendix C.

The FEA results are compared to the results from analytical results. The FEA results with higher stresses than the analytical results will result in the need to ensure the manufacture of the component with a stronger material. It is necessary to apply ISO strength tests before testing on the patient as a final validation of the FEA results (See Appendix B).

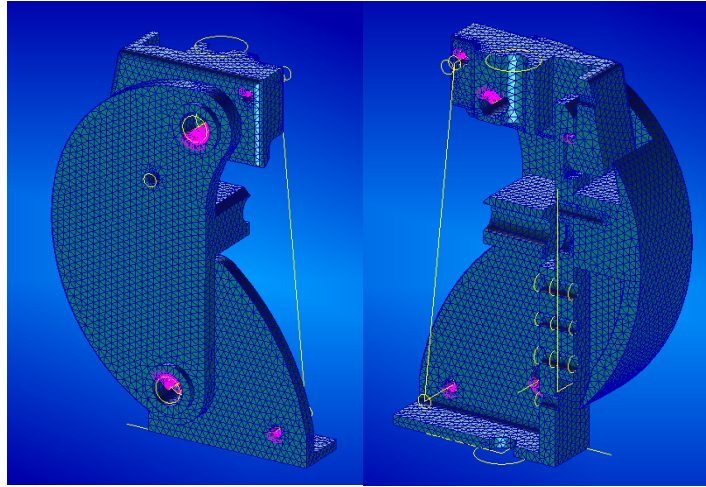


**Figure 21: Half model of the knee (Plotz 2016)**

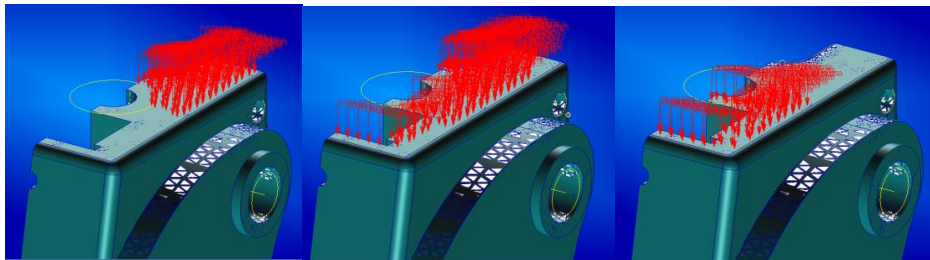


**Figure 22: FEA how forces are applied, a) Back pressure (439 kPa), b) Centre pressure (219 kPa), c) Front pressure (439 kPa) (Plotz 2016)**

Shown in Figure 23 is the fringe plot of the Von Mises stress when centre pressure is applied to the knee model. A concentration of 23.3 MPa can be seen in this figure where the lock is connected to the base. This stress is due to the constraints that are applied in this section which is located at three points rather than along the length of the bolt. The body is made of aluminium which has a fatigue strength of 138 MPa and the lock is made of steel with an ultimate strength of 300 MPa, therefore these stresses are not a design concern.

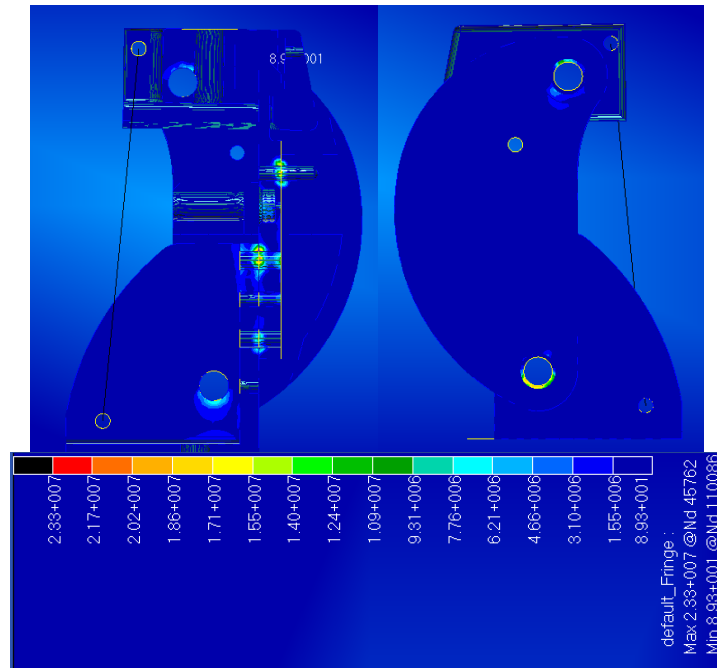


**Figure 23: Von Mises stress fringe plot - Centre pressure (Plotz 2016)**

A maximum stress of 15.5 MPa can be seen on the upper and lower sections of the body which hold the control and knee axes (Figure 23). This result is similar to the calculated value of 15.77 MPa (Table 22). As seen in Figure 24, similar stresses result when pressure is applied only to the back of the knee, however, it can be seen that a maximum stress of 56.7 MPa occurs when front pressure is applied, see Figure 25. This stress is higher than the compressive and tensile strengths of PLA, 17.9 MPa and 46.7 MPa respectively. This shows that these locations on the body component of the knee design will have a large amount of wear when walking. It is recommended that the top and body components of the knee are instead manufactured out of Delrin which has larger strength characteristics (Table 15, Appendix A.2). The density of Delrin is 1410 kg/m<sup>3</sup> (Ngan 2015) whereas the density of PLA is 1250 g/cm<sup>3</sup> (Swart n.d.), therefore by changing the material from PLA to Delrin the weight of the components will not be significantly affected. Delrin, however, is not a plastic used in 3D printing, therefore it will be required to instead make the component with a CNC machine. The pins used at these axes are made out of steel, as such, the pins will be strong enough.

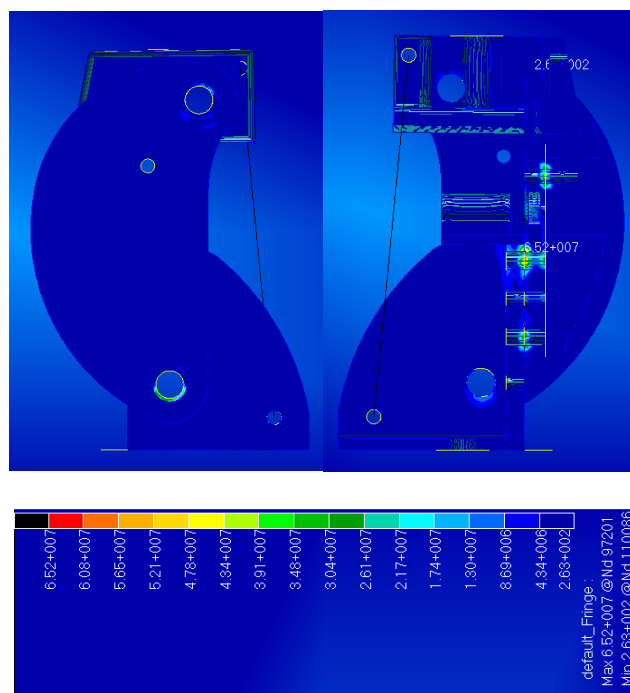


**Figure 24: Back pressure FEA analysis (Plotz 2016)**

Figure 26 shows the translational displacement of the knee joint when centre pressure is applied. As seen in this figure, the maximum displacement is at the lower front section of the top component. This displacement is small at 0.146 mm and will therefore not result in any unexpected motions. As seen in the figure the body experiences small amounts of deflection at the top half, this is a small amount, however, a change to Delrin will improve the deflection and strength here.

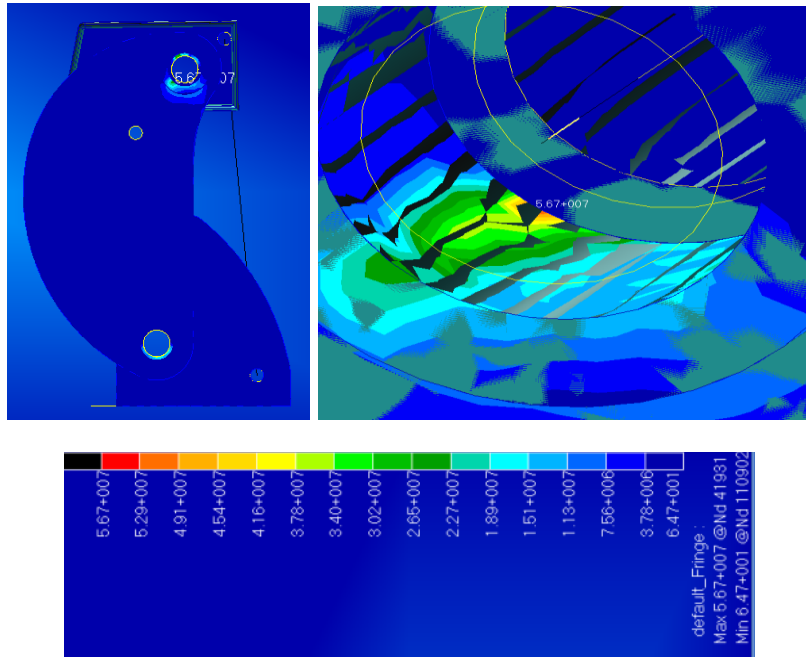


Figure 25: Front pressure applied, with close up (Plotz 2016)

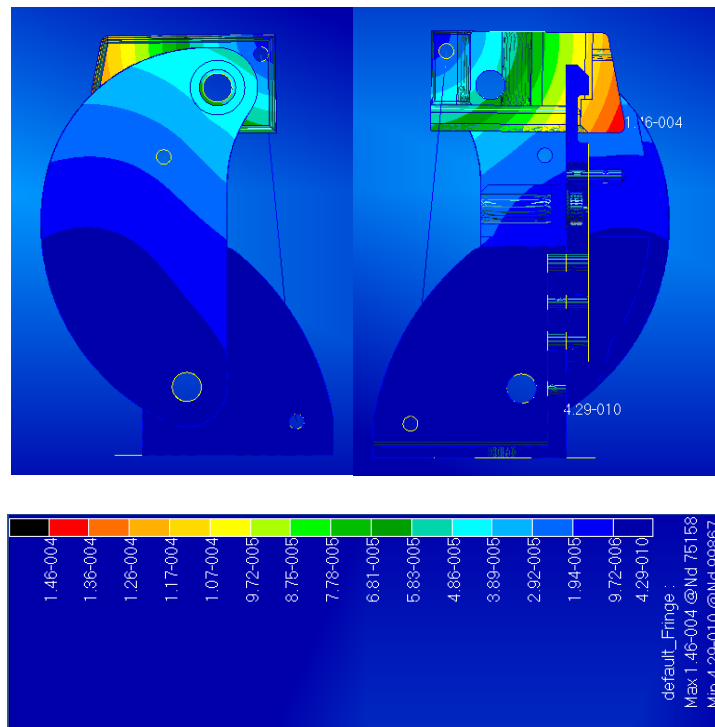


Figure 26: Displacement fringe plot – Centre pressure is applied (Plotz 2016)



## 4.4 Overall design

The final design is shown in Figure 27. As discussed in Sections 4.1, 4.2 and 4.3 most design parameters were achieved. Table 25 (Appendix C) summarised the engineering requirements and how they are achieved. The final design consists of a mechanical prosthetic that requires active control for movement. The design consists of a single-axis foot with a torsion spring of  $808.59 \text{ Nmm/}^\circ$  which can easily be replaced by a spring with a different stiffness. A urethane foot cover can easily be placed over the foot to allow for shoes to be worn. The footplate can be removed and replaced for size requirements as well as stiffness requirements. The pylon device consists of overlapping tubes with a clamp collar. The knee consists of a design based on the PASPL design of Ngan (2015) with a zone of instability of 54.8%. The extension assist mechanism consists of spring of stiffness  $3.34 \text{ N/mm}$  that can easily be removed and replaced with a spring of a different stiffness as required for the swing phase (ER3).



**Figure 27: Final prototype of the adjustable prosthetic leg**

All ADPs were achieved, most PDPs were achieved however the design has 5 mm less than the desired adjustability with no shock absorption, this is smaller than the 10 mm height adjustment mentioned by Friberg (1984). The design also allows for a height adjustment to any position within the 45 mm range, thus allowing small changes in growth to be accommodated for. Most of the KDPs were achieved however the maximum flexion is smaller than the desired range yet will allow for a normal gait pattern. The overall weight of the design is 933 g,

with the larger weights being closer to the torso. According to Zinke-Allmang (2009), the total weight of a leg is approximately 15% of the total body weight, therefore, the total leg weight would be between 2.2 and 2.7 kg. Though this total weight does include the whole leg (whereas this design only just above the knee) we can safely assume that this design has a low enough weight to allow for a natural gait.

The overall cost of the above-knee prosthetic design is R21 458.19, excluding the cost of a socket and foot cover. This includes a manufacturing cost of R17 006.08 as well as the cost of prosthetic adapters of R3 159.75. This would be the cost of the prosthetic for a three-year lifespan. In comparison, the lowest cost for a prosthetic device is between R378 480.93 – R 417 596.43 for a three year period (Section 2.3), excluding inflation considerations. It is clear from this data that this design is much cheaper than the cost of a prosthetic device. The overall costs are summarised in Table 27 in Appendix C.

During the manufacture of the prototype, it was concluded that a dorsiflexion bumper is unnecessary. This is due to the torsion spring, which is much stiffer than the required dorsiflexion bumper, thus the bumper became obsolete.

## 5 Design of the gait emulator

As discussed in Section 2.8, testing is ideal when it can be done on individuals. However, to ensure the safety of a component prior to testing a patient, other test procedures should be considered. In this chapter, a mechanical gait emulator is designed and developed to allow for testing of the prosthetic leg without the risk of injury to the patient.

### 5.1 Introduction

As stated by Eberhart et al. (1954)

“...it is obvious that any improvement – either in surgical and physiotherapeutic procedures or in braces and prostheses – must rest upon an accurate knowledge of the functional characteristics of the normal locomotor system”

As such, by knowing how a normal leg moves during a gait cycle, analysis to determine whether improvements are required on a prosthetic leg design can be done. Gait analysis is a useful tool to determine quantitative results of walking. During a gait analysis, kinetic and kinematic data are collected, as discussed in Section 2.2. This data can be used to analyse anomalies of a prosthetic with respect to a normal gait pattern. Adjusting the alignment of a prosthetic leg has an effect on the energy consumption of a transfemoral amputee more significantly than that of a transtibial amputee (Schmalz et al. 2002). Therefore, it is especially important to determine how making adjustments to an above-knee prosthetic can affect the gait of the patient.

By using devices such as the gait emulators designed by Richter et al. (2015) and by Ficanha et al. (2015) information can be determined about the gait characteristics of the prosthetic device prior to testing with human subjects. The use of a gait emulator will allow for the prevention of injury as well as repeatability, an aspect which has been noted as difficult to achieve when testing paediatric patients (Andrysek 2009). It is the goal of this research to determine how the adjustability of the design affects the normal gait characteristics.

The above-knee prosthetic leg designed in this thesis is made with regards to adjustability. The final design is adjustable in the following aspects:

- the height of the prosthetic,
- the length of the footplate,

- the stiffness of the extension assist spring i.e. swing phase control, (the ankle stiffness is not as easily adjustable, but can be changed)<sup>2</sup>

By designing a gait emulator that emulates the movement of the body above the knee, that is the hip kinematics, the adjustable aspects of the prosthetic can be analysed.

## 5.2 Desired output data

The goal of the gait emulator is therefore to determine the effect on adjustability on the design. As such, each age group will be considered and compared to by adjusting to the required height and foot length. The adjustability of the extension assist mechanism will also be determined by using three different spring stiffness'.

As discussed in Section 2.2, there are kinematic and kinetic data of the gait cycle that can be collected during the emulation. By emulating the hip kinematics as a control variable, the remainder of the kinematic data can be analysed. The data that will be emulated or collected during a gait analysis will include:

- Hip displacement (see section 5.2.1)
- Stride length and step frequency (see section 5.2.2)
- Flexion and extension angles of the ankle, knee and thigh (see section 5.2.3)

Kinematics is the branch of mechanics that is concerned with the motion of objects with no reference to the forces that can cause this motion (Dictionary 2017). The hip moves laterally, vertically and horizontally during gait due to balance requirements and the effect of walking (Mochon & McMahon 1980). The vertical motions will be analysed and the horizontal motion will be emulated from the movement of a treadmill. Lateral movements will not be emulated for simplicity purposes as these are smaller and exist for balance during gait (Richter et al. 2015). As noted in Section 2.2, a mature gait pattern is reached near to the age of 3, therefore the kinematic patterns of an adult can be emulated and scaled down to that of a child (Sutherland et al. 1980; Ivanenko et al. 2005; Chester et al. 2006).

### 5.2.1 Vertical excursion of the centre of mass

As discussed in Section 2.2, the centre of mass moves vertically in a sinusoidal pattern which has twice the frequency of gait. One sine curve occurs during the

---

<sup>2</sup> Though shims are part of the design of the knee prosthetic, they could not be implemented accurately in the prototype and will therefore not be tested during the gait emulation.

stance phase as the leg lifts the body up, and the other occurs during the swing phase (when the other leg causes the body to be lifted up), see Equation 1. As discussed in Section 5.1, it is desired to emulate the hip kinematics. Therefore the hip vertical excursion will be emulated.

The sinusoidal pattern occurs most prominently during the optimal speed, this is when the kinetic energy and potential energy are out of phase and therefore the amount of work is minimal as shown in Figure 28. Above this optimal speed, the recovery of mechanical energy through potential kinetic energy transfer decreases, this decrease in recovery has a greater effect for younger subjects. This reduction implies that a greater amount of work is supplied by the muscles. It was determined that an individual's chosen walking speed was similar to the optimal speed, this is equal to a slow to moderate pace. This optimal speed is around 0.8 m/s for a 2-year-old and increases progressively up to 1.4 m/s for a 12-year-old. Only the 'optimal' speed will be analysed to ensure that the sinusoidal pattern is emulated correctly and avoid any additional effects of energy. (Cavagna et al. 1983)

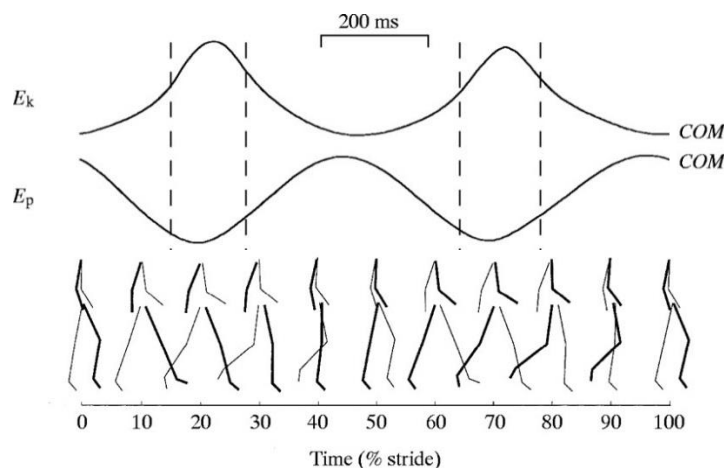


**Figure 28: The kinetic and potential energy curves during optimal speed (Schepens et al. 2004)**

Three methods exist to determine the location of the centre of body mass (CM) these are double integrating the GRF to determine the location of the CM; using a full body multi-segmented kinematic model (KM), and using the centre point of the pelvis as the CM. A study was done with able-bodied children (ages 6-17) as well as adults to determine which method was the most accurate. This data can be used for a wide range of children, due to previous research it is known that the gait cycle of a toddler is similar to that of older children and therefore this

data can be deemed feasible to work with. The GRF or KM results will be used due to their determined accuracy (See Section 2.2.1). The results for the vertical excursion of the CM can be seen in Table 10, along with calculations for the three age groups in this thesis using the results. (Ganley & Powers 2005; Ivanenko et al. 2005; Ounpuu et al. 1991; Cavagna et al. 1983; Eames et al. 1999; Chester et al. 2006)

**Table 10: The determination of DeltaZ using the data determined by Eames et al. (1999)**

		GRF	KM	CP	
		$\Delta Z$ (as % of height)			
(Eames et al. 1999)	Adults		2	2	2.3
	Children		1.9	1.9	2.3
		Height (mm)	$\Delta Z$ (mm)		
Table 14	3 year old	955	18	18	22
	4 year old	1027.5	20	20	24
	5 year old	1095	21	21	25

### 5.2.2 Speed and stride length

It is necessary to determine the speed and stride length or step frequency of gait so that  $T_c$  (See Equation 1) can be determined as well as the optimal speed for the sinusoidal motion to be most prominent.  $T_c$  can be determined according to Equations 5 and 6, based on the data acquired. Data was collected and the average optimal speed and  $T_c$  is summarised in Table 11. (Schepens et al. 2004; Rose-Jacobs 1983; Shriners Hospital 1987; Hof 1996; Schwartz et al. 2008)

$$T_c = \frac{\text{stride length}}{\text{optimal speed}} \quad (5)$$

$$\text{velocity} = \text{stride length} \left( \frac{m}{2 \text{ steps}} \right) * \text{cadence} \left( \frac{\text{steps}}{\text{min}} \right) * \left( \frac{\text{min}}{60 \text{ sec}} \right) \quad (6)$$

**Table 11: Average optimal speed and  $T_c$  values for ages 3 to 5 years**

Units	Optimal speed	Full Gait, $T_c$	
	m/s	Hz	s
Age			
3	0.76	1.00	1.00
4	1.00	1.13	0.89
5	0.90	0.98	1.02

### 5.2.3 Flexion and extension angles

As discussed in Section 5.1, the gait emulator will emulate the hip kinematics, therefore the hip extension and flexion angles will be emulated. In Section 2.2.1 the knee and ankle kinematics were discussed, it was shown that age does not have a large effect on the size or shape of the kinematic data curves, therefore normative kinematic data for a wide range of children can be used to compare the kinematic data of the prosthetic device. The data that will be used will be that collected from Gillette Children's Specialty Healthcare, GCSH (Pinzone et al. 2014)

As noted in Section 2.2.1, speed has an effect on the size of the flexion and extension angles, however, it has a small effect on the overall shape of the curves, as the speed increases the peaks occur earlier. However, as stated in Section 5.2.2, only the optimal speed will be considered.

### 5.2.4 Kinetics

The aim of the gait emulator tests is to determine whether the movement of the prosthetic is similar to a normal leg. Therefore, the moments and powers will not be analysed. The GRF of the foot, however, will be compared to existing data. This is so that the curve can be analysed to determine whether heel strike and toe-off occur as expected. The gait emulator is emulating the normal gait (so that an ideal gait is emulated) and determining how the prosthetic will respond, therefore additional factors that are due to weak muscles or deficiencies such as cerebral palsy will not be considered in this design.

From the description of the GRF in Section 2.2.2, it is concluded that the gait emulator should not apply any force to the leg to emulate the GRF graph, instead, the GRF during the emulation should be analysed to determine whether heel-strike, toe-off and accelerations occur as expected.

### **5.2.5 Measurement devices**

The Central Analytical Facilities (CAF) of Stellenbosch will be used for data capture of the gait emulator. Of the available equipment offered by CAF, it was determined that the Vicon Motion capture system, as well as the Bertec instrumented treadmill, would be ideal for this analysis. The Vicon motion capture system consists of 10 cameras which capture lightweight markers that are placed on the component being analysed in 3D space, in this case, the prosthetic leg. The movement of the component is then given as the x, y and z coordinates with respect to a set origin. These coordinates can then be used to determine kinematic data such as displacements and angles. This method works well for the prosthetic device as marker points can be determined easily for future analysis. Other methods of motion capture include EMG analysis, however, due to the lack of muscle signal from the prosthetic, this would not be feasible. (Cockcroft 2017; Vicon 2017)

The Bertec instrumented treadmill is a treadmill with speed control as well as an embedded force plate. This allows for tight control of the speed of the treadmill during testing while measuring the GRF of the prosthetic device during walking. The force data can be synced to the Vicon data so that events can be determined. (Bertec 2016; Cockcroft 2017)

## **5.3 Mechanical design**

To conclude, the vertical excursion of the hip (Section 5.2.1), the flexion and extension angles of the thigh (Section 5.2.3) and the horizontal movement should be controlled (Section 5.1). Therefore, this design will require three degrees of freedom. From this emulation, it is desired to compare the knee angles, ankle angles and GRF to existing data (Section 5.2). The designs of Ficanha et al. (2015) and Richter et al. (2015) are considered to determine a feasible solution for the desired emulation.

### **5.3.1 Existing gait emulator designs**

The design by Ficanha et al (2015) emulates vertical excursion and horizontal movement during the gait cycle. This is due to the design emulating the gait for a below knee prosthetic. The knee movement is emulated through the use of a universal joint, acting as a passive knee. Vertical displacement is done through the use of a lifting mechanism which uses a DC motor to raise a weighted bar with a cable. Horizontal movement is emulated with a rotating turntable – this is due to the design focus on the effect on an ankle-foot prosthetic during turning. This design emulates the gait cycle while allowing the passive effects of the ankle joint to be analysed. This design does not, however, consider above-knee prosthetics.



The design of Richter et al. (2015) uses a linear actuator to emulate vertical excursion and attached to this, a rotary actuator emulating thigh rotation, see Figure 29. The emulator is placed near a treadmill so that the horizontal movement of gait is emulated. Closed loop control is performed to ensure that the positioning of the system is with respect to an ideal gait. The test robot uses the linear and rotary actuators to apply the force due to weight and muscle action. Due to the coupling of the linear actuator to the rotary actuator, the response of the prosthetic device alone cannot be determined. For example, it would be difficult to determine the GRF of the prosthetic as well as the displacement of the hip during the stance phase. Therefore, it is concluded that an emulator design similar to the design of Richter et al. (2015) should be considered, however, the new design should allow for coupling and decoupling of the linear actuator. This would allow for the passive response of the prosthetic to be analysed more thoroughly.

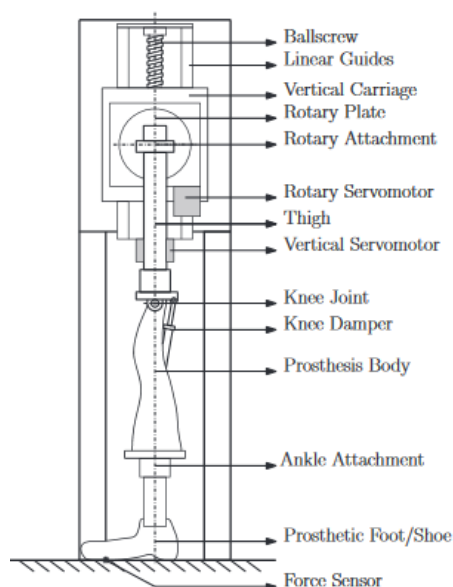


**Figure 29: Test robot by Richter et al. (2015)**

For the tests required, the linear actuator will be decoupled from the rotary actuator so that it can emulate the displacement of the hip during the swing phase but allow for any additional positive displacement to occur, see Figure 30. The displacement will then be measured externally to compare the response to existing data. With this design, further analysis with respect to forces can be done by coupling the linear actuator to the rest of the system, the plate that is

attached to the actuator can be fastened to the top plate through the use of bolts.

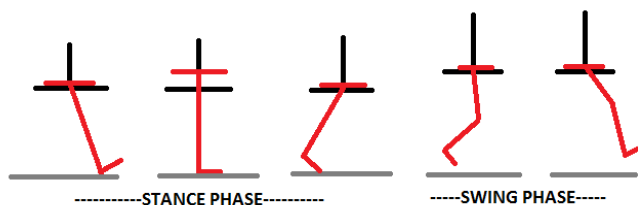


**Figure 30: Depiction of uncoupled actuator**

### 5.3.2 Linear actuator

The linear actuator is required to emulate the displacement of the hip during the swing phase of a normal gait cycle (see Figure 30). The actuator can ideally be used in further experiments by coupling it to the rotary actuator to emulate forces as described by Richter et al (2015), however, this will not be done here.

To emulate the hip displacement, it will be necessary to have position control. Due to laboratory environment constraints, it will be necessary to use an electric actuator instead of pneumatic one. There are a variety of linear actuator types available, however, the ball screw was determined to be the best choice as it can deliver precision positioning. A rod-style actuator is ideal as it can be designed to couple and decouple from the system (Lewotsky 2007).

The linear actuator is required to apply a force of 202 N, this includes the weight of the servo motor as well as the weight of a child (20 kg for safety), this allows for the range of weights of the child to be emulated. The stroke length required is 165 mm, this is determined from Equation 7 with data from Table 10 and Table 14 (Appendix A.2). This length allows the actuator to be used to position the prosthetic according to the length of the prosthetic rather than mechanically adjusting the structure.

$$Stroke = \left( Z_{avgmax} + \frac{\Delta Z_{max}}{2} \right) - \left( Z_{avgmin} + \frac{\Delta Z_{min}}{2} \right) \quad (7)$$

An actuator with a stroke length of 300 mm and rated 5.3 kN at 3000 rpm was readily available at Stellenbosch University, with this additional stroke length the final device can also be used on larger prosthetic legs in the future. Due to the length of the actuator, it was placed with rod facing down to allow the short

prosthetic device to reach the floor, the final structure can be seen in Figure 31. The linear actuator chosen is the SEW CMS50M, it requires three phase power and the use of a SEW Movidrive for control.

### 5.3.3 Rotary actuator

A servo motor will be used for the hip flexion and extension control. This is due to its ability to precisely track position. The servo motor shall track the position and ensure that the leg is in the correct position according to normal gait cycles, thus providing the power that is normally supplied by the hip. The servo motor can also provide torque to ensure a faster swing if necessary.

The total range of motion required is  $51.24^\circ$ , this is based on maximum flexion and extension angles of the hip determined by Chester et al. (2006). The maximum amount of torque required is 1.7 Nm, this is the total mass of the system moving around the centre of gravity to the maximum angle. The servo motor will also need to carry the total mass of the leg (933 g) at a distance of 0.23 m (this is due to the location of the treadmill centre).

A Faulhaber Series 3257 012CR DC-Micromotor (70 mNm) with a series 32/3 S Gearhead (14:1) and a Series IE2 – 16 encoder attached was available at Stellenbosch University. With the gear head attached, this motor has a torque of 0.98 Nm, with the use a 2:1 gear combination this torque could be increased to 1.96 Nm as well as increasing the encoder resolution to a 1792 ppr (Faulhaber 2011). The use of the additional gears along with bearings will also ensure that the distance to weight requirements mentioned previously will be met. The motor chosen in this design would need to be changed for a stronger motor if other prosthetic age groups are tested.

### 5.3.4 Structure design

The final test structure can be seen in Figure 31, Figure 59 and the parts list in Table 19 (Appendix A.6). The structure is made from aluminium extrusions to allow for small adjustments to be made in the positioning of each component. A top plate is used to hold the rotary actuator as well as the gears and bearings, this is to emulate the flexion and extension angles of the hip (Section 5.2.3). The plate is lifted by the linear actuator via a rigid lever that can be coupled to the plate if required (using screws). The vertical motion is constrained with the use of linear guides, this motion will emulate the vertical excursion of the hip (Section 5.2.1). Additional weights can be added to the top plate to emulate the overall weight of the child.

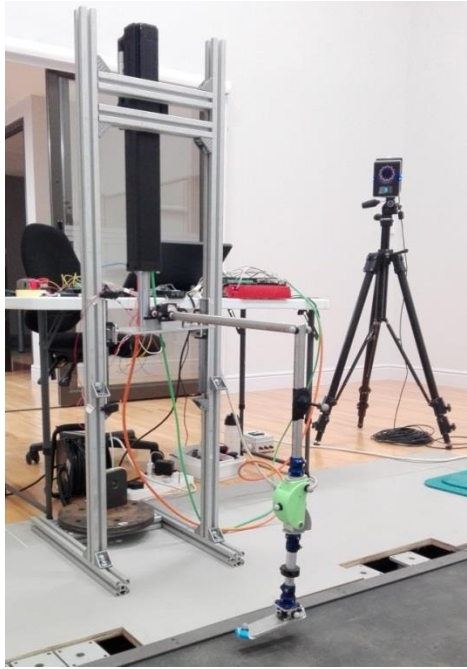


**Figure 31: Final test structure with prosthetic attached**

## 5.4 Control requirements and strategy

The control requirements for the test structure are discussed followed by the control strategy for closed loop feedback.

As discussed in Section 2.2, the hip displacement moves similarly to a sine wave. The hip displacement is due to the vaulting of the hip while one leg is straight followed by the vaulting due to the other leg. Therefore, we can emulate the hip displacement during the swing phase only, followed by no actuation during the stance phase thus allowing the prosthetic leg to cause the displacement alone. This is shown in Figure 32, 15000 encoder counts are equal to 20 mm. The control of the flexion and extension angles of the thigh will follow the curve shown in Figure 3.

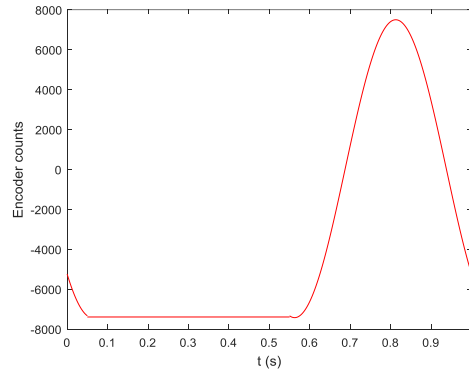


**Figure 32: Linear actuator requirements for only the swing-phase**

The control strategy diagram can be seen in Figure 33. The control of the rotary and linear actuators are via Arduino code, the treadmill and motion capture data is measured separately. An arduino was used due to its sensor abilities as well as data output to Matlab The linear actuator is controlled through PI feedback via the SEW Movidrive with a built-in external encoder (D1 and D2). Similarly, the rotary actuator is controlled through PI feedback with a motor driver and the encoder attached to the motor (D3, D4 and D5). The control is with respect to the required position in the gait cycle, with respect to time  $T_c$ .

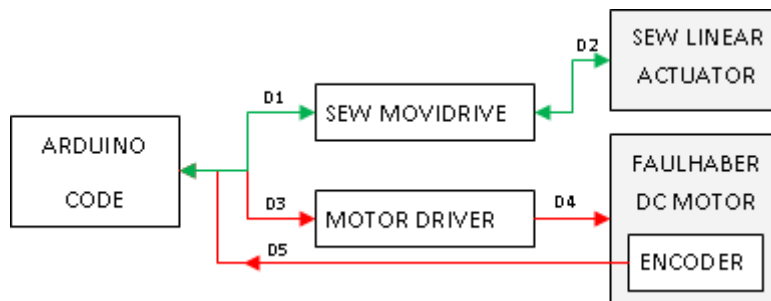


**Figure 33: Control strategy diagram of gait emulator**

For testing with the gait emulator, it was necessary to design a safety procedure, this can be found in Appendix D. This includes strategies to mitigate the risks of electric shock and moving equipment. To ensure safety from moving equipment a stop button was hard wired to the circuit and two limit switches were implemented to prevent the actuator moving beyond the determined bounds. Additionally, in the Movitools software (for the Movidrive which controls the

actuator), the current and torque limits were reduced due to the required force being much lower than the available force. To reduce the risk of high current a switch was implemented between the three phase power and the Movidrive, the wearing of shoes was required and warning signs were implemented.

The testing procedure is summarised in Figure 34. First, the setup of the Bertec treadmill, Vicon motion capture cameras and test structure is required. During the test procedure, each prosthetic group is tested, i.e. age group three, four and five for different spring stiffnesses. The emulator controls the placement and gait emulation of the prosthetic leg. The treadmill and Vicon system is turned on, followed by the gait emulation. While gait is being emulated the motion capture data and force plate data is recorded. The prosthetic leg is then lifted up and out of the way and the treadmill is turned off.

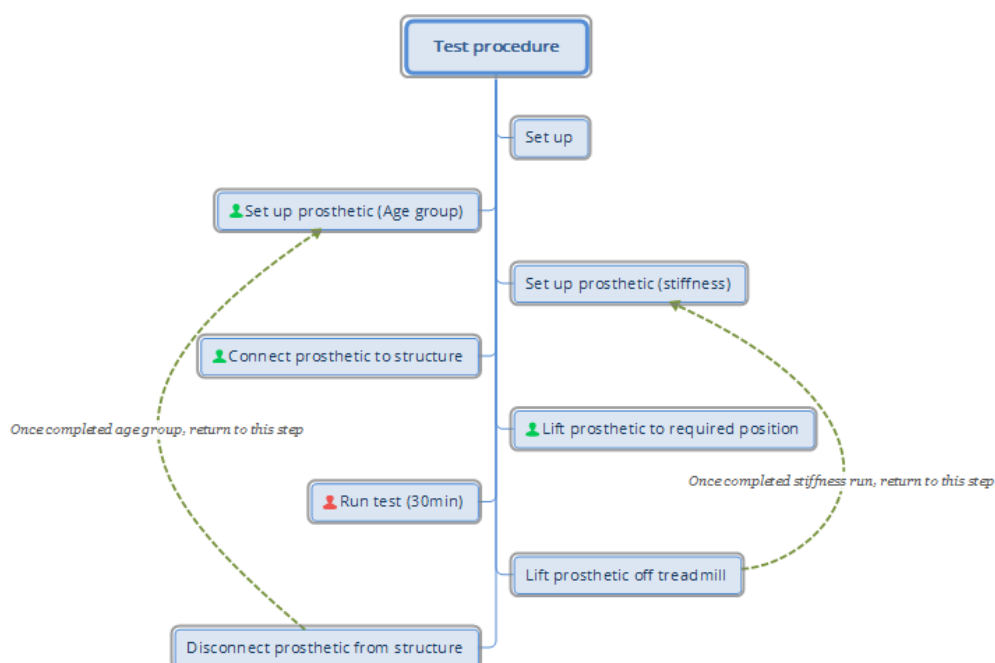


**Figure 34: Testing procedure**

The required spring stiffness was calculated to be 3.34 N/mm, due to the size constraints of the knee the stiffness was chosen to be 3.62 N/mm. For testing purposes, a spring with a lower stiffness and one with a higher was made so that the effect of the springs could be tested. These spring constants are 2.416, 3.623 and 4.269 N/mm.

It was concluded by Owings and Grabiner (2003) that to obtain accurate data from a treadmill gait cycle test, 400 steps were required. This number is based on the variability of a human subject when walking on a treadmill. For the emulation, there is no patient variability that would result from walking except the possibility of an accumulation of movement in the swing phase, therefore, a test cycle will be run only for the amount of time required to ensure that any variability can be noted, approximately 30 seconds.

## 5.5 Results

Marker points were placed as shown in Figure 35, this allows the Vicon system to determine the position of the prosthetic device in 3D space for future analysis. Basic geometry calculations were then done to find the angle made between two lines in 3D. Figure 66 in Appendix E shows some photos during these tests.



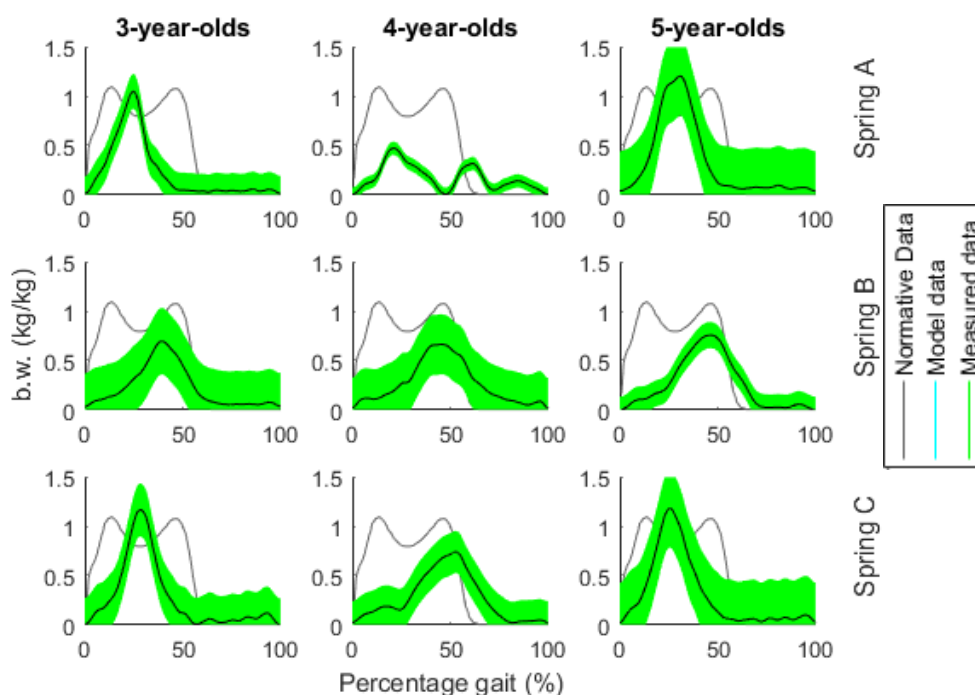
**Figure 35: Marker location points on prosthetic device**

*Key: THI: Thigh, KNE: Lateral Knee, ANK: Lateral Ankle, HEE: Heel, TOE: Toe, MMA: Medial malleolus, KAD: Knee alignment device, SHI: Shin, HIPA: Hip Anterior, HIPP: Hip Posterior*

The GRF data was analysed by first filtering the data with a 4<sup>th</sup> order low-pass Butterworth function followed by determining the occurrence of heel-strike so

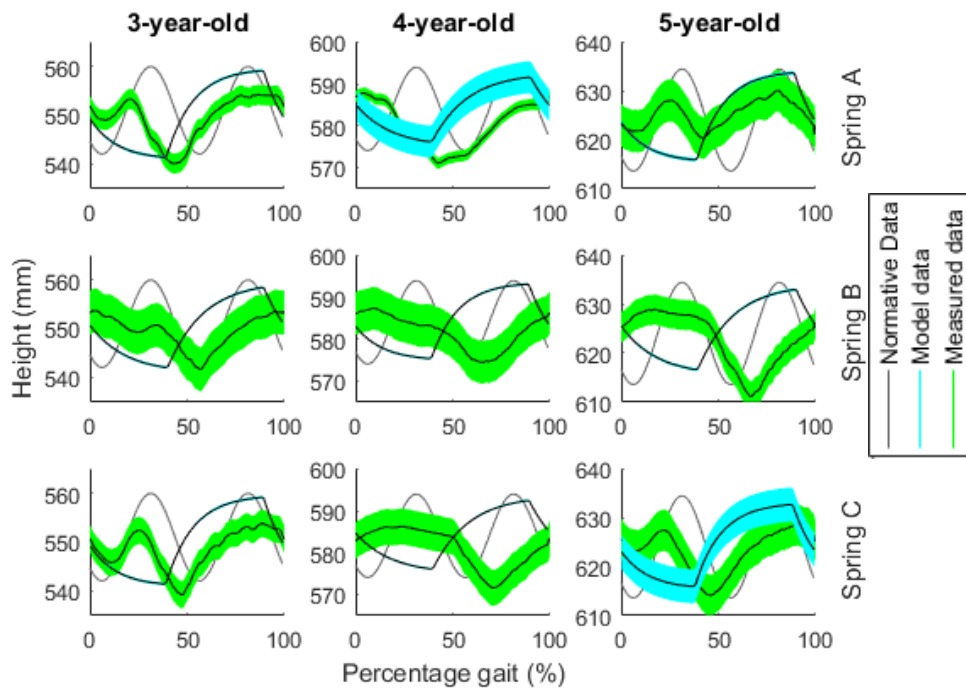
that data could be cut-up accordingly. Unfortunately, the use of the Arduino to control the linear actuator did not allow for the linear actuator to move faster as this resulted in a lag in the control which had dangerous repercussions in the movement of the linear actuator over the treadmill. As such it was determined that the gait could be more precisely controlled for a lower speed of 0.5 m/s and 0.75 m/s compared to the desired 1 m/s. With these lower speeds, it is expected that the overall energy of the system will not be ideal as desired (Schepens et al. 2004).

Figure 36, Figure 37, Figure 38, Figure 39 and Figure 40 show the data results from the gait emulation testing. In these figures normative data from Gillette Children's Specialty Healthcare, GCSH, is used for the angle data (Pinzone et al. 2014), GRF data is obtained from Schwartz et al. (2008) and the hip excursion is from Equation 1. In these figures, normative data is in grey, model data in blue and measured data in green. The data show the three, four and five-year-old data for springs A, B and C. The standard deviations are expressed as a shaded band around the mean, in some figures such as Figure 37, the standard deviation is very small in some cases. The data from the testing results are summarised in Table 12 and the standard deviations of the data in Table 13.



**Figure 36: GRF - gait emulator results**





**Figure 37: Vertical hip excursion - gait emulation results**

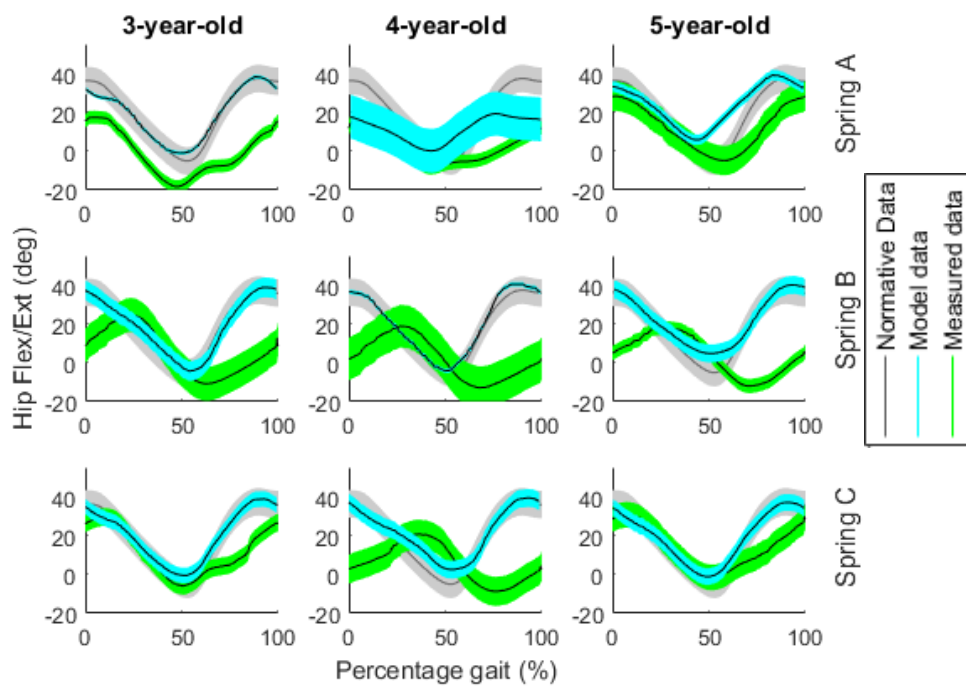


**Figure 38: Hip flexion and extension angles - gait emulation results**

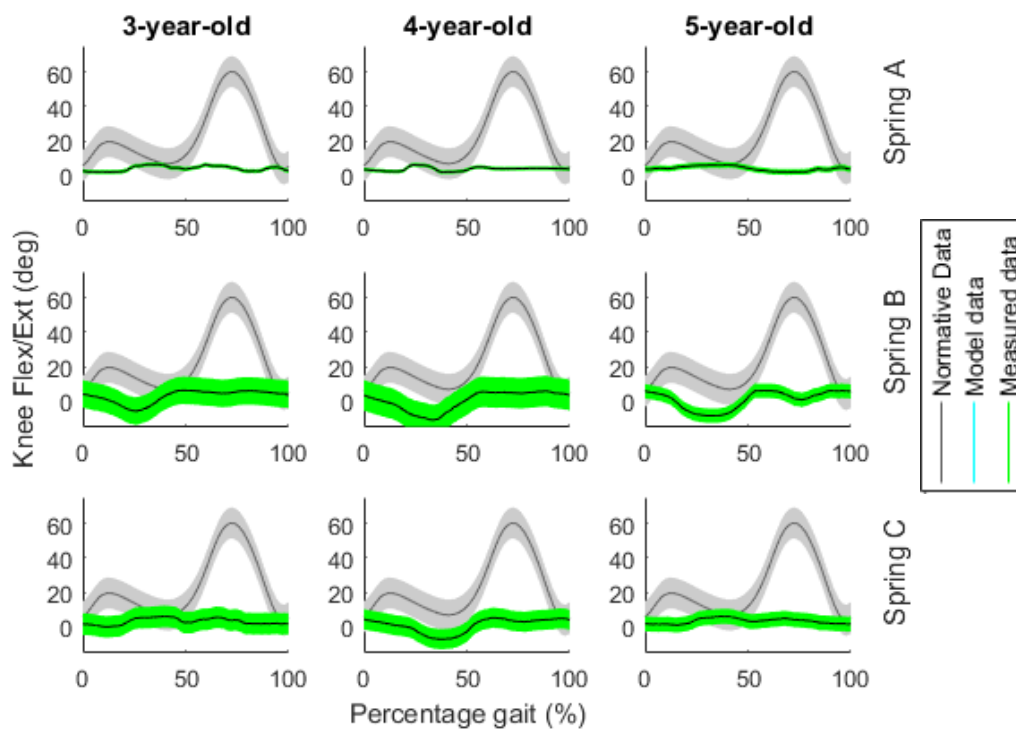


Figure 39: Knee flexion and extension angles - gait emulation results

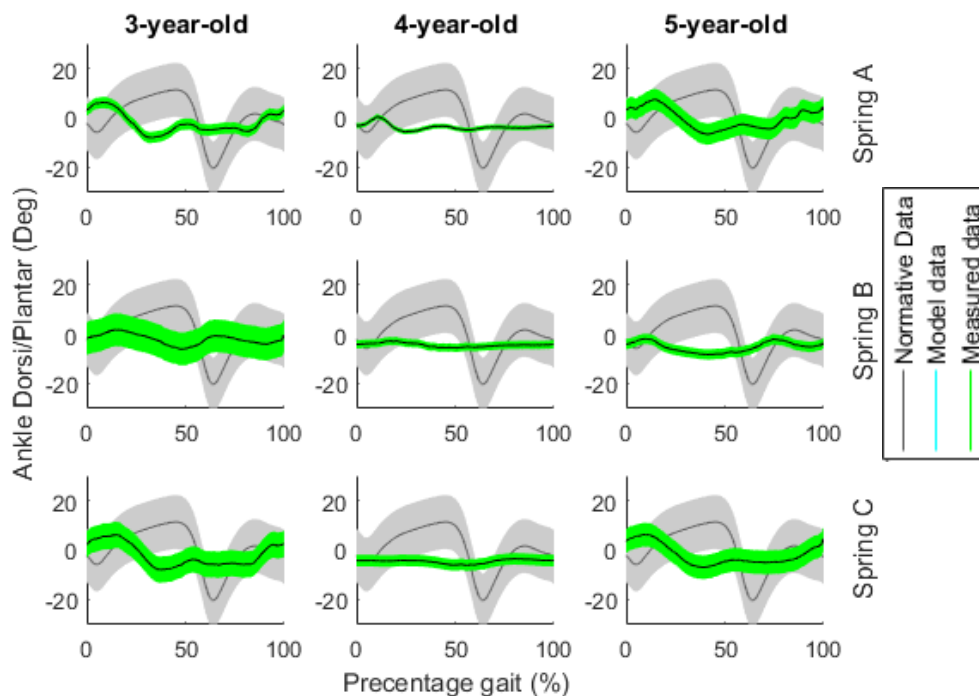


Figure 40: Ankle dorsi/plantar flexion - gait emulator results

**Table 12: Data from gait emulation testing**

	Data	Units	Minimum	Maximum	Standard deviation	Mean	Normative
GRF	Peak reached at:	%	24.68	53.70	10.88	36.71	14.02
	Toe-off reached at:	%	46.48	89.86	14.40	65.40	60.75
	GRF maximum	BW	0.66	1.21	0.24	0.93	1.10
Hip flexion and extension angles	Max peak at:	%	1.17	39.56	14.46	18.40	88.00
	Min peak at:	%	47.31	76.62	10.76	60.77	54.00
	Min peak value	°	17.29	30.61	5.54	23.39	37.32
	Min peak value	°	-18.54	-4.70	5.04	-11.31	-5.20
	ROM	°	29.43	35.83	2.40	32.78	47.11
Knee flexion and extension angles	Max peak value	°	5.08	6.15	0.34	5.81	60.41
	Min peak value	°	-11.08	1.97	5.37	-3.39	3.69
	ROM	°	16.76	3.84	5.23	9.21	70.81
Ankle dorsi-/plantar flexion angles	Max peak value	°	-3.72	8.41	5.03	2.65	11.37
	Min peak value	°	-8.29	-5.55	1.00	-6.90	-20.63
	ROM	°	16.36	2.47	5.49	9.55	28.33
Vertical excursion	Min peak value	%	43.15	70.61	11.51	55.20	57.00
	$\Delta Z$	mm	17.80	9.40	2.24	13.73	20.00

**Table 13: Standard deviation of gait emulator testing with respect to age and spring**

	Units	Age			Spring		
		3	4	5	A	B	C
Modelled hip flexion	°	1.40	3.58	1.93	3.31	1.53	2.07
Modelled vertical excursion	mm	0.08	0.63	0.53	0.62	0.10	0.52
GRF	BW	0.08	0.09	0.10	0.06	0.10	0.11
Vertical Excursion	mm	1.46	1.82	1.76	0.90	2.13	1.99
Hip flexion and extension	°	2.68	3.56	3.04	1.60	4.20	3.48
Knee flexion and extension	°	1.67	2.21	1.20	0.39	2.61	2.08
Ankle dorsi- and plantar flexion	°	1.92	0.54	1.49	0.84	1.60	1.52
Average measured data angles	°	2.09	2.10	1.91	0.94	2.80	2.36

## 5.6 Discussion

In this section, the results of the gait emulation are discussed. When not specified, the figures referred to in this section are found in Section 5.5. All data for the gait emulation is summarised in Table 12 and Table 13 in Section 5.5.

Figure 36 shows the GRF data, based on the BW of the prosthetic limb. Due to size constraints, the total weight applied was 2.8 kg. As can be seen in the figure, the four-year-old, spring A data is an outlier and will therefore not be considered further. In the remaining data, it can be seen that the peak of the GRF is reached more gradually than with the normative data, reaching a maximum peak of on average 0.93 BW (S.D. 0.24 BW) at 36.71% (S.D. 10.88%) rather than the norm of 1.1 BW at 14.02%. This curve is more similar to that of the “slow walk” GRF, shown in Figure 6 in Section 2.2.2, in which the occurrence of the GRF peak is reached at 18% with a maximum of 1 BW with no second peak. This corresponds well with the speeds used due to Arduino control requirements. By comparing the GRF response to the resultant reaction of an inverted pendulum, (see Figure 7) an inverted pendulum will only have one peak due to the leg remaining straight, this corresponds to Figure 39 which shows the knee remaining moderately straight.

As stated, the knee remains moderately straight. This is due to the timing of the vertical excursion and hip flexion, by lifting the hip up for the occurrence of the swing phase even slightly out of sync to the hip flexion the moment to unlock the knee is effectively reduced to zero. As discussed in Section 4.3.1, a moment of only 0.957 Nm is necessary to unlock the knee, i.e. a mass of only 0.0975 kg. Additionally, though the zone of instability is 1% smaller than the recommended 55.8%, this is not the cause of why the knee does not unlock as toe-off is still required. This is further shown in the data analysis in which the lowest vertical excursion occurs on average at 55.2% (S.D. 11.41) rather than the norm of 57% thus affecting the time of toe-off and the swing phase. This is as a result of the control of the components with the Arduino, which did not allow for a higher speed control of the linear actuator.

As discussed in Section 5.4 the linear actuator would not emulate the vertical excursion during the stance phase, thus allowing the resultant vertical excursion to be analysed. As shown in Figure 37 an initial delay in the modelled data of the vertical excursion was set such that the measured data would reach the lowest point at approximately 57% as seen in the three-year-old spring B data. This did not, however, always occur as expected as can be seen in the four-year-old spring C data. It is noted that vertical excursion during the stance phase is not prominent, however, the five-year-old data does show that the leg did lift up during the stance phase even as the ‘hip’ was being lowered. Due to the length of the L-beam for simulation purposes, it is determined that the moment

required to lift the leg was too great, however, it is still expected that a lower moment, such as for a normal child, the leg will be able to vault forward thus allowing for vertical excursion during the stance phase.  $\Delta Z$  is on average 13.73 mm (S.D. 2.24mm), which is much smaller than the norm of 20 mm. This is again due to Arduino control speed and results in a very small toe-clearance during the gait cycle.

Shown in Figure 38 are the hip flexion and extension angles. The modelled data accurately follows the normative curve, however, the resultant angles were not as accurate. As can be seen in the figure the swing phase did not occur as smoothly and the spring B data results are out of sync to that which was modelled. When compared to Figure 36 and Figure 37 it can be seen that this delay also occurred in the application of body weight during the stance phase as well as the occurrence of the lowest vertical excursion. This data has a large standard deviation due to the spring B data delay. The mean of the occurrence of the maximum peak value is 18.4% (S.D. 14.46%) in comparison to the norm of 88%. The occurrence of the minimum peak is at 60.77% (S.D. 10.76%) in comparison to the norm of 54%. The total average ROM is 32.78°, 14.33° less than normative data.

The standard deviation of the angle of the knee does increase as the spring stiffness increases (Spring A having the lowest S.D., see Table 13), however, there is consistently no knee flexion during the swing phase. The average ROM of the knee angle is 9.21° (S.D. 5.23) this is much smaller than the norm of 70.81° (see Section 5.3.3) (Chester et al. 2006). The knee did not reach the required flexion for an adequate swing-phase, thus there was little toe-clearance. The gait pattern was similar to skating in which the foot does not strike the treadmill/floor with the heel first but rather flat foot or the toe. Figure 41 shows a screen shot of the gait emulation in progress when insufficient toe-clearance occurred. As can be seen, due to insufficient toe-clearance the moment required to unlock the knee was reached thus unlocking the knee. This is a concern as the knee would buckle when walking. As such it is important in further testing to ensure that adequate patient control of the prosthetic through hip flexion will ensure the required toe-clearance is reached. Ngan (2015) found that less tripping occurred with the PASPL-Knee design, which this design is based on.

As shown in Figure 40, the ankle dorsi-/plantar flexion is minimal and does not follow the expected curve. Due to the ankle torsion spring being designed for the heaviest user it is expected that a small dorsiflexion angle would result due to the entire load not being applied. However, as can be seen from the data, further design on the plantar flexion bumper will be required to cause adequate plantar flexion angles. The size of these angles is also affected by the time of toe-off which occurs too late. The total ROM of the ankle is 9.55° (S.D. 5.49°), much smaller than the required 28.33° (Chester et al. 2006).



**Figure 41: Screenshot of gait emulation when insufficient toe-clearance**

The standard deviation for each set of data is summarised in Table 13. The average S.D.s for the measured data angles for the age groups three, four and five years is 2.09, 2.10 and 1.91° respectively. From this data, it can be concluded that the adjustability of the foot length and leg height did not affect the prosthetic design.

It is difficult to ensure the timing of toe-off with enough vertical excursion to ensure this knee flexion, it will be necessary to test this with an improved gait emulation design or when testing with a patient. When the data is compared to the data from the gait emulator designed by Richter et al. (2015) it is noted that the hip displacement and thigh angle were followed more exactly in Richter's tests. This is due to the higher level of control of the prosthesis – the thigh angles, vertical excursion and GRF were all controlled by the emulator, thus leaving no resultant variables. From these results, it can be concluded that a design that has more control over the variables can allow for a more effective analysis of each individual component. Therefore, it is recommended that in future to use the GRF as a part of the feedback loop to ensure that sufficient toe-off occurs.

## 6 Conclusion

The purpose of this thesis was to design and develop a lower limb prosthetic for toddlers between the ages of three and five years that could adjust to changes in growth, height and weight. This age range was chosen due to a need for adjustment approximately every three months (Lambert 1972) as well as the presence of a mature gait pattern by the age of three (Chester et al. 2006; Sutherland et al. 1980).

The engineering requirements were determined followed by a literature review to determine the design parameters for each individual component. Table 25 and Table 26 in Appendix C contain a summary of all Engineering Requirements (ERs) and Design Parameters (DPs) as well as how each was achieved. Most importantly the design is adjustable, allowing for users between the ages of three and five years:

- Height adjustable by 45 mm, this is less than the desired 50 mm but is within the range discussed by Friberg (1984) of less than 10 mm (ER1/PDP3). Growth plates are recommended if more adjustment is required (WillowWood 2016).
- Foot length adjustability through the use of three removable foot plates, this also allows for adjustability in foot stiffness requirements. (ER2/ADP6).
- Stiffness adjustment is achieved through the design of a removable extension assist spring in the knee design. This allows the prosthetist to determine the ideal spring stiffness without redesign. A torsion spring that simulates the stiffness of the ankle joint can also be replaced with a less stiff spring if required (ER3/ADP4/KDP7).

Strength and fatigue calculations were done on each component followed by a further Finite Element Analysis (FEA) of the ankle and knee to ensure the overall safety. The design has a maximum strength for a weight of 20 kg (ER4), with a lifespan of three years, an approximate of  $2.37 \times 10^7$  cycles (ER5). The calculations can be found in Appendix C.

The foot design consists of a single-axis foot with a torsion spring of  $808.59 \text{ Nmm/}^\circ$  to ensure the required ankle-rotational stiffness of a child as described by Shamaei (2011) (ADP4). The overall dimensions of the ankle design were based on the size requirements for the ankle, following this, a simple hinge joint was designed. A plastic spacer was used to ensure that the spring moved along the pin of the hinge joint without increasing the weight of the foot unnecessarily (ADP1). The Activity level of the foot prosthetic is between K2 and K3 (ADP3, Table 3). The deflection of the foot plate, torsion spring and bumpers absorbs shock to ensure a comfortable gait (ADP2).

The pylon device consists of static (PDP2) overlapping tubes with a clamp collar, the pylon can be adjusted to any height by a total of 45 mm, thus allowing for any small changes in growth. The tubes have a 22 mm outer diameter to ensure the use of standard paediatric adapters (Ossur 2016b) (ER11).

The knee design is based on the PASPL design by Ngan (2015), it is designed to have a zone of instability of 54.8% (ER9, KDP1). This knee ensures stability through a control axis and locking mechanism. The locking mechanism is kept in place with the use of a lock spring, a small moment of 0.1255 Nm is necessary to unlock the knee to allow swing phase to occur. This moment is created in the toe-off stage of the gait cycle. The extension assist mechanism consists of a spring of stiffness 3.34 N/mm that can easily be removed and replaced with a spring of a different stiffness as required for the swing phase (ER3, KDP7). It is necessary for the knee to allow a minimum of 50° of flexion to ensure toe-clearance is reached (Pinzone et al. 2014), however, it is recommended in the literature that a total of 150° is better for toddlers at play (Andrysek 2009). The final design of the knee has a total of 67.3° (KDP5), this allows for toe-clearance but the difficulty in playing or sitting.

The overall prosthetic design ensures the use of standard paediatric adapters to connect each prosthetic device to the next (ER11). The design uses materials sourced in South Africa (ER6) (Excluding the prosthetic adapters) and makes use of basic workshop facilities as well as laser cutting (ER7). Overall the design is cosmetically appealing and has no edges that would result in difficulty in putting on clothing (ER10), the plastic components can also be made in different colours for toddlers to enjoy.

A prototype was manufactured to test the functionality of the design, the prototype of the knee consists of a PLA body which was 3D printed. Future designs, however, require Delrin to be used due to the strength requirements determined in the FEA analysis of the knee in which a Von Mises stress of 56.7 MPa occurred when front pressure was applied (Plotz 2016). The overall weight of the design is 933 g, with the larger weights being closer to the torso, this is acceptable for toddler use due to the total weight of a toddler's leg being between 2.2 and 27 kg (Zinke-Allmang 2009; Selles 2002). The engineering requirement for low cost was reached for this design, the overall cost of the prototype is R21 458.19 for the three year period, excluding the cost of a socket and foot cover (ER8).

The Design Parameters (DPs) for each component was determined to ensure that the functional requirement of natural gait was met. To ensure that natural gait was achieved, yet still ensuring the safety of the design (ER9), a gait emulator was designed and developed. The gait emulator consists of a linear actuator which emulates the vertical excursion of the limb during the stance phase,



calculated to be a total height of approximately 20 mm and a rotary actuator emulating the hip flexion and extension moment of the hip, a range of motion of  $51.24^\circ$  (Chester et al. 2006). This was done through the control of an Arduino as well as a SEW Movidrive. The emulator makes use of a Bertec treadmill to emulate the horizontal motion of gait. The effect on the changes in height and foot length as well as the adjustability of the stiffness of the extension assist spring was considered.

From the results and discussion in Section 5, it is concluded that the Arduino microcontroller timing limitations affected the timing of the occurrence of toe-off. Toe-off is an essential factor to unlock the knee, unfortunately, with this control, this could not be achieved. It was concluded that the zone of instability, the moment required to unlock the knee and the extension assist spring did not affect the gait emulation. It is recommended that in future gait emulator tests, a faster controller is used as well as additional feedback control with respect to the GRF – thus ensuring that toe-off will occur in the gait cycle.

The standard deviation average for each age group's kinematic angles is  $2.09$ ,  $2.1$  and  $1.91^\circ$  for age groups three, four and five years respectively. This shows that the change in height and foot length had no effect on the overall functionality of the design. The effect of the adjustability of the spring cannot fully be determined due to the previously mentioned out of sync toe-off, however, it is noted that spring A has the lowest standard deviation of the knee angle at  $0.76^\circ$ , this spring is slightly less stiff than the original design stiffness,  $2.416$  N/mm. This is likely due to the low weight of the prosthetic limb during the emulation, thus a spring of a lower stiffness is recommended for lighter users.

During the gait emulation, the importance of toe-clearance in the knee design was determined. When insufficient toe-clearance occurs the knee unlocks during the stance phase resulting in the knee buckling. Though this is not expected when a proper heel strike occurs it will be important in the future to determine adequate toe-clearance occurs to prevent the knee buckling. It is recommended that if knee buckling does persist a larger lock moment should be considered by use of a stiffer lock spring.

From the emulation, it is also concluded that further analysis on the plantar flexion bumper is required to allow for a more controlled plantar flexion in the ankle. Additionally, due to poor toe-off, the torsion spring did not deflect as required, thus not allowing for the required push off, further analysis on the action of the torsion spring is required to determine its ability to increase the torsion and ROM of the ankle.

It can be concluded that a stable lower limb, above-knee prosthetic has been manufactured. The prosthetic can successfully support the gait of the user to

enable in assisted walking. The prosthetic is entirely adjustable to facilitate the three-year growth of a child between the ages of three and five years. These methods of adjustment can be used for older individuals while ensuring the overall strength is increased. The final design is low in cost thus ensuring a positive socioeconomic impact on South Africa.

## 7 References

Ace wire, Properties of common spring materials.

Afrose, M.F. et al., 2016. Effects of part build orientations on fatigue behaviour of FDM-processed PLA material. *Progress in Additive Manufacturing*, 1(1–2), pp.21–28. Available at: <http://link.springer.com/10.1007/s40964-015-0002-3> [Accessed August 30, 2016].

Andrysek, J., 2009. *Development of prosthetic knee joint technologies for children and youth with above-knee amputations*,

APC Prosthetic, 2016. Children’s Prosthetic Options – APC Prosthetics. Available at: <http://apcprosthetics.com.au/childrens-prosthetic-options/>.

Baker, R., 2011. Globographic visualisation of three dimensional joint angles. *Journal of Biomechanics*, 44(10), pp.1885–1891. Available at: <http://linkinghub.elsevier.com/retrieve/pii/S0021929011003514> [Accessed May 20, 2017].

Bay Plastics Ltd, 2016. Oil Filled Nylon : Oilon, Ertalon LFX & Nylube | Bay Plastics Ltd. Available at: <http://www.bayplastics.co.uk/oilfillednylon.htm> [Accessed July 13, 2016].

Beardmore, R., 2013. Shock Absorbers. Available at: [http://www.roymech.co.uk/Useful\\_Tables/Cams\\_Springs/Shock\\_absorbers.html](http://www.roymech.co.uk/Useful_Tables/Cams_Springs/Shock_absorbers.html).

Bertec, 2016. Instrumented Treadmills | Bertec Corporation. Available at: <http://bertec.com/products/instrumented-treadmills/> [Accessed July 25, 2017].

Bicycle riding, 2016. Bicycle Seat Post - Many Types To Choose From. Available at: <http://www.bicycle-riding.com/bicycle-riding/bicycle-parts/bicycle-seat-post/> [Accessed August 8, 2016].

Boonstra, A.M. et al., 2000. Children with congenital deficiencies or acquired amputations of the lower limbs: Functional aspects. *Prosthetics and Orthotics International*, 24(1), pp.19–27. Available at: <http://www.ncbi.nlm.nih.gov/pubmed/10855435> [Accessed July 21, 2017].

Brackx, B. et al., 2012. Passive Ankle-Foot Prosthesis Prototype with Extended Push-Off Regular Paper. *International Journal of Advanced Robotic Systems*, 10(101).

Buczek, F.L. et al., 2006. Performance of an inverted pendulum model directly applied to normal human gait. *Clinical Biomechanics*, 21(3), pp.288–296. Available at: <http://www.ncbi.nlm.nih.gov/pubmed/16325971> [Accessed August 22, 2017].

Budynas, R. & Nisbett, K., 2011. *Shigley’s Mechanical Engineering Design* 9th ed., McGraw-Hill.

Castellanos, D., Gomez, J. & Crystal, G., 2016. EML 4905 Senior Design Project Adjustable Lower Limb Prosthetics for Children Final Report Ethics Statement and Signatures.

Cavagna, G.A., Franzetti, P. & Fuchimoto, T., 1983. The mechanics of walking in children. *The Journal of physiology*, 343, pp.323–39. Available at:

- <http://www.ncbi.nlm.nih.gov/pubmed/6644619> [Accessed January 20, 2017].
- Ceri, C.N., 2013. Design analysis of the four-bar Jaipur-Stanford prosthetic knee for Developing countries. Available at: <https://dspace.mit.edu/handle/1721.1/83688> [Accessed July 12, 2017].
- Chester, V.L., Tingley, M. & Biden, E.N., 2006. A comparison of kinetic gait parameters for 3–13 year olds. *Clinical Biomechanics*, 21(7), pp.726–732. Available at: <http://www.sciencedirect.com.ez.sun.ac.za/science/article/pii/S0268003306000507> [Accessed May 19, 2017].
- Choi, H.J. & Kim, B.K., 2008. Generation of a Energy Efficient Biped Robot’s Walking Trajectory based on a Jacobian.
- Clements, C., 2016. Modern Prosthetic Limbs - How Prosthetic Limbs Work | HowStuffWorks. Available at: <http://science.howstuffworks.com/prosthetic-limb2.htm> [Accessed June 7, 2016].
- Cockcroft, J., 2017. Neuromechanics Unit (Human Movement Analysis). Available at: <http://www.sun.ac.za/english/faculty/science/CAF/units/neuromechanics> [Accessed July 25, 2017].
- Cummings, D. & Kapp, S., 1992. Lower-Limb Pediatric Prosthetics: General Considerations and Philosophy - Journal of Prosthetics and Orthotics, 1992 | American Academy of Orthotists & Prosthetists. *American Academy Orthotists & Prosthetists*, 4(4), pp.196–206. Available at: [http://www.oandp.org/jpo/library/1992\\_04\\_196.asp](http://www.oandp.org/jpo/library/1992_04_196.asp).
- Cupp, T. et al., 1999. Age-related kinetic changes in normal pediatrics. *Journal of pediatric orthopedics*, 19(4), pp.475–478. Available at: [http://journals.lww.com/pedorthopaedics/Abstract/1999/07000/Age\\_Related\\_Kinetic\\_Changes\\_in\\_Normal\\_Pediatrics.10.aspx](http://journals.lww.com/pedorthopaedics/Abstract/1999/07000/Age_Related_Kinetic_Changes_in_Normal_Pediatrics.10.aspx) [Accessed December 14, 2016].
- D-Rev, 2015. Mobility Impact Dashboard | D-Rev. Available at: <http://d-rev.org/impact/remotion/> [Accessed June 20, 2016].
- Dictionary, 2017. Kinematics | Define Kinematics at Dictionary.com. Available at: <http://www.dictionary.com/browse/kinematics> [Accessed February 1, 2017].
- Eames, M.H.A., Cosgrove, A. & Baker, R., 1999. Comparing methods of estimating the total body centre of mass in three-dimensions in normal and pathological gaits. *Human Movement Science*, 18, pp.637–646. Available at: [www.elsevier.com/locate/humov](http://www.elsevier.com/locate/humov) [Accessed January 18, 2017].
- Eastlack, M.E. et al., 1991. Interrater reliability of videotaped observational gait-analysis assessments. *Physical therapy*, 71(6), pp.465–72. Available at: <http://www.ncbi.nlm.nih.gov/pubmed/2034709> [Accessed December 14, 2016].
- Eng, J.J. & Winter, D.A., 1995. Kinetic analysis of the lower limbs during walking: what information can be gained from a three-dimensional model? *J. Biomechanics*, 28(6), pp.753–758.

- Engineering Toolbox, 2016. Modulus of Elasticity or Young's Modulus - and Tensile Modulus for common Materials. Available at: [http://www.engineeringtoolbox.com/young-modulus-d\\_417.html](http://www.engineeringtoolbox.com/young-modulus-d_417.html) [Accessed June 2, 2017].
- Faulhaber, 2011. Faulhaber catalog.
- FDA, 2016. Classify Your Medical Device. Available at: <https://www.fda.gov/MedicalDevices/DeviceRegulationandGuidance/Overview/ClassifyYourDevice/> [Accessed July 12, 2017].
- Fillauer Companies, 2011. Prosthetic Product Information Guide.
- Fillauer LLC, 2016. Mini Shock Pylon.
- Fisk, J., 1992. 31: Introduction to the Child Amputee | O&P Virtual Library. Available at: <http://www.oandplibrary.org/alp/chap31-01.asp>.
- Friberg, O., 1984. Biomechanical significance of the correct length of lower limb prostheses: a clinical and radiological study. *Prosthetics and orthotics international*, 8(3), pp.124–9. Available at: <http://www.ncbi.nlm.nih.gov/pubmed/6240634> [Accessed August 31, 2016].
- Furse, A., Cleghorn, W. & Andrysek, J., 2011. Development of a Low-technology Prosthetic Swing-phase Mechanism. *Journal of Medical and Biological Engineering*, 31(2), pp.145–150.
- Ganley, K.J. & Powers, C.M., 2005. Gait kinematics and kinetics of 7-year-old children: a comparison to adults using age-specific anthropometric data. *Gait & Posture*, 21(2), pp.141–145.
- Gard, S.A. & Childress, D.S., 2001. What Determines the Vertical Displacement of the Body During Normal Walking? - Journal of Prosthetics and Orthotics, 2001 | American Academy of Orthotists & Prosthetists. Available at: [http://www.oandp.org/jpo/library/2001\\_03\\_064.asp](http://www.oandp.org/jpo/library/2001_03_064.asp) [Accessed January 18, 2017].
- Greene, M.P., 1983. Four Bar Linkage Knee Analysis.
- Hanger Clinic, 2016. Lower Extremity Componentry Prosthetics – Hanger Clinic. Available at: <http://www.hangerclinic.com/limb-loss/adult-lower-extremity/Pages/Lower-Extremity-Componentry.aspx> [Accessed June 7, 2016].
- Haun, D.G., 2012. Pyramid receptacle for coupling a prosthetic limb to a socket. Available at: <http://www.google.ac/patents/US8252066> [Accessed July 14, 2017].
- Healthyfeetstore, 2016. Kids' Shoe Sizing Guide with Sizing Chart - Shopping Online for Infant, Toddler, Children, & Youth Shoes. Available at: <http://www.healthyfeetstore.com/kids-shoe-sizing-guide-with-sizing-chart.html> [Accessed June 6, 2016].
- Hof, A., 1996. Normalised Temporal-Spatial parameters.
- Imasen, 2009. IMASEN ENGINEERING CORPORATION / Lapoc System Prostheses / Children's

- Prosthetic Foot System. Available at: <http://www.imasengiken.co.jp/en/lapoc/infant.html> [Accessed May 25, 2016].
- ISO, 2006. ISO 10328:2016(en), Prosthetics — Structural testing of lower-limb prostheses — Requirements and test methods. Available at: <https://www.iso.org/obp/ui/#iso:std:iso:10328:ed-2:v1:en> [Accessed June 10, 2016].
- Ivanenko, Y.P. et al., 2005. Kinematics in Newly Walking Toddlers Does Not Depend Upon Postural Stability. *PresS. J Neurophysiol*.
- Jones, R.H. & Nelson, C.C., 1965. "Pylon-Prosthetic"; Devices for Lower Extremity Congenital Skeletal Limb Deficiencies.
- Kaufman, K. et al., 2016. Reliability of 3D gait data across multiple laboratories.
- Kinetic revolutions, 2016. Kinetic Revolutions | Adjustable Pylons. Available at: <http://www.kineticrevo.com/#!adjustable-pylons/c4vj> [Accessed June 7, 2016].
- Kirtley, C., 2016. Resolution of Forces, Friction, and the ground reaction vector. Available at: <http://www.clinicalgaitanalysis.com/teach-in/friction.html> [Accessed May 20, 2017].
- Klasson, B.L., 1995. Carbon fibre and fibre lamination in prosthetics and orthotics: some basic theory and practical advice for the practitioner. *Prosthetics and Orthotics International*, 19, pp.74–91.
- Klodd, E. et al., 2010. Effects of prosthetic foot forefoot flexibility on gait of unilateral transtibial prosthesis users. *JRRD*, 47(9).
- Klute, G.K., Berge, J.S. & Segal, A.D., 2004. Heel-region properties of prosthetic feet and shoes. *Journal of Rehabilitation Research and Development*, 41(4), pp.535–546. Available at: <http://www.rehab.research.va.gov/jour/04/41/4/Klute.html>.
- Lambert, C., 1972. Amputation surgery in the child. *Orthop Clin North Am*, 3, pp.473–482.
- LegWorks, 2016. For Prosthetists — LegWorks. Available at: <http://legworks.com/for-prosthetists>.
- Levesque, C., Gauthier-Gagon, C. & Beaugard, M., 1992. An\_Endoskeletal\_Hip\_Disarticulation\_Prosthesis\_for.8.pdf. Available at: [http://journals.lww.com/jpojournal/Citation/1991/06000/An\\_Endoskeletal\\_Hip\\_Disarticulation\\_Prosthesis\\_for.8.aspx](http://journals.lww.com/jpojournal/Citation/1991/06000/An_Endoskeletal_Hip_Disarticulation_Prosthesis_for.8.aspx).
- Lewotsky, K., 2007. Choosing the Right Linear Actuator. Available at: [http://www.motioncontrolonline.org/content-detail.cfm/Motion-Control-Technical-Features/Choosing-the-Right-Linear-Actuator/content\\_id/1051](http://www.motioncontrolonline.org/content-detail.cfm/Motion-Control-Technical-Features/Choosing-the-Right-Linear-Actuator/content_id/1051) [Accessed January 23, 2017].
- Liu, M.Q. et al., 2008. Muscle contributions to support and progression over a range of walking speeds. *Journal of biomechanics*, 41(15), pp.3243–52. Available at: <http://www.ncbi.nlm.nih.gov/pubmed/18822415> [Accessed May 12, 2017].

- Loder, R.T. et al., 2004. Long-term Lower Extremity Prosthetic Costs in Children With Traumatic Lawnmower Amputations. *Archives of Pediatrics & Adolescent Medicine*, 158(12), p.1177. Available at: <http://archpedi.jamanetwork.com/article.aspx?doi=10.1001/archpedi.158.12.1177> [Accessed July 11, 2016].
- Machine Design, 2014. Machine Design: LESSON 8. DESIGN OF KNUCKLE JOINT. Available at: <http://ecoursesonline.iasri.res.in/mod/page/view.php?id=125517>.
- Matweb, 2016. ASM Material Data Sheet. Available at: <http://asm.matweb.com/search/SpecificMaterial.asp?bassnum=MA6061t6>.
- McHugh, J., 2007. Blade Runner | WIRED. Available at: <http://www.wired.com/2007/03/blade/> [Accessed June 22, 2016].
- Military in-step, 2014. Military inStep: Prosthetic Feet. Available at: <http://www.amputee-coalition.org/military-instep/feet.html> [Accessed May 24, 2016].
- Mochon, S. & McMahon, T.A., 1980. Ballistic walking: an improved model. *Mathematical Biosciences*, 52(3), pp.241–260.
- Mohd, T., 2014. Prosthetic knee joints. Available at: <http://www.slideshare.net/megaancient/prosthetic-knee-joints> [Accessed June 20, 2016].
- Myers, 2016. Email interview.
- Narang, Y.S., 2013. Identification of Design Requirements for a High-Performance, Low-Cost, Passive Prosthetic Knee Through User Analysis and Dynamic Simulation.
- Ngan, C., 2015. DESIGN AND EVALUATION OF A PROSTHETIC KNEE JOINT BASED ON AUTOMATIC STANCE-PHASE LOCK (ASPL) TECHNOLOGY FOR CHILDREN WITH TRANSFEMORAL AMPUTATIONS.
- Nike, 2016. Nike tri-star sole. Available at: [http://www.nike.com/za/en\\_gb/launch/c/2016-04/womens-nike-free-tr-6?ref=https%253A%252F%252Fwww.google.com](http://www.nike.com/za/en_gb/launch/c/2016-04/womens-nike-free-tr-6?ref=https%253A%252F%252Fwww.google.com) [Accessed June 24, 2016].
- Nilsson, J. & Thorstensson, A., 1989. Ground reaction forces at different speeds of human walking and running. *Acta physiologica Scandinavica*, 136(2), pp.217–27. Available at: <http://www.ncbi.nlm.nih.gov/pubmed/2782094> [Accessed August 31, 2016].
- Ossur, 2016a. flex-foot® junior kits fleX-foot junior kit With male pyramid. Available at: [www.ossur.com](http://www.ossur.com) [Accessed June 6, 2016].
- Ossur, 2016b. Standard Adapters. Available at: <https://www.ossur.com/prosthetic-solutions/products/all-products/standard-adapters> [Accessed August 28, 2017].
- Otto, J., 2014. 3D Printing: Opportunity for Technicians? | July 2014 | The O&P EDGE | oandp.com. Available at: [http://www.oandp.com/articles/2014-07\\_01.asp](http://www.oandp.com/articles/2014-07_01.asp) [Accessed July 13, 2016].

- Ottobock, 2013. About feet — Ottobock UK. Available at:  
[http://www.ottobock.co.uk/prosthetics/info\\_for\\_new\\_amputees/prosthetic-technology-explained/about\\_feet/](http://www.ottobock.co.uk/prosthetics/info_for_new_amputees/prosthetic-technology-explained/about_feet/) [Accessed May 25, 2016].
- Ottobock, 2016. Keeping your leg on — Ottobock USA. Available at:  
<http://www.ottobockus.com/prosthetics/info-for-new-amputees/prosthetics-101/keeping-your-leg-on-%28suspension%29/> [Accessed June 10, 2016].
- Ounpuu, S., Gage, J.R. & Davis, R., 1991. Ounpuu et al 3D LE Joint Kinetics in Normal Ped Gait J Pediatr Orthop 1991.pdf. *Journal of Pediatric Orthopaedics*, 11(3), pp.341–9. Available at:  
[https://www.researchgate.net/publication/21100112\\_Three-Dimensional\\_Lower\\_Extremity\\_Joint\\_Kinetics\\_in\\_Normal\\_Pediatric\\_Gait](https://www.researchgate.net/publication/21100112_Three-Dimensional_Lower_Extremity_Joint_Kinetics_in_Normal_Pediatric_Gait).
- Pinzone, O. et al., 2014. The comparison of normative reference data from different gait analysis services. *Gait & Posture*, 40(2), pp.286–290. Available at:  
<http://linkinghub.elsevier.com/retrieve/pii/S0966636214002835> [Accessed July 17, 2017].
- Plotz, J., 2016. *FEA analysis of knee and ankle component for vacation training*,
- Radcliffe, C., 1955. Functional Considerations in the Fitting of Above Knee Prostheses | O&P Virtual Library. Available at: [http://www.oandplibrary.org/al/1955\\_01\\_035.asp](http://www.oandplibrary.org/al/1955_01_035.asp) [Accessed March 1, 2016].
- Radcliffe, C.W., 2003. Biomechanics of Knee Stability Control with Four-Bar Prosthetic Knees.
- Radcliffe, C.W., 1994. Four-bar linkage prosthetic knee mechanisms: kinematics, alignment and prescription criteria. , 18(1), pp.59–1.
- Richter, H. et al., 2015. Dynamic modeling, parameter estimation and control of a leg prosthesis test robot. *Applied Mathematical Modelling*, 39, pp.559–573.
- Rihs, D. & Polizzi, I., 2001. Prosthetic Foot Design.
- Rose-Jacobs, R., 1983. Development of Gait at Slow, Free, and Fast Speeds in 3-and 5-Year-Old Children. *Physical therapy*, 63(8), pp.1251–1259.
- Rush, 2016. RUSH Kid™ |. Available at: <http://rushfoot.com/patient-home/the-rush-feet/rush-kid/> [Accessed June 23, 2016].
- Schache, A.G. & Baker, R., 2007. On the expression of joint moments during gait. *Gait & Posture*, 25(3), pp.440–452. Available at:  
<http://linkinghub.elsevier.com/retrieve/pii/S0966636206001615> [Accessed May 20, 2017].
- Schepens, B. et al., 2004. Mechanical work and muscular efficiency in walking children. *Journal of Experimental Biology*, 207(4).
- Schmalz, T., Blumentritt, S. & Jarasch, R., 2002. Energy expenditure and biomechanical characteristics of lower limb amputee gait: the influence of prosthetic alignment and different prosthetic components. *Gait & posture*, 16(3), pp.255–63. Available at:  
<http://www.ncbi.nlm.nih.gov/pubmed/12443950> [Accessed December 14, 2016].



- Schwartz, M.H., Rozumalski, A. & Trost, J.P., 2008. The effect of walking speed on the gait of typically developing children - ClinicalKey. *Journal of Biomechanics*, 41(8), pp.1639–1650. Available at: <https://www-clinicalkey-com.ez.sun.ac.za/#!/content/playContent/1-s2.0-S0021929008001450> [Accessed January 26, 2017].
- Selles, R.W., 2002. *Weighing weight : effect of below-knee prosthetic inertial properties on gait*, s.n.].
- Shamaei et al., 2011. On the Mechanics of the Ankle in the Stance Phase of the Gait.
- Shriners Hospital, 1987. Clinical gait analysis data.
- Smith, D., 2006. inMotion: Congenital Limb Deficiencies and Acquired Amputations in Childhood, Part 1. Available at: [http://www.amputee-coalition.org/inmotion/jan\\_feb\\_06/congenital\\_limb\\_part1.html](http://www.amputee-coalition.org/inmotion/jan_feb_06/congenital_limb_part1.html) [Accessed May 24, 2016].
- Snyder, R.G. et al., 1977. Anthropometry of infants, children, and youths to age 18 for product safety design. , 1. Available at: <https://deepblue.lib.umich.edu/handle/2027.42/684>.
- Stansfield, B.W. et al., 2001. Normalized speed, not age, characterizes ground reaction force patterns in 5-to 12-year-old children walking at self-selected speeds. *Journal of pediatric orthopedics*, 21(3), pp.395–402. Available at: <http://www.ncbi.nlm.nih.gov/pubmed/11371828> [Accessed November 23, 2016].
- Strait, E. & Resident, P., 2006. Prosthetics in Developing Countries.
- Sutherland, D. et al., 1980. The development of mature gait The Development of Mature Gait\*. *J Bone Joint Surg Am*, 62, pp.336–353.
- Swart, W., Department of Mechanical and Mechatronic Engineering 3D Printing Guide. Available at: [http://www.sun.ac.za/english/faculty/eng/mechanical-mechatronic/Documents/Undergraduate/Current UG/2016-11-23 MM\\_3D\\_printing\\_doc.pdf](http://www.sun.ac.za/english/faculty/eng/mechanical-mechatronic/Documents/Undergraduate/Current UG/2016-11-23 MM_3D_printing_doc.pdf) [Accessed June 2, 2017].
- Thompson, D., 2002. Energy and power during the gait cycle. Available at: <http://coph.ouhsc.edu/dthomps/web/gait/epow/pow1.htm> [Accessed June 29, 2016].
- Trulife, 2011. Child’s Play Energy.
- Vicon, 2017. Biomechanics and Sport | VICON. Available at: <https://www.vicon.com/motion-capture/biomechanics-and-sport> [Accessed July 25, 2017].
- WillowWood, 2016. Pediatric Pylons & Pylon Adapters | WillowWood | Free the body. Free the spirit. Available at: <https://www.willowwoodco.com/products-services/pediatric/pediatric-modular-components/pediatric-pylons-pylon-adapters/> [Accessed June 7, 2016].
- Zinke-Allmang, M., 2009. *Physics for the Life Sciences* Nelson Education Ltd., ed., Toronto. Available at: <https://www.amazon.com/Physics-Life-Sciences-M-Zinke-Allmang/dp/0176442596>.

## Appendix A Information for the design of the prosthetic

### A.1 Data of the growth and development of a child

**Table 14: Measurement data**

	Measurement (mm) Reference	Age (year)		
		3	4	5
Foot length	(Snyder et al. 1977)	147	161	170
Foot-breadth	(Snyder et al. 1977)	61	65	68
Shoe size	Min	159	168	178
	(Healthyfeetstore 2016) Max	165	171	181
Buttock-Knee length	(Snyder et al. 1977)	284	314	339
Knee height	(Snyder et al. 1977)	270	299	323
Standing CG	(Snyder et al. 1977)	560	594	645
Total height	UK growth chart	955	1028	1095
Weight (kg)	(Snyder et al. 1977)	14.1	16.2	18.3

## A.2 Design data

Table 15: Material properties

	Material	Grade	Characteristic	Symbol	Value	Ref**	
Metal	Aluminium	Generic	Modulus of elasticity	E.al (GPa)	69	[1]	
			Density	$\rho$ .al (g/m <sup>3</sup> )	2700	[1]	
			Ultimate tensile strength	S.u (MPa)	110	[1]	
			Shear strength	$\tau$ .u (MPa)	207	[2]	
			Allowable compressive stress	$\sigma$ .c (MPa)	110	[1]	
			Fatigue strength*	S.f (MPa)	138	[3]	
		2024 T3 Aluminium		Ultimate tensile strength	S.u (MPa)	482	[3]
		Steel	Generic	Modulus of elasticity	E.st (GPa)	200	[1]
	Density			$\rho$ .st (g/m <sup>3</sup> )	8500	[1]	
			1006 HR steel	Ultimate tensile strength	S.u (MPa)	300	[3]
	Yield strength			S.y (MPa)	170	[3]	
	Music wire		Modulus of elasticity	E.st (GPa)	207	[4]	
			Ultimate tensile strength	S.u (MPa)	1586	[4]	
Fibre	Titanium alloy		Modulus of elasticity	E.al (GPa)	105	[1]	
			Density	$\rho$ .al (g/m <sup>3</sup> )	4510	[1]	
			Ultimate tensile strength	S.u (MPa)	900	[1]	
			Yield strength	S.y (MPa)	730	[1]	
	Glass			Modulus of elasticity	E (GPa)	70	[5]
				Tensile stress at failure	S.u (MPa)	3400	[5]
	Carbon			Modulus of elasticity	E (GPa)	210	[5]
				Tensile stress at failure	S.u (MPa)	2600	[5]
	Plastic	Nylon 6		Ultimate tensile strength	S.u (MPa)	70	[2]
				Compressive yield strength	S.y (MPa)	55	[2]
Polypropylene			Ultimate tensile strength	S.u (MPa)	40	[2]	
			Compressive yield strength	S.y (MPa)	40	[2]	
HDPE			Ultimate tensile strength	S.u (MPa)	15	[2]	
			Compressive yield strength	S.y (MPa)	20	[2]	
Polyacetal resin (Delrin)			Ultimate tensile strength	S.u (MPa)	70	[6]	
			Compressive yield strength	S.y (MPa)	70	[6]	
PLA			Compressive strength	$\sigma$ .c (MPa)	17.9	[7]	
			Tensile strength	S.u (MPa)	46.7	[7]	
ABS		Compressive yield strength	$\sigma$ .c (MPa)	7.58	[7]		
		Ultimate Tensile Strength	S.u (MPa)	34	[7]		

\*Corresponds to  $50 \times 10^7$  cycles of completely reversed stress

\*\*[1] = (Engineering Toolbox 2016), [2] = (Matweb 2016), [3] = (Budynas & Nisbett 2011), [4] = (Ace wire n.d.), [5] = (Klasson 1995), [6] = (Ngan 2015), [7] = (Swart n.d.)

### A.3 Foot design

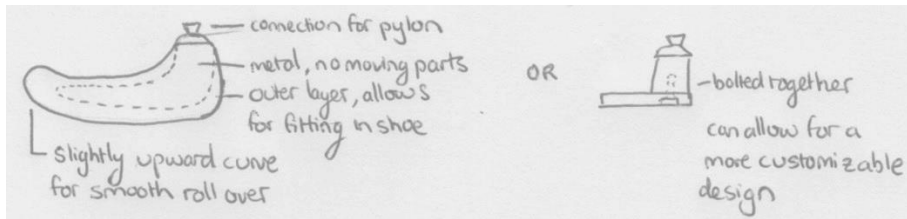


**Figure 42: Design Option 1: SACH foot**

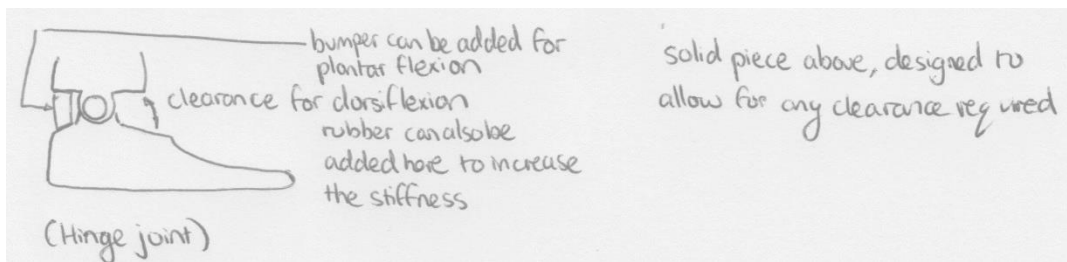


**Figure 43: Design Option 2: Single-axis foot**

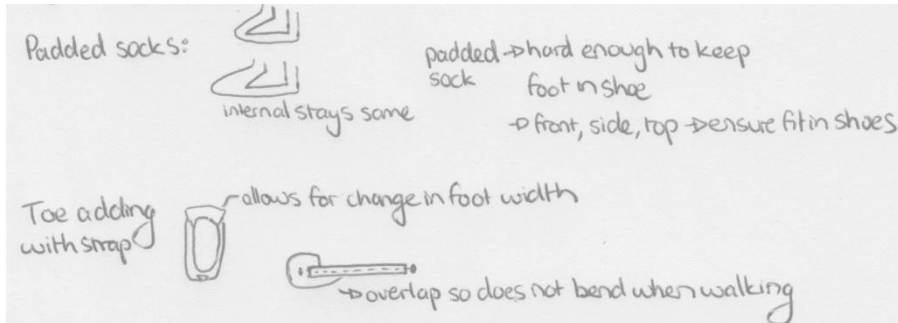


**Figure 44: Length adjustment option 1: Padded Socks/Straps**

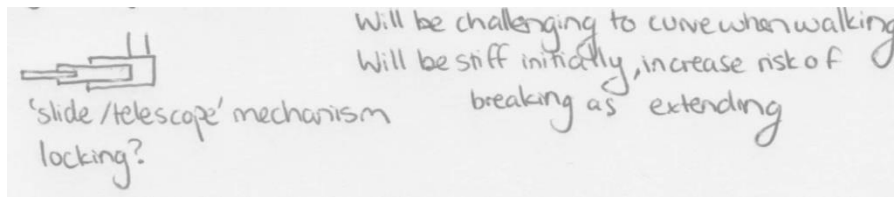


**Figure 45: Length adjustment option 2: Slide mechanism**

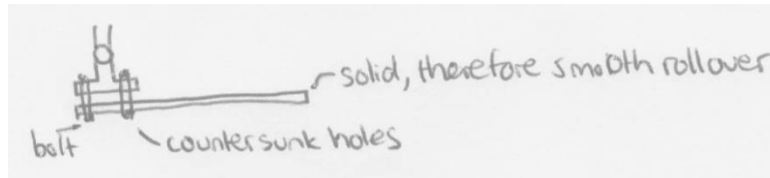


**Figure 46: Length adjustment Option 3: Replace flat foot component**



**Figure 47: Auxetic tri-star sole (Nike 2016)**

## A.4 Pylon design



Figure 48: Adjustable pylons (Kinetic revolutions 2016)

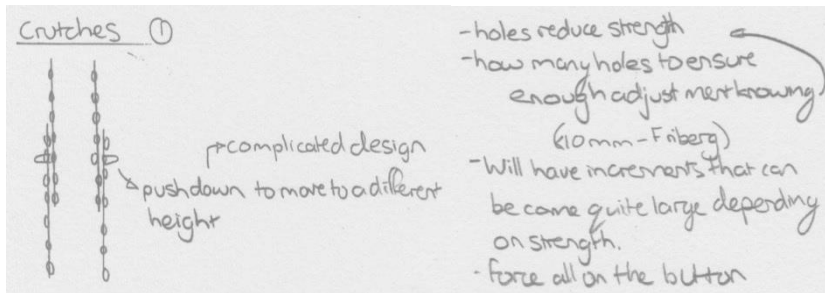


Figure 49: Leg design 1 version 1: Based on crutches

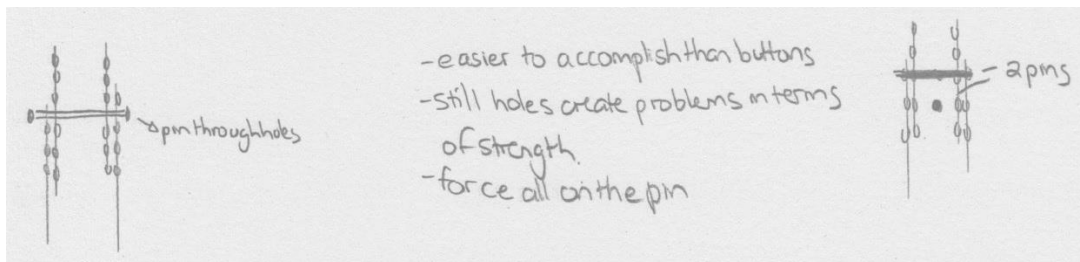


Figure 50: Leg design 1 version 2: Based on pin adjustments

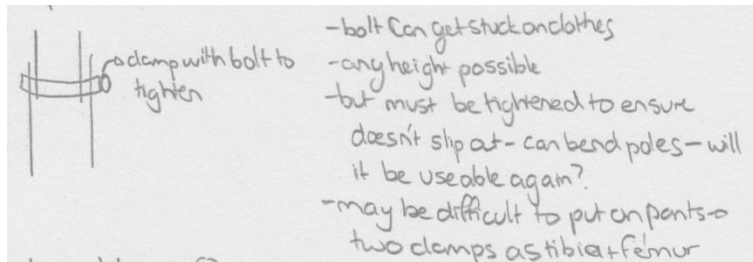


Figure 51: Leg design 2: Clamp design

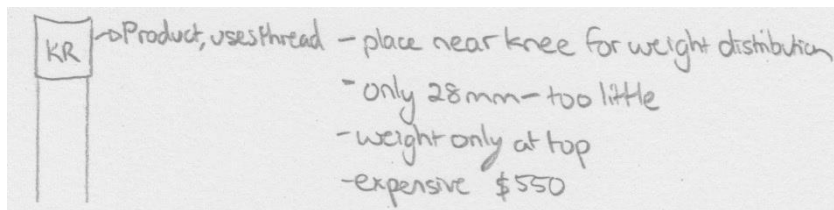


Figure 52: Leg design 3 version 1: Use of the Kinetic Revolution (2016) adjustable pylon

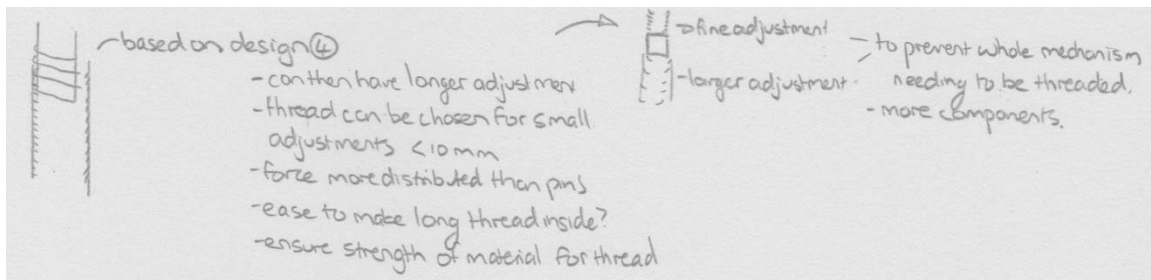


Figure 53: Leg design 3 version 2: Use of screw design

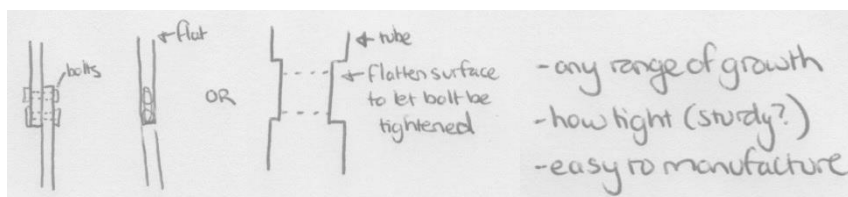
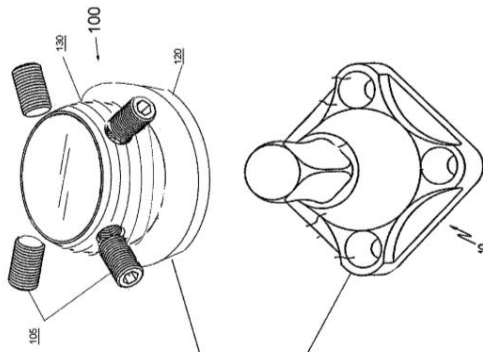
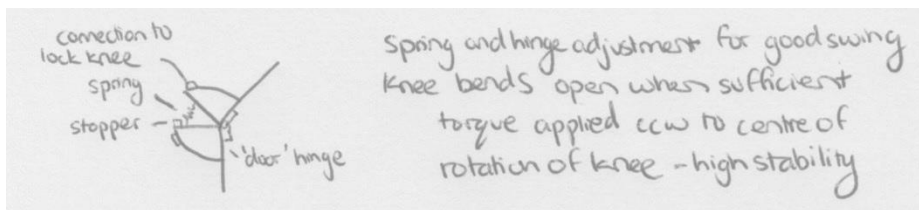


Figure 54: Leg design 4: Key/slot design



**Figure 55: Pyramid adapter (Haun, 2012)**

## A.5 Knee design



**Figure 56: Design Option 1: Single-axis with spring**

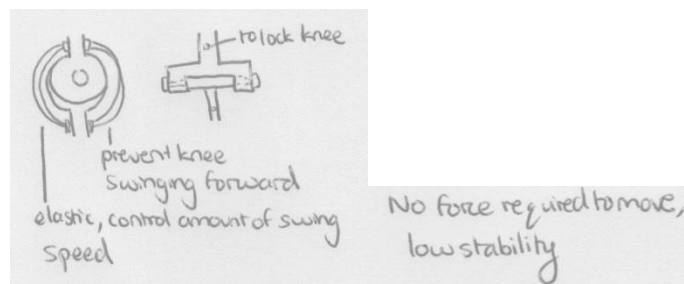


**Figure 57: Design Option 2: Single-axis, no spring**



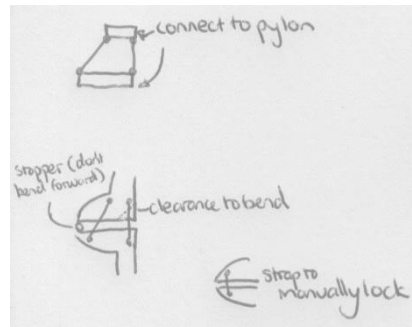


**Figure 58: Design option 3: polycentric knee**

## A.6 Parts lists for final designs

**Table 16: Parts list for foot and ankle design**

PART NO.	DESCRIPTION	AMOUNT	MATERIAL	SIZE	WORKSHOP	3D	OFF SHELF
<b>A01</b>	OUTER FOOT BRACKET	1	ALUMINIUM	39X10.5X20	*		
<b>A02</b>	INNER FOOT BRACKET	2	ALUMINIUM	42X57X22.3	*		
<b>A03</b>	ANKLE TORSION SPRING	1	MUSIC WIRE		MADE		
<b>A04</b>	SPACER	1	PVC	D13.5X20.5	*		
<b>A05</b>	FOOT PLATE	1	ALUMINIUM	68X170X	LASER		
<b>A06</b>	ANKLE PIN	1	ALUMINIUM	8X68	*		
<b>A07</b>	DORSI FLEXION BUMPER	1	PVC	M11X12	*		
<b>A08</b>	PLANTAR FLEXION BUMPER	1	PVC	M11X9	*		
<b>A09</b>	SILICON BUTTONS	2	SILICON	M11X8	*		*
<b>A10</b>	M3 BOLT	4	STEEL	M3X10			*
<b>A11</b>	M4 BOLT	2	STEEL	M4X10			
<b>A12</b>	EXTERNAL CIRCLIP 8	1	STEEL	D8			*

**Table 17: Parts list for pylon design**

PART NO.	DESCRIPTION	AMOUNT	MATERIAL	SIZE	WORKSHOP	3D	OFF SHELF
S01	Bottom shaft	1	ALUMINIUM	22x1 pipe (75 mm)	*		
S02	Top shaft	2	ALUMINIUM	22x2 pipe (111mm)	*		
S03	Clamp	1	STEEL	22 inner diam			*

**Table 18: Parts list for the knee design**

PART NO.	DESCRIPTION	AMOUNT	MATERIAL	SIZE	WORKSHOP	3D	OFF SHELF
K01	BODY	1	PLASTIC	53X104X59.4	*(HOLES)	*	
K02	LOCK	1	TOOL STEEL	15X6X80	*		
K03	BOTTOM	1	ALUMINIUM	52X34X34	*		
K04	TOP	1	PLASTIC		*(HOLES)	*	
K05	EXTENSION ASSIST BOTTOM SHAFT	1	18-8 STAINLESS STEEL	M4X34	*		
K06	EXTENSION ASSIST MAIN SHAFT	1	18-8 STAINLESS STEEL	M8X80	*		
K07	EXTENSION ASSIST TOP SHAFT	1	18-8 STAINLESS STEEL	M4X34	*		
K08	SPRING BOTTOM ANCHOR	1	PVC 17-4 STAINLESS	M16X44	*		
K09	TOP SHAFT	1	STEEL	D8X52	*		
K10	M4 X20	1	STEEL				*
K11	M5 X10	2	STEEL				*
K12	M5 WASHER	2	STEEL				*
K13	M4 WASHER	1	STEEL				*
K14	CIRCLIP M6	1	STEEL	M6			*
K15	KNEE SPRING TOP ANCHOR	1	ALUMINIUM BRONZE	D16	*		
K16	SLEEVE BUSHING	4	PLASTIC	D10X8	*		
K17	SHIM DOWEL BUMPER	1	SILICONE TUBE 303 STAINLESS	D5X17	*		
K18	NYLOCK NUT	1	STEEL	D20 X5			
K19	BOTTOM SHAFT	1	17-4 STAINLESS STEEL	D8X52	*		

<b>K20</b>	M8 WASHER FRICTION CONTROL	2	PLASTIC 18-8 STAINLESS	M8X2	
<b>K21</b>	SCREW	1	STEEL	M4X56	*
<b>K22</b>	M8 SET SCREW	1	STEEL 18-8 STAINLESS	M8X10	
<b>K23</b>	TOP SHIM DOWEL	1	STEEL	D4X50	*
<b>K24</b>	TOP SHIM	2	UHMW STAINLESS STEEL	39X35X1.6	*
<b>K25</b>	LOCK INSERT	1	SHEET	21X19X5	*
<b>K26</b>	LOCK SPRING	1	POLYURETHANE	D6.35MM	
<b>K27</b>	EXTENSION ASSIST SPRING	3	COMPRESSION	ID12.6XFL44	*
<b>K29</b>	M3 X 10	1	STEEL		*

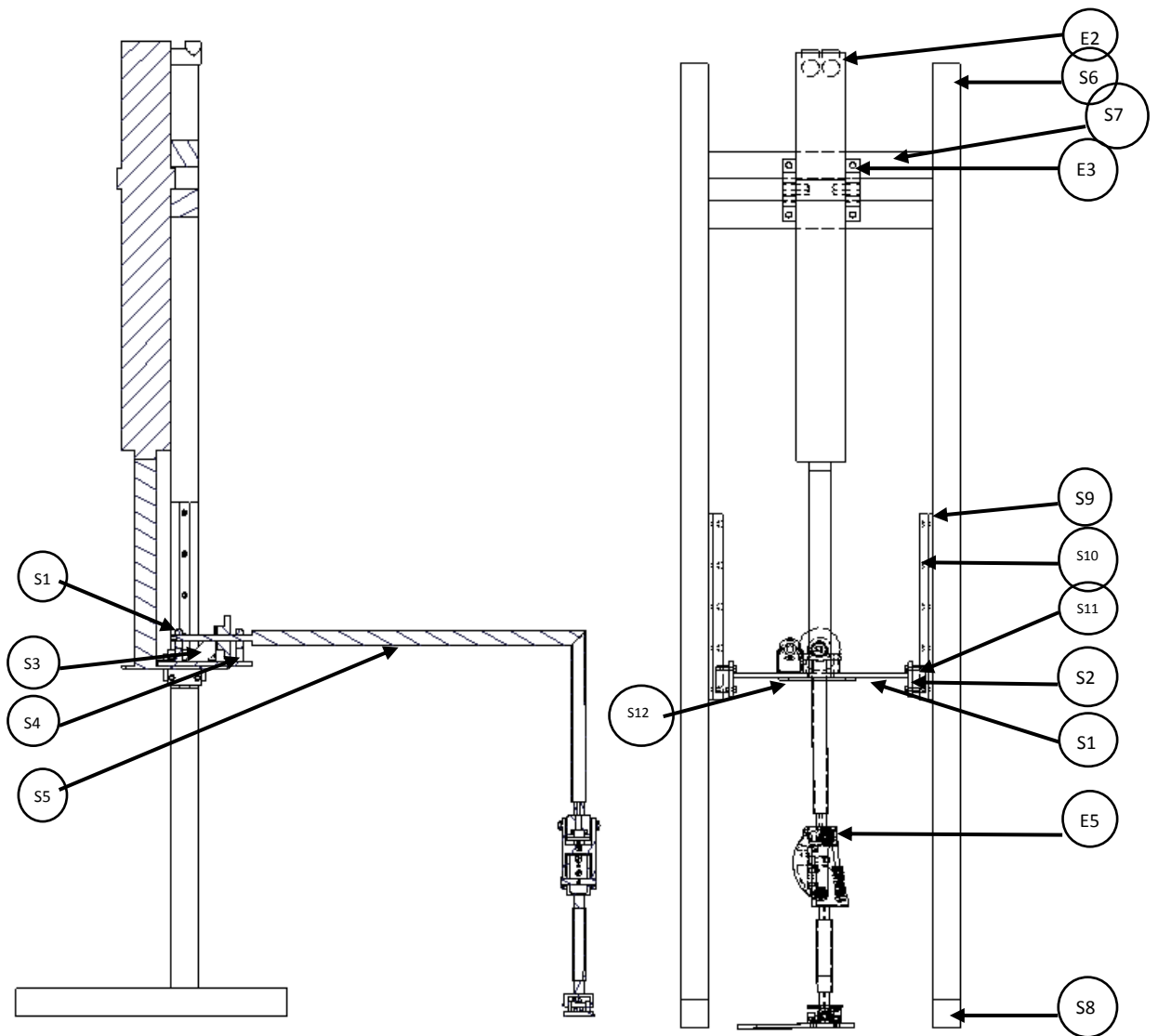


Figure 59: Final assembly drawing of test structure

**Table 19: Parts list for test structure, see Figure 59**

PART NO.	DESCRIPTION	AMOUNT	MATERIAL	SIZE	WORKSHOP	3D	OFF SHELF
JTS1	TOP PLATE	1	AL	257X140X6	*		
JTS2	SIDE FOR PLATE	2	AL	50X50X6	*		
JTS3	MOTOR BRACKET	1	N/A	N/A	*		
JTS4	HEIGHT BLOCK	1	ST	58X20X10	*		
JTS5	L-BEAM	3	ST	VERTICAL: 249; 279; 305	*		
JTS6	VERTICAL BEAM	2	AL		1360		*
JTS7	MIDDLE BEAM	2	AL		329		*
JTS8	BASE BEAM	2	AL		400		*
JTS9	SPACER	2	ST	270X40X6	*		
JTS10	LINEAR GUIDE RAIL	2	ST		270		*
JTS11	LINEAR CARRIAGE	2	ST	N/A			*
JTS12	LINEAR ACTUATOR PLATE	1		150X110X6	*		
JTS13	GEAR MOD 2	1			60		*
JTS14	GEAR MOD 2	1			30		*
JTS15	PILLOW BEARING	2		BOREHOLE 10			*
JTE1	MOTOR	1		N/A			*
JTE2	LINEAR ACTUATOR	1		N/A			*
JTE3	LINEAR ACTUATOR MOUNTS	2		N/A			*
JTE4	BERTEC TREADMILL	1		N/A			*
JTE5	ADJUSTABLE ABOVE KNEE PROSTHETIC	1		N/A	*		
JTE6	WEIGHTS	N/A		KG: 7; 2.6; 3			*
JTP1	ARDUINO MEGA 2560	1		N/A			*
JTP2	MOTOR DRIVER	1		N/A			*
JTP3	MOVIDRIVE B	1		N/A			*
JTP4	ETHERNET ADD ON	1		N/A			*
JTP5	EMERGENCY BUTTON	1		N/A			*
JTP6	LIMIT SWITCH	2		N/A			*

## Appendix B Structural strength test requirements

### B.1 Overview of tests

There are two types of tests, Principal Structural Tests and Separate Structural tests, each involving static and cyclic tests. These tests are done to determine the

- Proof strength
- Ultimate strength
- Fatigue strength
- Static strength in torsion and security against clamped components

### B.2 Test loads

The test loading levels supplied in the ISO standard are for adults, P5, P4 and P3 with a weight of 100 kg, 80 kg and 60 kg respectively. The loads in the principal tests have further conditions known as I and II. Condition I is related to the instant of maximum loading occurring early in the stance phase of walking, while condition II is related to the instant of maximum loading occurring late in the stance phase of walking (ISO 2006). The requirements for the prosthetic developed in this thesis is for a child of maximum weight 20 kg (for safety), which is much lower than the lowest loading level P3. Due to this large difference in weight of the lowest level compared to the required level the forces were analysed to determine a feasible method to downscale the force components.

Colombo et. al. (2010) considered comparing the height and weight of a Hybrid III dummy to the P3 level to determine a scaling ratio. The correct weight, however, was not considered as the settling force of condition I (736 N = 75 kg) was used instead of the stated 60 kg for the P3 individual. An alternative method is considered here in which the weight of the individual could be compared to the test forces. This method is feasible as the force of weight is being compared to a testing force. The only force that required scaling was  $F_{cr}$  the cyclic range, the remainder of the forces are related to  $F_{cr}$  according to formulas supplied in the standard.

The weight of each level, in Newtons, was plotted alongside the  $F_{cr}$  value. It was further assumed that an individual of 0 kg weight would result in 0 N force. A trendline could then be determined from the data. This method was done for the  $F_{cr}$  value for condition I, II and for the separate ankle foot prostheses test (see

Figure 60 and Figure 61). The scaled values can be found in Table 20. As can be seen in the graphs the best fit was a polynomial, this is most likely due to the small amount of data available. Though the straight line is conservative as the weight of the individual gets larger, the second order polynomial is more conservative at lower weights. Therefore it will be more conservative to use the polynomial values. Test forces that are the same for all test loading levels were not scaled. The test forces for separate test on knee locks are the same for all loading levels, therefore, cannot be scaled. However, the test forces are much higher than any other test forces required for the prostheses. Most of these forces correlate to approximately the P4 level for principal tests, therefore it is determined valid that the test loading requirements shall be the same values as for the principal tests for the first condition.

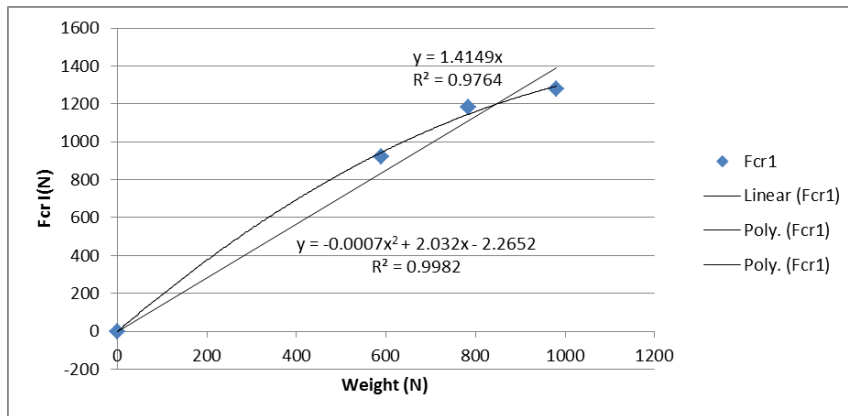


**Figure 60: Fcr with respect to weight for condition I**

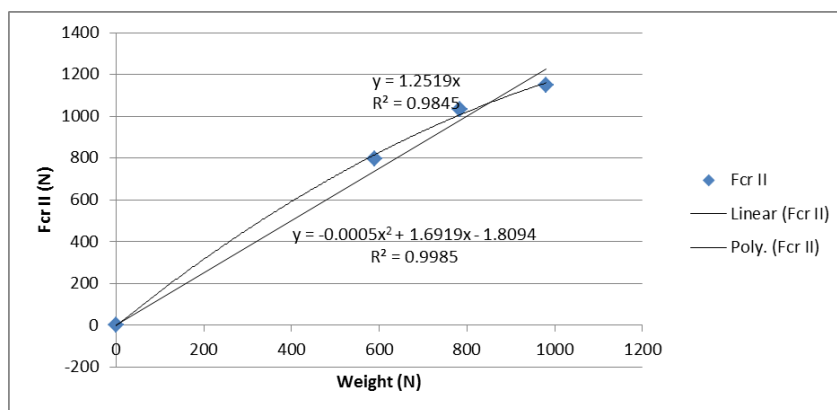


**Figure 61: Fcr with respect to weight for condition II**

### B.3 Offsets and dimensions

Refer to Figure 62, there are three axes, the u-axis, o-axis and f-axis. The u-axis is related to the height of the individual loading levels, in the ISO standard, the heights are the same for all loading levels, however, it is stated that if necessary these heights may be adjusted. F and o offsets are supplied depending on the individual loading level and the condition of the test. The axes are described below.

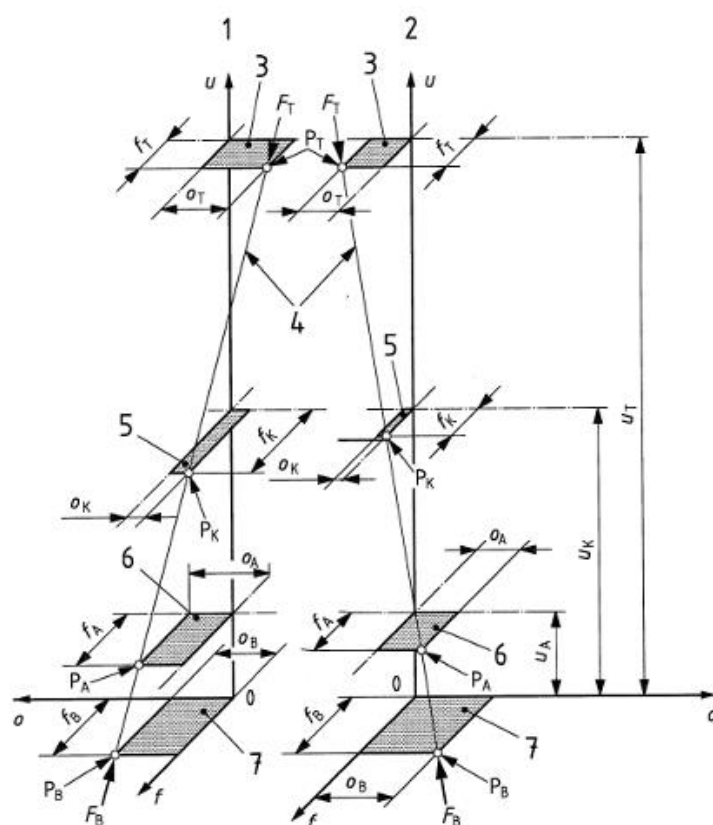


**Figure 62: Specific configuration with  $u_b=0$ , showing coordinate systems with reference planes, reference lines, reference points and test force, F, for right and left-sided application (ISO 2006)**

*Key: 1: Right leg, 2: Left leg, 3: Top reference plane, T; 4: Load line; 5: Knee reference plane, K; 6: Ankle reference plane, A; 7: Bottom reference plane, B; PT: Top load application point, PK: Knee load reference point, PA: Ankle load reference point, PB: Bottom load application point.*

- U-axis extends from origin, passes through the effective ankle-joint centre and the effective knee joint centre, positive direction upwards



- O-axis extends from the origin 0 perpendicularly to the u-axis and parallel to the effective knee-joint centre line. Positive direction outwards (left for left prostheses)
- F-axis extends from the origin 0 perpendicularly to both the o-axis and the u-axis. It's positive direction is forward towards the toe.

For this design the effective knee-joint centre line is through the monocentric axis, the top axis; and the effective ankle-joint centre line is  $\frac{1}{4}$  of the foot length (from the heel), and along the centre of the widest part of the foot. The test load is applied as shown in the figure at the location of the supplied offsets. Due to the forces being scaled due to the extreme differences in weights it will also be necessary to scale the offsets. Without scaling both larger than necessary internal moments can occur. The scaled values can be found in Table 20.

### B.3.1 Scaling of heights

The knee height of all loading levels is 500 mm (for P3, P4 and P5), this is quite different from the height of a five-year-old which is 323 mm (Table 14). It is determined through the statements in the ISO standard, quoted below, that it will be necessary to scale the heights of the force locations to ensure that the correct moments are caused for the smaller test subjects. It would also be preferable to scale the offsets in a similar fashion as was done to the test forces so that the correct moments can be caused by the ISO tests.

“10.3.6 The fixed total length shall be determined by the dimension  $u_{t-ub}$  and shall be achieved by selecting either one of the combinations specified in Table 5 for different types of the test sample or any other relevant combination. The combination of a selected length selected shall be recorded.” (ISO 2006)

The  $u$  (height) values were determined with the assumption that the child's knee height to ankle height ratio and knee height to total length (of prosthetic) ratio is similar to that of a child's proportions, see Equation 8 (this will not be very accurate, however, it is not specified how  $u$  values are determined only that they are not specifically related to the mechanical locations of the axis (ISO 2006)).

That is: 
$$ratio_{ka} = \frac{u_{kadult}}{u_{Aadult}} = \frac{500}{80} = 6.25$$

Therefore 
$$u_{Achild} = \frac{u_{kchild}}{ratio_{ka}} = \frac{323}{6.25} = 51.68 \text{ mm}$$

And 
$$ratio_{Tk} = \frac{u_{Tadult}}{u_{kadult}} = \frac{650}{500} = 1.3 \quad (8)$$

Therefore 
$$u_{Tchild} = u_{kchild}ratio_{Tk} = 323 * 1.3 = 419.9 \text{ mm}$$

### B.3.2 Scaling of offsets

The height of each test loading individual is the same as discussed in the section above, however, the offset values are different depending on the weight of the individuals – therefore it can be assumed that the offsets can be scaled in a manner similar to the scaling of the loads. In annexe B of the standard, it is stated that the ankle and knee offsets are related to the internal moment caused in the knee, which is in turn related to the axial force. The axial force  $F_u$  is related to  $F_{cr}$ , which was determined in the previous section, by Equation 9.

$$F_u = \sqrt{\left| F^2 - \left( \frac{M_{Ao} - M_{Ko}}{u_k - u_A} \right)^2 - \left( \frac{M_{Af} - M_{Kf}}{u_k - u_A} \right)^2 \right|} \quad (9)$$

The moment values are related to  $F_{cr}$ , the moment was plotted against the  $F_{cr}$  value and it was determined that a linear correlation was the most feasible as can be seen in Figure 63 and Figure 64. The offsets were then determined by the formulas in Equation 10.

$$f_A = \frac{M_{Ao}}{F_u}, o_A = -\frac{M_{Af}}{F_u}, f_K = \frac{M_{Ko}}{F_u}, o_K = -\frac{M_{Kf}}{F_u} \quad (10)$$

Due to steep gradients for some of the offsets and shallow gradients for others, it is difficult to correlate exact values, however, these values were not further adjusted as this method correlates to the method of scaling the loads.

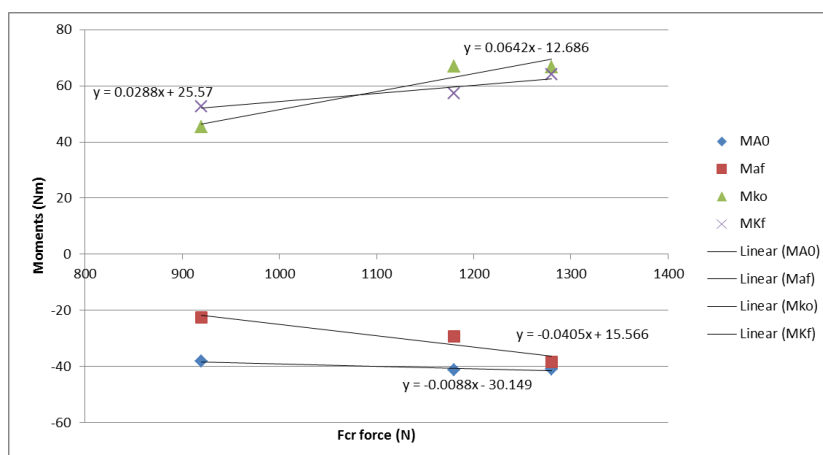
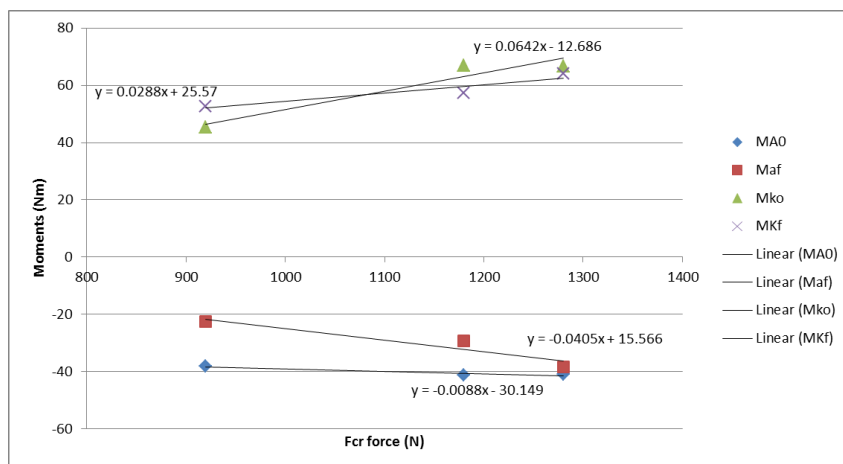


Figure 63: Moment vs Fcr for condition I



**Figure 64: Moment vs Fcr for condition II**

### B.3.3 Additional dimensions

The angles for the ankle foot test were kept the same as these can be assumed to be related to gait rather than to the height or weight of an individual. The offset dimensions for the knee lock will be kept as is to allow for a conservative test for knee locks.

**Table 20: Structural test forces (Principal tests)**

Principal tests					
	Test procedure and test load	Name	Unit	Principal tests	
				I	II
Principal structural tests	Dimensions	uT	mm	419.90	
		uK	mm	323.00	
		uA	mm	51.68	
		uB	mm	0.00	
		fb	mm	-99.60	100.55
		ob	mm	14.83	-42.49
		fA	mm	-79.44	92.52
		oA	mm	-1.33	-43.09
		fK	mm	26.40	50.38
		oK	mm	-86.18	-46.28
		ft	mm	64.20	90.58
		ot	mm	-116.48	-43.24
		Stabilizing test force	Fstab	N	50.00
	Settling force	Fset	N	296.44	249.43
	Proof test force	Fpa	N	1556.33	1309.48
	Proof test force	Fsp	N	648.47	545.62
	Ultimate static test force	Fsu, lower level	N	972.71	818.43
		Fsu, upper level	N	1296.94	1091.23
	Minimum test force	Fcmin	N	50.00	
	Cyclic range	Fcr	N	370.56	311.78
Maximum test force	Fcmax	N	420.56	361.78	
Mean test force	Fcmean	N	235.28	205.89	
Cyclic amplitude	Fca = 0.5*Fcr	N	185.28	155.89	
Final static force	Ffin = Fsp	N	648.47	545.62	
Number of cycles			2x10 <sup>6</sup>		

**Table 21: Structural test forces (Separate tests)**

Separate tests					
Static test in torsion	Settling twisting moment	Mu-set	Nm	3.00	
	Stabilizing twisting moment	Mu-stab	Nm	1.00	
	Maximum twisting moment	Mu-max	Nm	50.00	
Ankle foot test	Dimensions	alpha	°	15.00	
		beta	°	20.00	
		gama	°	7.00	
(Static)	Proof test force	F1sp, F2sp	N	648.47	
	Ultimate static test force	F1su F2su, lower level	N	972.71	
		F1su F2su, upper level	N	1296.94	
(Cyclic)	Minimum test force	F1cmin, F2cmin	N	50.00	
	Cyclic range	F1cr, F2cr	N	370.56	
	Maximum test force	F1cmax, F2cmax	N	420.56	
	Mean test force	F1cmean, F2cmean	N	235.28	
	Cyclic amplitude	F1ca, F2ca	N	185.28	
	Final static force	F1fin, F2fin	N	648.47	
	Number of cycles			2x10 <sup>6</sup>	
	Max knee flexion Knee locks	Length	Le	mm	258.4
Dimensions		Ultimate static test force	Fsu		1296.94
		fk	mm	-50	
		ok	mm	0	
		fa	mm	-50	
		oa	mm	0	
Stabilizing test force		Fstab	N	50	
Settling force		Fset	N	296.44	
Proof test force		Fsp	N	1556.33	
Ultimate static test force		Fsu	N	1296.94	
Minimum test force		Fcmin	N	50	
Cyclic range		Fcr	N	370.56	
Maximum test force		Fcmax	N	420.56	
Mean test force		Fcmean	N	235.28	
Cyclic amplitude		Fca = 0.5*Fcr	N	185.28	
Final static force		Ffin = Fsp	N	648.47	
Number of cycles				1x10 <sup>6</sup>	

## Appendix C Design calculations

**Table 22: Calculation results for each design component**

	Part	Analysis	Symbol(Unit)	Value
Ankle	Hinge joint (Al)	Bending failure of pin	$\sigma_{\max}$ (MPa)	12.8
		Safety factor	n	8.59
	Torsion spring (St)	Stiffness	K (Nmm/°)	808.59
		Stress	$\sigma_{\max}$ (MPa)	1303.33
	Footplate (Al)	Energy (Heel strike)	U (J)	3.92
		Energy (Torsion spring)	U (J)	2.29
		Energy (Dorsiflexion bumper)	U (J)	3.6
		Energy (Plantarflexion bumper)	U (J)	5.84
		Deflection	$\delta_{\max}$ (mm)	6.02
		Deflection angle	$\theta_{\max}$	3.04
		Von Mises stress	$\sigma'$ (MPa)	129.28
	Bumpers	Ideal stiffness, dorsi-	K (N/mm)	211.75
		Ideal stiffness, plantar-	K (N/mm)	91.89
	Leg	(Al 2024*)	Deflection	$\delta_{\max}$ (mm)
		Von Mises stress of bottom part	$\sigma'_{\text{bot}}$	116.24
		Von Mises stress of top part	$\sigma'_{\text{top}}$	139.8
		* $>$ Sut generic Al, $<$ Su of 2024 Al		
Knee	Lock (1006 HR St)	Deflection	$\delta_{\max}$ (mm)	$4.18 \times 10^{-18}$
		Maximum stress	$\sigma_{\max}$ (MPa)	1.43
		Fatigue life	$N_{\text{cyc}}$	$5.73 \times 10^{38}$
	Body (PLA)	Compressive force (Standing)	$\sigma_{\max}$ (MPa)	1.94
		Tensile force	$\sigma_{\max}$ (MPa)	1.94
	Top (PLA)	Compressive force (Standing)	$\sigma_{\max}$ (MPa)	1.94
		Tensile force	$\sigma_{\max}$ (MPa)	1.94
		Bending failure of pin (Standing)	$\sigma_{\max}$ (MPa)	15.77
	Lock lip (St)	Deflection	$\delta_{\max}$ (mm)	$2.59 \times 10^{-6}$
		Von Mises stress	$\sigma'$ (MPa)	16.8
		Fatigue life	$N_{\text{cyc}}$	$1.05 \times 10^{20}$
	Axis (1006 HR St)	Von Mises stress	$\sigma'$ (MPa)	66.68
		Fatigue life	$N_{\text{cyc}}$	$2.65 \times 10^{14}$

**Table 23: Summary of ankle FEA results**

	Property	Units	Value	Location
Centre pressure (219 kPa)	Max Von Mises	MPa	24.4	At interface between top and bottom hinge components
	Max translation	mm	$1.45 \times 10^{-2}$	Front of top component
Back pressure (439 kPa)	Max Von Mises	MPa	112	At interface between top and bottom hinge components
	Max translation	mm	$6.27 \times 10^{-2}$	Back of the top component
Front pressure (439 kPa)	Max Von Mises	MPa	110	At interface between top and bottom hinge components
	Max translation	mm	$6.43 \times 10^{-2}$	Front of top component

**Table 24: Summary of knee FEA results**

	Property	Units	Value	Location
Centre pressure (219 kPa)	Max Von Mises (Lock constrained)	MPa	226	Lock to body
	Max translation (Lock constrained)	mm	2.51	Top component
	Max Von Mises	MPa	23.3	Lock to body
	Max translation	mm	0.146	Top
Back pressure (439 kPa)	Max Von Mises (Lock constrained)	MPa	65.2	Lock to body connection
	Max translation (Lock constrained)	mm	0.284	At top back of body
Front pressure (439 kPa)	Max Von Mises (Lock constrained)	MPa	56.7	Body at axis
	Max translation (Lock constrained)	mm	0.65	

**Table 25: Summary of engineering requirements for final design**

Engineering requirements	ER ref no.	Units	Range/Goal	Actual
Height adjustments	ER1 /PDP3	mm	50	45
Foot length adjustments	ER2/A DP6	mm	159-181	Achieved Separate foot plate for each size.
Stiffness adjustment	ER3/A DP4	Nmm/°	808.59	Replaceable
	ER3/K DP7	N/mm	3.34	Replaceable springs
Overall strength	ER4	N/A	Handle 20 kg	Designed to ensure
Fatigue strength/ 3-year lifespan	ER5	N/A	lifespan: $2.37 \times 10^7$ cycles, corrosion resistant	Designed to ensure
Locally sourced materials	ER6	N/A	From South Africa	All except prosthetic adapters from SA
Easy to manufacture	ER7	N/A	Use of basic workshop facilities	Basic workshop facilities used, laser cutting and 3D printing.
Material and manufacture cost	ER8	R	Cost less than R378,480.93 – R417,596.43	Achieved, R21,458.19
Safe	ER9	N/A	For toddler overall use, especially stability	Safe, high stability designed for
Cosmetically appealing	ER10/ PDP4	N/A	To the eye, putting on clothing	Colourful for toddlers, easy to put on clothes
Standardized	ER11	N/A		Use of paediatric adapters.



**Table 26: Summary of Design parameters, see Table 25 for additional ERs**

Design Parameters	DP ref no.	Unit	Range	Actual
Lightweight	ADP1	g	276-400	227
	PDP1	g	114-160	227
	KDP3	g	130-369	479
Shock absorption	ADP2		N/A	Achieved, The deflection of the footplate, as well as the torsion spring.
	PDP2		N/A	Low to none - static
Activity level	ADP3	N/A	K3	Achieved, K2-K3
Ankle stiffness	ADP4		Dorsi: 8.77	Achieved
			Plantar: 19.56	Achieved
Length and breadth	ADP5	mm	159-181	Achieved Separate foot plate for each size.
Stance-phase stability	KDP1	Posterior	Ideal 55.8%	Lock spring, and axis alignment: 54.8%
Swing-phase control	KDP2	N/A		Extension assist spring, shims
Toe-clearance	KDP4	N/A	N/A	Requires testing
Maximum knee flexion angle	KDP5		150-165	Minimum for natural gait achieved: 67.3°. No additional flexion
Thigh portion length	KDP6	mm	In line with the other thigh	Knee axis is at actual knee joint

**Table 27: Overall cost of final design**

Cost of:	R	Additional information
Components	1292.36	Includes cost of laser cutting and spring forming, excludes adapter costs
Machine and manufacture	362.92	3D printing
	15198.25	
	1444.91	
Prosthetic adapters	3159.75	Workshop cost rates
<b>Total</b>	<b>21458.19</b>	

All data for prosthetic components - determined iteratively and then adjusted due to drawings.

$$g := 9.81 \frac{m}{s^2}$$

$$m_{ch} := 18.3 \text{ kg} \quad (3)14.1, (4)16.2, (5)18.3 \text{ kg (Snyder et. al., 1977)}$$

$$m_{ch} := 20 \text{ kg}$$

$$m_{leg} := 15 \text{ kg} \quad (\text{Zinke-Allmang, 2009})$$

$$W_{ch} := m_{ch} \cdot (1 - m_{leg}) \cdot g = 166.77 \text{ N} \quad \text{Weight of child without leg}$$

$$\rho_{al} := 2.7 \frac{g}{cm^3} \quad E_{al} := 69 \text{ GPa} \quad (\text{Engineering toolbox, 2016})$$

$$\rho_{st} := 8.5 \frac{g}{cm^3} \quad E_{st} := 200 \text{ GPa}$$

$$E_{wire} := 207 \text{ GPa} \quad (\text{Ace wire, 2016})$$

$$m_{adap} := 38.5 \text{ g}$$

#### Socket

$$l_{so} := 17 \text{ cm} + 1 \text{ mm} \quad \text{Foot length: 14.7cm (2-3.5yo) to 17cm (4.5 to 5.5yo)} \\ \text{1 mm clearance added} \quad 16.1 \quad 6.5$$

$$b_{so} := 6.8 \text{ cm} + 15 \text{ mm} \quad \text{Foot breadth: 6.1 cm (2-3.5yo) to 6.8cm (4.5 to 5.5yo)} \\ \text{15 mm clearance added}$$

$$h_{so} := 4.6 \text{ mm}$$

$$m_{soal} := l_{so} \cdot b_{so} \cdot h_{so} \cdot \rho_{al} = 0.1763 \text{ kg}$$

$$m_{pl} := 140 \text{ g} \quad \text{Assumed, based on the weight of a 5 year-old's shoe}$$

$$m_{so} := m_{soal} + m_{pl} = 0.3163 \text{ kg} \quad (140(5), 100(4), 80(3))$$

#### Knee

$$l_k := 101 \text{ mm}$$

$$m_k := 0.34 \text{ kg}$$

#### Foot

$$l_{fo} := 0.0332 \text{ m} \quad \text{height of foot component}$$

$$m_{fo} := 0.2667 \text{ kg}$$

$$l_{e_{fo}} := 17 \text{ cm} \quad \text{Foot length: 14.7cm (2-3.5yo) to 17cm (4.5 to 5.5yo)}$$

$$b_{fo} := 4.3 \text{ cm} \quad \text{Foot breadth: 6.1 cm (2-3.5yo) to 6.8cm (4.5 to 5.5yo)}$$

#### Shank

$$l_{sh} := 32.3 \text{ cm} - l_{fo} - l_k - 14.2 \text{ mm} = 0.1608 \text{ m}$$

$$m_{sh} := 0.0751 \text{ kg}$$

#### GRF

GRF is equivalent to the weight of the child above the component analysed, however it will be simplified to be the weight of the child for safety.

$$m_{ch} = 20 \text{ kg}$$

$$GRF := m_{ch} \cdot g = 196.2 \text{ N}$$

## C.1 Foot and ankle calculations

### Design of the spring stiffness:

Based on Shamaei et. al. (2011) and the data from Liu et. al.(2008). Shamaei discusses the ability to use a torsion spring to copy the stiffness of the ankle. The ankle stiffness is determined and then a spring is designed. Required spring stiffness:

$$K := (2.46) N \frac{m}{kg \text{ rad}} = 42.9351 N \frac{mm}{kg \text{ deg}} \quad \text{Liu et al (2008), an average age of 12.9 years.}$$

$$K_{\text{desired}} := K \cdot m_{\text{ch}} = 858.702 N \frac{mm}{deg}$$

This is the desired stiffness however it would be preferred if it was less stiff, there is no data referring to much younger participants and this stiffness may be too high.

$$Nu := 1.5 \quad \text{No. of active coils}$$

$$D_k := 22.5 \text{ mm}$$

$$d_k := 4.5 \text{ mm}$$

$$MD := D_k - d_k = 0.018 \text{ m}$$

$$\text{index} := \frac{MD}{d_k} = 4$$

This index must be 4 or higher, this is the main reason why a smaller spring is not feasible.

$$R_t := \frac{E_{\text{wire}} \cdot d_k^4}{10.8 \cdot MD \cdot Nu \cdot 360 \text{ deg}} = 808.5937 N \frac{mm}{deg}$$

This is the final spring rate, as can be seen it is lower than  $K_{\text{desired}}$  however this is for a much smaller, therefore lighter user.

$$\theta_{\text{spring}} := 18 \text{ deg}$$

$$TQ := R_t \cdot \theta_{\text{spring}} = 14.5547 \text{ N m}$$

This is the torque that will result at 18 deg, which has been determined to be the maximum flexion angle (Shamaei, 2011).

$$K_B := \frac{4 \cdot \text{index} - 1}{4 \cdot \text{index} - 4} = 1.25$$

$$SKTO := \frac{10.2 \cdot TQ}{d_k^3 \cdot K_B} = 1303.3333 \text{ MPa}$$

$$\text{minimum tensile strength: } 1586 \text{ MPa}$$

The strength of the spring must be considered to ensure that the required torque results in a smaller stress than the minimum tensile strength, this is another reason why a smaller spring is not feasible.

The moments created by the designed spring are now compared to the desired moment (by the ideal spring). As can be seen these moments are similar.

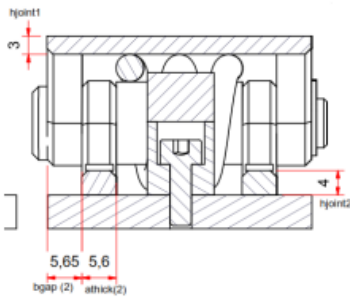
$$K_{\text{desired}} \cdot \theta_{\text{spring}} = 15.4566 \text{ N m}$$

$$R_t \cdot \theta_{\text{spring}} = 14.5547 \text{ N m}$$

However, according to excess springs(2016), a maximum spring deflection of only 16 deg is possible (for. strength purposes)

## (a) Design of the hinge joint (Machine design, 2014)

The values  $d_p$ ,  $d_{os}$ ,  $d_{od}$ ,  $t$  and  $t_1$  are adjusted to ensure the strength of the hinge joint. Hinge joint, final values shown.



$$\begin{aligned}d &:= 8 \text{ mm} \\b_{\text{gap}} &:= 5.65 \cdot 2 \text{ mm} = 0.0113 \text{ m} \\d_0 &:= d + 4 \text{ mm} \cdot 2 = 0.016 \text{ m} \\b_{\text{top}} &:= 50 \text{ mm} \\a_{\text{thick}} &:= 5.6 \cdot 2 \text{ mm} = 0.0112 \text{ m} \\h_{\text{joint1}} &:= 3 \text{ mm} \\h_{\text{joint2}} &:= 4 \text{ mm}\end{aligned}$$

To determine the dimensions for the hinge joint, failure in different parts are considered. The stresses developed should be less than the corresponding permissible values of stress. A high safety factor is desired due to unforeseen forces such as additional weight and impact.

The stress in the components is first compared to aluminium.

$$S_u := 110 \text{ MPa} \quad \text{Ultimate tensile strength (Engineering toolbox)}$$

$$\tau_u := 207 \text{ MPa} \quad \text{Shear strength (Matweb, 2016)}$$

$$\sigma_c := S_u \quad \text{Allowable compressive stress for the material}$$

Shear failure of pin: (must be smaller or equal to  $\tau_u$ )

$$\tau := \frac{\text{GRF}}{2 \cdot \left( \frac{\pi}{4} \cdot d^2 \right)} = 1.9516 \text{ MPa} \quad n := \frac{\tau_u}{\tau} = 106.0648$$

Crushing failure of pin in eye: (must be smaller or equal to  $\sigma_c$ )

$$\sigma_{\text{crushing}} := \frac{\text{GRF}}{b_{\text{gap}} \cdot d} = 2.1704 \text{ MPa} \quad n_2 := \frac{\sigma_c}{\sigma_{\text{crushing}}} = 50.683$$

Crushing failure of pin in fork: (smaller or equal to  $\sigma_c$ )

$$\sigma_{\text{crushing}} := \frac{\text{GRF}}{2 \cdot a_{\text{thick}} \cdot d} = 1.0949 \text{ MPa} \quad n_3 := \frac{\sigma_c}{\sigma_{\text{crushing}}} = 100.4689$$

Bending failure of pin: (smaller or equal to  $S_u$ )

$$\sigma_b := \frac{\text{GRF}}{2} \cdot \frac{\frac{a_{\text{thick}}}{3} + \frac{b_{\text{gap}}}{4}}{\frac{\pi}{32} \cdot d^3} = 12.7995 \text{ MPa} \quad n_4 := \frac{S_u}{\sigma_b} = 8.5941$$

Tensile failure of eye: (smaller or equal to  $S_u$ )

$$\sigma_t := \frac{\text{GRF}}{b_{\text{gap}} \cdot (d_0 - d)} = 2.1704 \text{ MPa} \quad n_5 := \frac{S_u}{\sigma_t} = 50.683$$

Shear failure of eye: (smaller or equal to  $\tau_u$ )

$$\tau := \frac{\text{GRF}}{b_{\text{gap}} \cdot (d_0 - d)} = 2.1704 \text{ MPa} \quad n_6 := \frac{\tau_u}{\tau} = 95.3761$$

Tensile failure of fork: (smaller or equal to  $S_u$ )

$$\sigma_t := \frac{\text{GRF}}{2 \cdot a_{\text{thick}} \cdot (d_0 - d)} = 1.0949 \text{ MPa} \quad n_7 := \frac{S_u}{\sigma_t} = 100.4689$$

Shear failure of fork: (smaller or equal to  $\tau_u$ )

$$\tau := \frac{\text{GRF}}{2 \cdot a_{\text{thick}} \cdot (d_0 - d)} = 1.0949 \text{ MPa} \quad n_8 := \frac{\tau_u}{\tau} = 189.0642$$

The components could be designed incredibly small however due to the spring stiffness required and thus the size requirements, the overall size of the hinge is much larger, therefore strength will not be a problem.

**Design of strength of foot**

The force modes can be separated into 3 phases, (1) Heel-strike, only heel touches the floor; (2) flat-foot, whole foot touches; (3) toe-off, only toes. Deflection, strength and fatigue will be analysed.

**(1) Heel-strike**

This involves an impact force applied to the ankle of the foot.

Energy to be absorbed:

$$h_{\text{step}} := 20 \text{ mm} \quad \text{Assumed}$$

$$\text{Energy}_{\text{total}} := \text{GRF} \cdot h_{\text{step}} = 3.924 \text{ J} \quad \text{Energy to be absorbed}$$

$$\text{Energy}_{\text{spring}} := \frac{1}{2} \cdot R_t \cdot \theta_{\text{spring}}^2 = 2.2862 \text{ J} \quad \text{Energy that the spring will absorb}$$

$$\frac{\text{Energy}_{\text{spring}}}{\text{Energy}_{\text{total}}} \cdot 100 = 58.2631 \quad \text{Percentage energy that spring absorbs. Remainder will be absorbed by bumpers.}$$

**Design for bumpers**

The bumper must deflect to ensure that movement is possible in the ankle, the desired deflection is calculated below.

$$M_{\text{spring}} := R_t \cdot 16 \text{ deg}$$

$$F_{\text{spring2}} := \frac{M_{\text{force}} - M_{\text{spring}}}{\frac{50 \text{ mm}}{2}} = 816.66 \text{ N}$$

Dorsiflexion bumper: (This is the bumper at the back of the ankle)

$$d_{\text{dorsi}} := \frac{50 \text{ mm}}{2} \cdot \tan(8.77 \text{ deg}) = 0.0039 \text{ m}$$

$$k_{\text{dorsi}} := \frac{F_{\text{spring2}}}{d_{\text{dorsi}}} = 211.7454 \frac{\text{N}}{\text{mm}} \quad \text{The ideal stiffness of the bumper}$$

$$\text{Energy}_{\text{dorsi}} := F_{\text{spring2}} \cdot d_{\text{dorsi}} = 3.1497 \text{ J} \quad \text{Energy absorbed by dorsiflexion bumper}$$

Plantar flexion bumper: (Front of ankle)

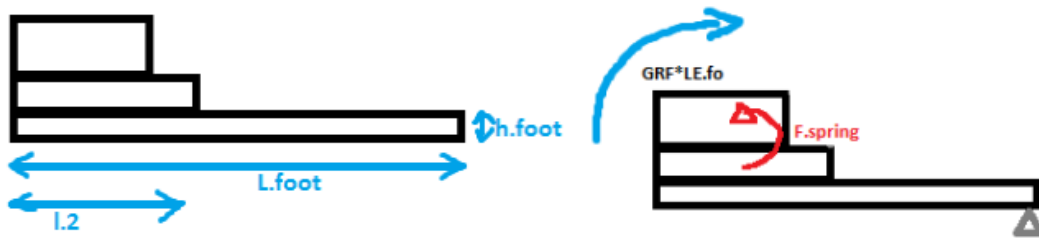
$$d_{\text{plantar}} := \frac{50 \text{ mm}}{2} \cdot \tan(19.57 \text{ deg}) = 0.0089 \text{ m}$$

$$k_{\text{plantar}} := \frac{F_{\text{spring2}}}{d_{\text{plantar}}} = 91.8901 \frac{\text{N}}{\text{mm}} \quad \text{The ideal stiffness of the bumper}$$

$$\text{Energy}_{\text{plantar}} := F_{\text{spring2}} \cdot d_{\text{plantar}} = 7.2579 \text{ J} \quad \text{Energy absorbed by plantarflexion bumper}$$

(2) Flat-foot

The forces experiences here is the movement of the body over the foot.



Though the foot will rotate over the end, and therefore it is similar to a pin support, the analysis will be done as though it were a fixed support so that maximum deflection can be considered. Deflection and fatigue strength is compared alongside one another, it is necessary for the foot to last the lifespan.

$$Le_{fo} = 0.17 \text{ m}$$

$$h_{foot} := 6 \text{ mm}$$

$$b_{foot} := b_{fo}$$

Dependent on fatigue strength

Based on the foot breadth, can be made thinner if necessary.

$$I_{x1} := \frac{b_{foot} \cdot h_{foot}^3}{12} = 7.74 \cdot 10^{-10} \text{ m}^4$$

$$M_{force} := GRF \cdot Le_{fo} = 33.354 \text{ J}$$

How forces are applied to test deflection

$$\sigma_x := \frac{(M_{force}) \cdot \frac{h_{foot}}{2}}{I_{x1}} = 129.2791 \text{ MPa}$$

Von mises stress

$$\delta_{max} := \frac{(GRF)}{3 \cdot E_{al}} \cdot \left( \frac{(Le_{fo})^3}{I_{x1}} \right) = 6.0164 \text{ mm}$$

This deflection is at the end, and we need to ensure that there is not too much deflection that a sturdy toe off is still achievable.

$$\theta_{max} := \frac{GRF \cdot Le_{fo}^2}{2 \cdot E_{al} \cdot I_{x1}} = 3.0416 \text{ deg}$$

$$\theta_{max} + 16 \text{ deg} = 19.0416 \text{ deg}$$

This falls in line with previously measured dorsiflexion

$$S_f := 138 \text{ MPa}$$

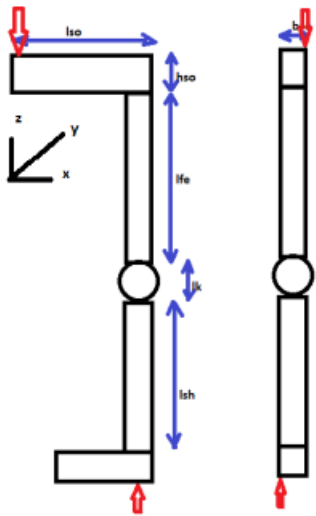
Corresponds to  $50(10)^7$  cycles of completely reversed stress.

The fatigue strength is the highest stress that a material can withstand for a given number of cycles without breaking. The von Mises stress is lower than this and therefore the foot will be strong enough.

## C.2 Pylon calculations

### FBD of leg

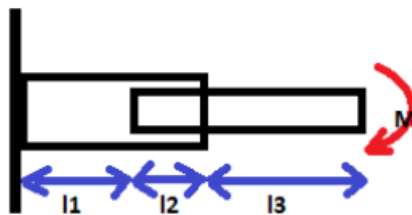
A moment would be created when standing however, due to this analysis being for standing on one leg, it can be assumed that the moment arm would be quite small as shown in the figure.



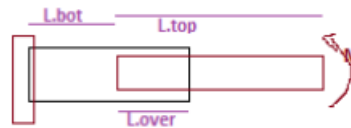
### Analyse shank

The FBD shown below is to determine the maximum deflection, this is when the leg is assumed to be fixed to the floor, as otherwise some of the moment would result in movement.

FBD



(Beam formulas)



Data

$$L_{bot} := 45 \text{ mm}$$

5 cm requirement for adjustment, shortened due to available space

$$L_{over} := 36 \text{ mm}$$

Due to saint venant principle:  $>1 \cdot \text{shaft diameter}$

$$L_{overrem} := 45 \text{ mm}$$

For adjustments

$$L_{top} := 24.5 \text{ mm} + L_{overrem} + L_{over} = 10.55 \text{ cm}$$

Shortened due to available space.

**Deflection of the shank**

$$P_{sh} := 20 \text{ kg} \cdot g = 196.2 \text{ N}$$

The force applied to the shin, larger weight for safety.

Moments are created due to the centre of gravity being off-centre. It is assumed that the child's weight creates a larger moment than the moment created by the prosthesis when swinging.

$$M_{shz} := P_{sh} \cdot (170 \text{ mm} - 50.667 \text{ mm}) = 23.4131 \text{ N m}$$

It is assumed that the front of the leg is a 1/3 of the foot (through analysis of literature).

$$M_{shy} := \frac{b_{fo}}{2} \cdot P_{sh} = 4.2183 \text{ N m}$$

$$M_{max} := \sqrt{M_{shy}^2 + M_{shz}^2} = 23.7901 \text{ N m}$$

Combined moments

$$\delta_{fmaxx} := \frac{M_{max}}{2 \cdot E_{al}} \left( \frac{L_{bot}^2}{I_{bot}} + \frac{L_{over}^2}{I_{over}} + \frac{L_{overrem}^2}{I_{skinny}} + \frac{(L_{top} - L_{over} - L_{overrem})^2}{I_{top}} \right) = 0.2765 \text{ mm}$$

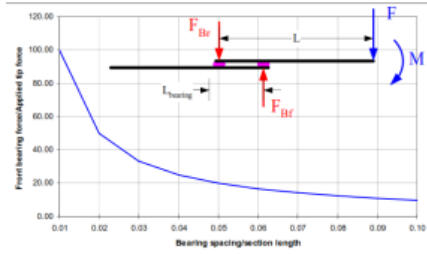


**Stress analysis**

The stress analysis is done as though the beam were a cantilevered beam as shown in the figure. Deflection cannot be determined if the top part of the toe is a simple support, therefore the analysis will also be for a fixed support cantilevered beam. These calculations are based on the discussion by Slocum (2008).

$$\gamma := \frac{L_{\text{over}}}{L_{\text{top}}} = 0.3412$$

From the figure, F is 0, as only moments are applied to the leg.



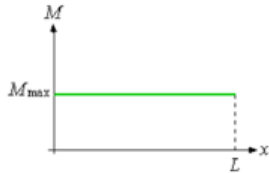
$$F_{Br} := \frac{M_{shz}}{L_{\text{over}}} = 650.3648 \text{ N}$$

$$F_{Bf} := F_{Br} = 650.3648 \text{ N}$$

This is the resultant force at the end when splitting the leg in two

$$F_{\text{end}} := F_{Br} - F_{Bf} = 0$$

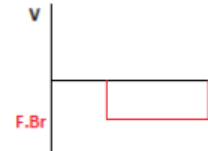
BMD - the moment will be the same through out the beam.



Firstly the stress for the bottom part:

When split into two, a shear force due to overlapping beams results.

SFD



The resulting stress due to the clamp is quite small p353 Shigley

$$\sigma_{\text{maxbot}} := \frac{M_{\text{max}} \cdot \frac{D_{\text{bot}}}{2}}{I_{\text{bot}}} + \frac{p_{sh}}{A_{\text{bot}}} = 74.7678 \text{ MPa}$$

Smallest I to determine max  $\sigma$   
Includes the compressive force

$$V_{\text{maxbot}} := -F_{Br} = -650.3648 \text{ N}$$

$$\tau_{\text{maxbot}} := \frac{2 \cdot V_{\text{maxbot}}}{A_{\text{bot}}} = -19.716 \text{ MPa}$$

p97 Shigley

$$\sigma'_{\text{bot}} := \frac{1}{\sqrt{2}} \cdot \left( \sqrt{\left( 2 \cdot \sigma_{\text{maxbot}} \right)^2 + 6 \cdot \left( 2 \cdot \tau_{\text{maxbot}} \right)^2} \right) = 116.2444 \text{ MPa} \quad \text{p223 no } \sigma_y, \text{ no } \sigma_z$$

Secondly the stress for the top part:

$$\sigma_{\text{maxtop}} := \frac{M_{\text{max}} \cdot \frac{D_{\text{skinny}}}{2}}{I_{\text{skinny}}} + \frac{P_{\text{sh}}}{A_{\text{skinny}}} = 91.3663 \text{ MPa} \quad \text{Smallest } I \text{ and } D \text{ to determine max } \sigma$$

$$V_{\text{maxtop}} := F_{\text{Br}} = 650.3648 \text{ N}$$

$$\tau_{\text{maxtop}} := \frac{2 \cdot V_{\text{maxtop}}}{A_{\text{skinny}}} = 21.7913 \text{ MPa} \quad \text{p97 Shigley}$$

$$\sigma'_{\text{top}} := \frac{1}{\sqrt{2}} \cdot \left( \sqrt{\left( 2 \cdot \sigma_{\text{maxtop}} \right)^2 + 6 \cdot \left( 2 \cdot \tau_{\text{maxtop}} \right)^2} \right) = 139.8027 \text{ MPa}$$

#### Fatigue of shank

Analysis for aluminium due to the previous discussion.

$$N_{\text{cyc}} := 2.37 \cdot 10^7$$

$$S_{\text{ut}} := 482 \text{ MPa} \quad \text{Aluminium 2024 T3 based on previous discussion}$$

$$S_{\text{f}} := 138 \text{ MPa} \quad \text{Corresponds to } 50(10)^7 \text{ cycles of completely reversed stress.}$$

The fatigue strength is the highest stress that a material can withstand for a given number of cycles without breaking. The largest stress is 133MPa, but not for a completely reversed stress, therefore this is acceptable.

#### Strength of slit

The slit in the lower shaft can experience fatigue however it is more likely that the clamp will break before the shaft breaks and therefore no further analysis is required.

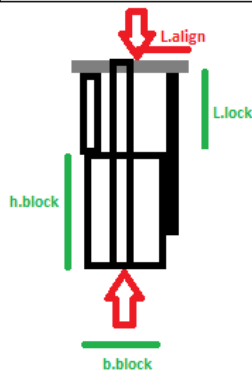
### C.3 Knee calculations

#### Forces on the knee

The forces on the knee can cause bending in the components which is undesired it is therefore important to analyse the deflection and the fatigue strength of the components. The PASPL-knee can be simplified into the figure below for strength and deflection calculations.

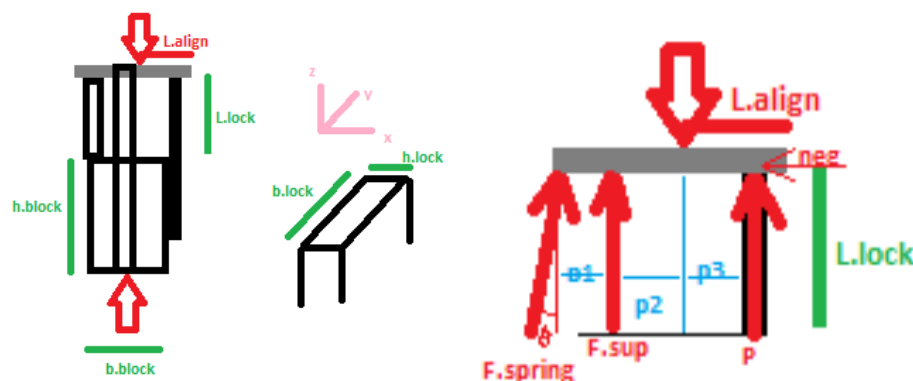
#### Simplified prosthetic knee

Negligible self-weight



#### Deflection and fatigue of standing

With the spring force (preload) and supports:



The deflection and strength of the lock is the most important, the lock can be analysed as a cantilevered beam with a fixed support with a compression force and a bending moment.

$$L_{align} = 18 \text{ mm}$$

distance from adapter to lock

$$L_{lock} = (80 - 59) \text{ mm} = 0.021 \text{ m}$$

The part that isn't supported.

$$b_{lock} = 15 \text{ mm}$$

$$h_{lock} = 3 \text{ mm}$$

3mm -> The thinnest part

$$A_{lock} = b_{lock} \cdot h_{lock} = 4.5 \cdot 10^{-5} \text{ m}^2$$

$$I_{lock} = \frac{h_{lock}^3 \cdot b_{lock}}{12} = 3.375 \cdot 10^{-11} \text{ m}^4$$

$$F_{spring} = 12.36 \text{ N}$$

From table 4-7

49.45x25% -> The preloaded force supplied

$$\theta_{spring} = 5 \text{ deg}$$

From figure (approximation)

$$p_1 = 19 \text{ mm}$$

From drawing

$$p_2 = 7 \text{ mm}$$

From drawing

$$p_3 = L_{align}$$

moment about axis

$$p = \frac{(F_{spring}) \cdot \cos(\theta_{spring}) \cdot p_1 + GRF \cdot p_2}{p_3 + p_2} = 64.2939 \text{ N}$$

Assume a negligible shear

and the supports:

The top part would absorb and lock isnt fixed, this force will occur as the top part moves down to rest on lock.down to rest on lock.

$$F_{sup} := \frac{-F_{spring} \cdot \cos(\theta_{spring}) + GRF - P}{2} = 59.7966 \text{ N} \quad \text{On each}$$

$$M_{ylock} := GRF \cdot p_3 - 2 \cdot F_{sup} \cdot (p_2 + p_3) - F_{spring} \cdot \cos(\theta_{spring}) \cdot (p_1 + p_2 + p_3) = 1.28 \cdot 10^{-16} \text{ Nm}$$

#### Compressive force on sides

The outer component will experience some compressive force when standing.

$$F_{sup} = 59.7966 \text{ N} \quad \text{This will be supplied to each side.}$$

$$F_{sup} := F_{sup} \cdot 2$$

$$b_{side} := 7.69 \text{ mm}$$

By using the formula for hinge joints, the tensile failure and shear failure can be checked.

$$d_0 := 22 \text{ mm}$$

$$d := 8 \text{ mm}$$

Crushing failure of the fork (smaller or equal to  $\sigma_c$ )

$$\sigma_{crush} := \frac{F_{sup}}{2 \cdot b_{side} \cdot (d)} = 0.972 \text{ MPa}$$

Tensile failure of fork: (smaller or equal to  $S_u$ )

$$\sigma_t := \frac{F_{sup}}{2 \cdot b_{side} \cdot (d_0 - d)} = 0.5554 \text{ MPa}$$

Shear failure of fork: (smaller or equal to  $\tau_u$ )

$$\tau := \frac{F_{sup}}{2 \cdot b_{side} \cdot (d_0 - d)} = 0.5554 \text{ MPa}$$

The compressive strength of PLA is 17.9MPa, Tensile strength is 46.7MPa. The compressive strength of ABS is 7.9MPa, tensile strength 34 MPa. These are both larger than the stresses the component experiences.

#### Design of axis points of the rod

$$d_{pin} := 8 \text{ mm}$$

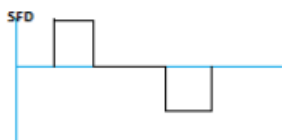
$$a_{thick} := 34 \text{ mm}$$

$$d_{top} := 27 \text{ mm}$$

$$A_{pin} := \pi \cdot \frac{d_{pin}^2}{4} = 5.0265 \cdot 10^{-5} \text{ m}^2$$

$$I_{pin} := \frac{\pi \cdot d_{pin}^4}{64} = 2.0106 \cdot 10^{-10} \text{ m}^4$$

SFD and BMD





Shear failure of pin: (must be smaller or equal to  $\tau_u$ )

$$\tau := \frac{F_{\text{sup}}}{2 \cdot \left( \frac{\pi}{4} \cdot d_{\text{pin}}^2 \right)} = 1.1896 \text{ MPa}$$

Crushing failure of pin in eye: (must be smaller or equal to  $\sigma_c$ )

$$\sigma_{\text{crushing}} := \frac{F_{\text{sup}}}{b_{\text{side}} \cdot d_{\text{pin}}} = 1.944 \text{ MPa}$$

Bending failure of pin: (smaller or equal to  $S_u$ )

$$\sigma_b := \frac{F_{\text{sup}}}{2} \cdot \frac{\frac{a_{\text{thick}}}{3} + \frac{b_{\text{side}}}{4}}{\frac{\pi}{32} \cdot d_{\text{pin}}^3} = 15.7693 \text{ MPa}$$

And for the top component

Tensile failure of eye: (smaller or equal to  $S_u$ )

$$\sigma_t := \frac{F_{\text{sup}}}{b_{\text{side}} \cdot (d_{\text{top}} - d_{\text{pin}})} = 0.8185 \text{ MPa}$$

Shear failure of eye: (smaller or equal to  $\tau_u$ )

$$\tau := \frac{F_{\text{sup}}}{b_{\text{side}} \cdot (d_{\text{top}} - d_{\text{pin}})} = 0.8185 \text{ MPa}$$

#### Deflection of the lock



$$\delta_{12} := \frac{M_{y\text{lock}} \cdot L_{\text{lock}}^2}{2 \cdot E_{\text{st}} \cdot I_{\text{lock}}} = 4.1813 \cdot 10^{-18} \text{ mm}$$

#### Strength of lock

The bending moment and the compressive force results in a stress:

$$\sigma_{\text{max}} := \left( \frac{M_{y\text{lock}} \cdot h_{\text{lock}}}{I_{\text{lock}}} - \frac{P}{A_{\text{lock}}} \right) = -1.4288 \text{ MPa}$$

$$\sigma_{\text{bend}} := \frac{M_{y\text{lock}} \cdot h_{\text{lock}}}{I_{\text{lock}}} = 1.1378 \cdot 10^{-8} \text{ Pa}$$

$$\sigma_{\text{axial}} := \frac{P}{A_{\text{lock}}} = 1.4288 \text{ MPa}$$

$$\sigma_{\text{bend}} := \frac{y_{\text{lock}} \cdot I_{\text{lock}}}{I_{\text{lock}}} = 1.1378 \cdot 10^{-8} \text{ Pa}$$

$$\sigma_{\text{axial}} := \frac{P}{A_{\text{lock}}} = 1.4288 \text{ MPa}$$

#### Fatigue of lock

$$N_{\text{cyc}} := 2.37 \cdot 10^7$$

$$S_{\text{ut}} := 300 \text{ MPa} \quad \text{Sut and Sy for 1006 HR steel Table A-20}$$

$$S_{\text{y}} := 170 \text{ MPa}$$

$$S'_{\text{e}} := 0.5 \cdot S_{\text{ut}} = 150 \text{ MPa} \quad \text{eqn 6-8} \quad \text{IF SUT > 1400 MPA then 700MPa}$$

$$a := 57.7 \quad \text{HR Table 6-2 (CD 4.51 -0.265)}$$

$$b := -0.718 \quad \text{HR Table 6-2 (HR 57.7 -0.718)}$$

$$k_{\text{a}} := a \cdot \left( \frac{S_{\text{ut}}}{\text{MPa}} \right)^b = 0.9607$$

$$k_{\text{b}} := 1 \quad \text{eqn 6-21 not a rotating shaft..}$$

$$k_{\text{c}} := 1 \quad \text{made 1 due to combined phenomenon}$$

$$k_{\text{d}} := 1 \quad \text{Table 6-4}$$

$$k_{\text{e}} := 0.753 \quad \text{Table 6-5 99.9\% reliability}$$

$$S_{\text{e}} := k_{\text{a}} \cdot k_{\text{b}} \cdot k_{\text{c}} \cdot k_{\text{d}} \cdot k_{\text{e}} \cdot S'_{\text{e}} = 108.5148 \text{ MPa}$$

$$q := 0.92 \quad \text{Figure 6-20}$$

$$K_{\text{tbend}} := 1.41 \quad \text{Figure A-15-6}$$

$$K_{\text{fbend}} := 1 + q \cdot (K_{\text{tbend}} - 1) = 1.3772$$

$$K_{\text{taxial}} := 1.62$$

$$K_{\text{faxial}} := 1 + q \cdot (K_{\text{taxial}} - 1) = 1.5704$$

$$\sigma_{\text{abend}} := \frac{\sigma_{\text{bend}}}{2} = 5.6889 \cdot 10^{-9} \text{ Pa} \quad \text{Fluctuates between 0 and } \sigma$$

$$\sigma_{\text{mbend}} := \frac{\sigma_{\text{bend}}}{2} = 5.6889 \cdot 10^{-9} \text{ Pa}$$

$$\sigma_{\text{aaxial}} := \frac{\sigma_{\text{axial}}}{2} = 7.1438 \cdot 10^5 \text{ Pa}$$

$$\sigma_{\text{maxial}} := \frac{\sigma_{\text{axial}}}{2} = 7.1438 \cdot 10^5 \text{ Pa}$$

$$\sigma'_{\text{a}} := K_{\text{fbend}} \cdot \sigma_{\text{abend}} + K_{\text{faxial}} \cdot \frac{\sigma_{\text{aaxial}}}{0.85} = 1.3198 \cdot 10^6 \text{ Pa} \quad \text{p318}$$

$$\sigma'_{\text{m}} := K_{\text{fbend}} \cdot \sigma_{\text{mbend}} + K_{\text{faxial}} \cdot \frac{\sigma_{\text{maxial}}}{0.85} = 1.3198 \cdot 10^6 \text{ Pa}$$

$$n_{\text{steel}} := \left( \frac{\sigma'_{\text{a}}}{S_{\text{e}}} + \frac{\sigma'_{\text{m}}}{S_{\text{y}}} \right)^{-1} = 50.1847 \quad \text{Conservative: Mod-Goodman}$$

$$\sigma_{\text{rev}} := \frac{\sigma'_{\text{a}}}{1 - \left( \frac{\sigma'_{\text{m}}}{S_{\text{ut}}} \right)} = \frac{153566861642212}{115841541501961} \text{ MPa}$$

p285

$$f := 0.775$$

$$a := \frac{(f \cdot S_{\text{ut}})^2}{S_{\text{e}}} = 4.9815 \cdot 10^8 \text{ Pa}$$

$$b := -\frac{\log_{10}\left(\frac{f \cdot S_{ut}}{S_e}\right)}{3} = -0.1103$$

$$N_{cyc} := \left(\frac{\frac{\sigma_{rev}}{n_{steel}}}{a}\right)^{\frac{1}{b}} = 5.7338 \cdot 10^{38}$$

This safety factor is high enough that the lock will be able to support more of the load so that the plastics components are protected.

#### Impact strength of locking mechanism

According to Ngan (2015) the swing-phase control mechanisms have the function of preventing impact as the knee moves to fully extend. (p33) The lifespan seen from the fatigue phase is still have give also so high that some impact will also so high that some impact will the necessary lifespan.

## **Appendix D Safety procedure**

### **D.1 Introduction**

The following safety procedures have been determined and set out for the use of the three phase power supply in the biomedical laboratory (or other available laboratories) in Stellenbosch University. These procedures are designed to ensure the safety of the individual as well as bystanders. The use of the biomedical laboratory will be used to test the control of a linear actuator, the driver requiring a three phase supply.

### **D.2 Overview of work to be performed**

The testing of the position feedback control of a linear actuator is required. The motor controller, Movidrive, requires a three phase power supply. The Movidrive shall first be tested with a smaller rotary motor, this will allow testing to ensure that the control is feasible without the risk of the linear actuator stroke and forces. During these tests, emergency stops shall also be tested as well as limit switches to ensure safety in the control design. Once the control is determined acceptable, the linear actuator will be installed so as to prevent any additional movement. The Movidrive will then be connected to the linear actuator to test the position feedback control.

### **D.3 General lab instructions**

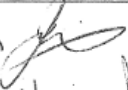



- Closed shoes should be worn at all times
- All individuals in the laboratory should be informed before devices are turned on
- All individuals should be aware of where the emergency stop button is and how it must be used.
- No after hours working alone
- The connection to the three phase supply will have a switch to switch off the power before uninstalling any devices.

### **D.4 Safety Risks**



**Table 28: Risk analysis**

<b>Risk</b>	<b>Risk Type</b>	<b>Design Impact</b>	<b>Mitigating steps</b>
Moving equipment	P, E	Emergency stop required Installation to ensure no additional movement.	Ensure emergency stop is working. Disconnect power before working on equipment. Ensure all are aware of moving parts before initializing the control. Set limit switches to a lower threshold than the actuator's actual threshold.
Electric shock	P	Provide emergency stop. Visual feedback that power is switched on. Insulate live wires.	Ensure emergency stops are easily accessible Wear shoes at all times.

J Theron   
 D. van den Heever   
 W. Swart 


## Appendix E Gait emulation testing



**Figure 65: Testing the prosthetic leg using Bertec treadmill and Vicon motion capture**



**Figure 66: Second figure of testing of the prosthetic leg using Bertec treadmill and Vicon motion capture**